A PRIMER ON WEATHER AND CLIMATE

Roger A. Pielke, Ph.D.
Professor of Atmospheric Science
Colorado State University

©2002
All Rights Reserved
Library of Congress Catalogue Card Number:
ISBN:
PRINTED IN THE UNITED STATES OF AMERICA

November 20, 2002

Contents

1 Introduction 1

2 Evolution of the Earth's Atmosphere 3

3 Surface Budgets 5

4 Vertical Structure of the Atmosphere 23

5 Horizontal Structure of the Atmosphere 39

6 Cloud Processes 57

7 Climatology and Climate Change 69

8 The Atmospheres of Other Planets 83

9 Practical Applications 87

Chapter 1

Introduction

Atmospheric Sciences represent components of the basic fields of physics and chemistry which focus on the structure and dynamics of the earth's atmosphere. Mathematical tools such as differential equations and vector analysis, and large computer systems are used to evaluate the physical, biological, and chemical relations which describe the workings of the atmosphere. Planetary science and stellar science refer to equivalent studies of the atmospheres of other astronomical bodies.

The atmospheric sciences have traditionally been divided into three topical areas – *meteorology, climatology,* and *aeronomy.* In meteorology, the focus of study is the day-to-day, hour-to-hour changes in weather within the lower stratosphere and troposphere. Climatology, on the other hand, concentrates on a statistical description of the weather in the same region of the atmosphere but over long time periods ranging from a month to millions of years. Meteorology is the science from which weather forecasts are prepared, whereas climatology provides information such as the most likely date for the first frost in the fall. Studies above the lower stratosphere are referred to as being in the field of aeronomy.

In recent years, the term *climate system science* has been used to describe a broader earth system perspective. Climate system science includes the physical, biological, and chemical processes in the atmosphere, oceans, continental ice sheets, and land.

Chapter 2

Evolution of the Earth's Atmosphere

The evolution of the earth's atmosphere is not completely understood. It is felt that the current atmosphere has resulted from a gradual release of gases from the interior, rather than being the primordial atmosphere which developed by outgassing during the original formation of the planet. Current volcanic gaseous emissions include carbon dioxide (CO_2), sulfur dioxide (SO_2), chlorine (Cl), fluorine (F), water (H_2O), and diatomic nitrogen (N_2), as well as traces of other substances. Approximately 85% of the emissions are in the form of water vapor. Carbon dioxide is about 10% of the effluent.

A requirement during the early evolution of the atmosphere on the earth is that water must have been able to exist as a liquid, since the oceans apparently have been present for at least 3 billion years. Since the solar output was about 25% less 4 billion years ago, enhanced levels of carbon dioxide and perhaps ammonia (NH_3) appear to have been required to retard longwave radiative heat loss to space. The initial life forms that evolved in this environment must have been anaerobic (i.e., survived in the absence of oxygen) and needed a capability to resist the biologically destructive short ultraviolet radiation, which was not absorbed by an ozone, O_3, layer as it is now. Once the organisms developed the capability for photosynthesis (in which visible sunlight on plants produces diatomic oxygen), oxygen was produced in large quantities, eventually reaching the current levels. This also permitted the development of the ozone layer as O_2 was dissociated into monatomic oxygen and recombined with O_2 to form ozone. The capability for primitive forms of plants to photosynthesize developed between 2 and 3 billion years ago. Previous to the evolution to photosynthetic organisms, oxygen was produced in only limited quantities as a result of the decomposition of water vapor into molecular oxygen by ultraviolet sunlight (Table 2.1).

The current percent composition of the earth's atmosphere in terms of total molecules is diatomic nitrogen (N_2) 78.08%; diatomic oxygen (O_2) 20.95%; argon (A) 0.93%, water (H_20) from about 0 to 4%); and carbon dioxide (CO_2) 0.0325%. The inert gases neon (Ne), helium (He), and krypton (Kr), and other constituents such as nitrogen oxides, compounds of sulfur and ozone are found in lesser amounts.

Table 2.1: History of the Earth, Its Atmosphere, and Life[a] (from Levine, J.S., 1985: The photochemistry of the early atmosphere. In: *The Photochemistry of Atmospheres. Earth, the Other Planets, and Comets.* Academic Press, Inc. 3-38).

Event	Years ago[b]
Formation of the sun, the earth and its atmosphere(?)	4.6 B
Oldest known sedimentary rocks	3.8 B
Origin of life(?)	3.8 B
Oldest stromatolites	3.5 B
Microbial fossils (proalgae?)	2.8 B
Atmospheric O_2 reaches 1%	2.0 B
Gunflint blue-green algae	2.0 B
Oldest eukaryotic cells	1.4 B
Atmospheric O_2 reaches 7%	670 M
First known metazoans	670 M
Atmospheric O_2 reaches 10%	550 M
Atmospheric O_3 shields surface from solar UV radiation	550 M
First hard-shelled animals	550 M
Atmospheric O_2 reaches 100%	400 M
Large fishes and first land plants	400 M

[a] Adapted from Cloud (1983)
[b] B $\equiv$ Billion, M $\equiv$ million

Chapter 3

Surface Budgets

The earth's atmosphere is bounded at the bottom by water and land. Heating of this surface is accomplished by three physical processes – *radiation, conduction*, and *convection.*

The electromagnetic radiation that influences the temperature of the atmosphere and at the surface is traditionally divided into two types – insolation from the sun which is referred to as *shortwave radiation* (with predominant wavelengths of 0.39 to 0.76 μm (microns)) and emittance from the surface and the atmosphere which is called *longwave radiation* (with typical wavelengths of 4 to 30 μm). The wavelength of the emitted electromagnetic radiation depends on the temperature of the radiating body as specified by Plank's law. The sun, with its surface temperature of around 6,000 K emits at a much shorter wavelength than the earth which has surface and atmospheric temperatures around 250 K to 300 K (Figure 3.1).

A fraction of shortwave radiation is absorbed by atmospheric gases including water vapor and warms the air directly, but most of this energy reaches the surface in the absence of clouds. Scattering of a fraction of the shortwave radiation, particularly of the shortest wavelength by air molecules, which is referred to as *Rayleigh scattering*, produces our blue skies.

When clouds are present, a large percentage (upwards to about 80%) of the solar insolation is reflected back out into space (the fraction of back reflected shortwave radiation is called the *albedo*). Of the solar radiation reaching the surface, a fraction is reflected back into the atmosphere. Values of the surface albedo range from 0.95 for fresh snow to 0.10 for dark, organic soils. On land, this reflection occurs entirely at the surface. In water, however, shortwave radiation penetrates to significant depths (upwards to several hundred meters) before the insolation is completely attenuated. The heating by solar radiation in water, therefore, is distributed through a depth, which results in smaller temperature changes at a level than would occur with the same insolation over land at the surface.

The magnitude of solar radiation reaching the surface depends on latitude, time of year, time of day, and orientation of the land surface with respect to the sun (Figure 3.2). In the northern hemisphere north of 23-1/2°, for example, solar insolation at local noon is less on north facing slopes than on land oriented toward the south (Figure 3.3).

Figure 3.1: (a) Solar irradiance at the top of the atmosphere (TOA) and at the surface for a clear atmosphere as a function of wavelength. The sun has an elevation of 30° above the horizon (from Kneizys et al., 1988 as reproduced by Liou, K.N., 1992: Radiation and cloud processes in the atmosphere. Oxford Monographs on Geology and Geophysics No. 20, 487 pp.) (b) Earth's radiation as observed by an earth-orbiting satellite (from Kunde et al., 1974 as reproduced by Liou, K.N., 1992).

Figure 3.2: A schematic illustration of the orbit of the earth around the sun to illustrate the annual progression of seasons.

Figure 3.3: Relation of direct solar insolation to slope orientation with respect to the sun. The solar irradiance is perpendicular to the line segment A-B. Because of the angle of incidence of the insolation with respect to the slope angle, the north facing slope receives this insolation along the slope distance $A'_N - B'_N$, while this insolation is received across the distance $A'_S - B'_S$ on the south facing slope. Since the $A'_N - B'_N$ distance is larger than the distance $A'_S - B'_S$, there would be less insolation per unit distance on the north facing slope.

Solar radiation is composed of the two components: *direct* and *diffuse*. Direct shortwave radiation is that which reaches a point without being absorbed or scattered from its line of propagation by the intervening atmosphere. The image of the sun's disk as a sharp distinct object represents that portion of the solar radiation that reaches the viewer directly (Figure 3.4a). Diffuse radiation, in contrast, reaches the observer after first being scattered from its line of propagation. On an overcast day (Figure 3.4b), for example, the sun's disk is not visible and all of the shortwave radiation is diffuse.

Longwave radiation is emitted by the atmosphere and propagates both upward and downward. The total amount of longwave energy emitted is proportional to the fourth power of the temperature of the emitting material (e.g., the ground surface, the atmospheric layer). The magnitude of this radiation reaching the surface depends on the temperature at the height of emission and the amount of absorption between the height of emission and the surface. A larger fraction of the longwave radiation is absorbed when the intervening atmosphere has large amounts of water vapor and carbon dioxide. Clouds with liquid water contents on the order of 2.5 g m^{-3} absorb almost 100% of the longwave radiation within a depth of 12 m into the cloud. Clouds with lower values of liquid water content require greater depths before complete absorption is attained (e.g., a cloud with a water content of 0.05 g m^{-3} requires about 600 m for complete absorption). Clouds which are at least this thick emit longwave radiation from their base corresponding to the temperature of the lowest levels of the cloud.

The magnitude of heat flux by conduction below the surface depends on the *thermal conductivity* and the vertical gradient of temperature in the material beneath the surface. Soils such as dry peat, with its very low thermal conductivity (i.e., 0.06 W $m^{-1}K^{-1}$), permit little heat flux, while concrete has a thermal conductivity almost 100 times as large (i.e., 4.60 W $m^{-1}K^{-1}$) which results in substantial heat flux through this material. Figure 3.5 illustrates the annual cycle of soil temperature beneath a grassy area in Fort Collins. In water, this thermal conductivity of heat is relatively unimportant since, in contrast to land surfaces, solar insolation extends to substantial depths into the water, and water can be mixed vertically.

Vertical mixing (*convection*) occurs in the atmosphere as well as in the water. Also referred to as *turbulence*, this mechanism of heat flux occurs in the atmosphere in two forms. When the surface is substantially warmer than the overlying air, mixing will spontaneously occur in order to redistribute the heat. This process, referred to as *free convection*, occurs when the atmospheric lapse rate of temperature decreases at a rate greater than $-1°C/100$ m ($-1°C/100$ m is called the *adiabatic lapse rate*). In the ocean, the temperature increase with depth which results in free convection is dependent on temperature, salinity, and depth. At the surface with a temperature of 20°C, a salinity of 34.85 parts per thousand, an increase of temperature with depth of greater than about 0.19°C/km will result in free convection.

Mixing can also occur due to the shearing stress of the wind on the surface. As a result of surface friction, the average wind velocity at the surface must be zero unless the surface is moving. Winds above the surface are decelerated when the vertical shear of the wind becomes large enough to result in vertical mixing. This process by which heat (and other atmospheric

Figure 3.4: Photo of sky conditions with direct sunlight (from Pielke, R.A., 2002: *Mesoscale meteorological modeling.* 2nd Edition, Academic Press, San Diego, CA., 676 pp.)

Figure 3.4: Continued. Photo of diffusive sunlight sky conditions (from Pielke, R.A., 2002: *Mesoscale meteorological modeling.* 2nd Edition, Academic Press, San Diego, CA, 676 pp.)

Figure 3.5: Soil temperatures at 0700 MST for Fort Collins, Colorado for October 1, 1991 – September 30, 1992 (courtesy of Nolan Doesken, Research Associate, Colorado Climate Center, Colorado State University, Fort Collins, Colorado).

properties) are mixed as a result of wind shear is called *forced convection*. Free and forced convection are also referred to as *convective* and *mechanical turbulence*, respectively. This convection occurs as either *sensible turbulent heat flux* in which heat is directly transported to or from the surface, or as *latent turbulent heat flux* in which heat is used to evaporate water from the surface. When this mixing does not occur, plumes from power plant stacks, for example, spread very little in the vertical and wind speeds are weak and change little with time (Figure 3.6).

The temperature at the interface of the atmosphere and the surface results from the contributions of heat by radiation, conduction, and convection. The magnitude of these contributions depends on the wind, temperature, and moisture structure in the immediate overlying atmosphere, the intensity of solar insolation, and the physical characteristics of the surface. The temperature which occurs at the interface is of critical importance in determining the habitability of a location.

The water budget at the air-surface interface is also of crucial importance in influencing atmospheric processes. The surface gains water through precipitation (rain and snow) and by direct condensation and deposition (dew and frost). On land, precipitation is often large enough for some of it to percolate into the ground or occurs as runoff into streams, rivers, lakes, and the oceans. Some of the precipitation which remains on the surface such as in puddles or on vegetation immediately evaporates back into the atmosphere.

Liquid water is also converted to water vapor by *evapotranspiration* as vegetation extracts water from within the soil and emits it through stoma on the leaves, and by evaporation from the surface of the soil directly when water from below is diffused upward. Evaporation occurs at the surface of water bodies at a rate which is inversely proportional to the relative humidity immediately above the surface. Evaporation is rapid in dry air but much slower when the lowest levels of the atmosphere are almost saturated. Evaporation from soils is dependent on the rate at which moisture is supplied by capillary suction within the soil, while evapotranspiration is dependent on the water available to plants within the root zone and whether or not the stoma are open on the plant leaf surfaces. Water which evaporates and evapotranspires into the atmosphere is often transported long distances over the earth before it precipitates out.

The input, transport, and removal of water from the atmosphere is part of the *hydrologic cycle* (Figure 3.7). At any one time, only a very small fraction of the earth's water is present within the atmosphere – if it were all condensed out, it would only cover the surface of the earth to an average of about 2.5 cm.

Surface budgets for other constituents of the earth's atmosphere can also be determined. The *nitrogen budget* (Figure 3.8), for example, involves the chemical transformation of diatomic nitrogen (N_2), which makes up 78% of the atmospheric gases, into compounds containing ammonium (NH_4^+), nitrite (NO_2^-), and nitrate (NO_3^-). Referred to as *nitrification*, bacteria such as Rhizobium (which are called *nitrifying bacteria*) that live on the roots of legumes such as peas and clover, perform this conversion. Lightning also produces this nitrogen conversion. These compounds eventually are converted back to N_2 after the plants die or are eaten by *denitrifying* bacteria. These bacteria in their consumption of plants and of

Figure 3.6: Photo of smoke plume from a power plant which rises into a region without substantial vertical mixing (courtesy of Douglas A. Latimer, Latimer and Associates, Inc., Boulder, Colorado).

Figure 3.7: The hydrologic cycle at global scale. [From National Research Council, 1991: *Opportunities in the Hydrologic Sciences*, National Academy Press, Washington, D.C., 348 pp.]

Figure 3.8: The nitrogen cycle (10^{12} grams N/year) (from Jaffe, D.A., 1992: The nitrogen cycle. In: *Global Biogeochemical Cycles*, Academic Press, San Diego, CA, 261-284).

the excrement and corpses of plant-eating animals, convert much of the nitrogen compounds back to N_2. Some of these compounds are also converted to N_2 by a series of chemical processes associated with ultraviolet light from the sun. The combustion of petroleum by motor vehicles also produces oxides of nitrogen which as enhanced the natural concentrations of these compounds. Part of the smog which occurs in urban areas is associated with the substantially higher levels of these compounds of nitrogen in such areas.

The *sulfur budget* (Figure 3.9) is another atmospheric constituent of major importance. Sulfur is input to the atmosphere as a result of weathering from sulfur containing rocks and by intermittent volcanic emissions. Organic forms of sulfur are incorporated into living organisms and represent an important component in the structure and function of proteins. Sulfur also appears in the atmosphere in the form of the gas sulfur dioxide (SO_2) and as part of particulate compounds containing sulfate (SO_4). These forms of sulfur are directly dry deposited, or precipitated out onto the earth's surface. When wetted, these compounds convert to caustic sulfuric acid (H_2SO_4).

During the last century, man has been inputting significant quantities of sulfur into the atmosphere through the combustion of fossil fuels. In and near regions of urbanization and heavy industrial activity, the enhanced deposition and precipitation of sulfur in the form of sulfuric acid, and of nitrogen oxides in the form of nitric acid (HNO_3) resulting from vehicular emissions have been associated with damage to fish populations, forests, and the exteriors of building and statues. Referred to as the *acid rain* problem, sulfuric and nitrogen oxides are precipitated in both rain and snow, as well as deposited to the surface during dry weather where subsequent wetting results in the production of H_2SO_4 and HNO_3.

The *carbon budget* (Figure 3.10) in the atmosphere is of critical importance to climate and to life. Carbon appears in the earth's atmosphere primarily as carbon dioxide (CO_2), which is produced naturally by the respiration of living organisms, during the decay of these organisms, through the weathering of carbon containing rock strata, and from volcanic emissions. Plants utilize CO_2, water, and solar insolation to convert CO_2 to diatomic oxygen (O_2). This process, referred to as *photosynthesis*, results in about a 3% drop in CO_2 concentrations in the northern hemisphere during the growing season (spring to fall). CO_2 is also absorbed by ocean waters with the rate of exchange to the ocean greater for colder water temperatures. Currently CO_2 comprises about 0.03% of the gaseous composition of the atmosphere. In past geologic times, CO_2 levels are thought to have been significantly higher than they are today and to have had a significant effect on the climate and ecology. During the Carboniferous Period of around 300 million years ago, for example, moderately warm and humid climates and high concentrations of CO_2 were associated with extensive lush vegetation. After these plants died and decomposed, they were converted to sedimentary rocks and became the coal deposits currently used for industrial combustion.

In the atmosphere, certain wavelengths of longwave radiation are absorbed and then re-emitted by CO_2. Since the lower levels of the atmosphere are warmer than layers higher up, the absorption of upward propagating electromagnetic radiation, and a re-emission of a portion of it back downward, permits the lower atmosphere to remain warmer than it would

Figure 3.9: Major fluxes of the global biogeochemical sulfur cycle (a) excluding, and (b) including human activity (from Charlson, R.J., T.L. Anderson, and R.E. McDuff, 1992: The sulfur cycle. Chapter 13 in: *Global Biogeochemical Cycles*, Butcher, Charlson, Orians, and Wolfe, Editors, Academic Press, San Diego, CA, 285-300).

Figure 3.10: The global carbon cycle. The boxes are in Pg C, and the fluxes (arrows) are in 10^{15} grams of carbon per year of CO_2 (from Moore, B. III, 1992: Four simple ocean carbon models. In: *Modeling the Earth System*, UCAR/Office for Interdisciplinary Earth Sciences, Boulder, CO, 197-224).

be otherwise. Erroneously referred to as the *greenhouse effect*[1], higher concentrations of CO_2 in the air appear to be associated with a warmer lower troposphere. In recent years, there has been increasing concern that the burning of coal and the resultant release of CO_2 will warm the lower atmosphere to the point that substantial melting of the Greenland and Antarctic icecaps will occur. This would result in an elevated sea level capable of inundating coastal cities.

[1] A greenhouse retains heat primarily because solar radiation enters through the glass, but mixing of air into the greenhouse from above is constrained by the glass (Figure 3.11).

Figure 3.11: Schematic of (a) actual greenhouse, and (b) atmospheric greenhouse (see also Figure 7.2b).

Chapter 4

Vertical Structure of the Atmosphere

The atmosphere is divided into several distinct layers defined as whether the temperature increases or decreases with height (Figure 4.1). The lowest major layer is the *troposphere* in which the temperature generally decreases with height. This layer contains most of the earth's clouds and is the region in which what we refer to as *weather* primarily occurs.

The lower levels of the troposphere are usually strongly influenced by the earth's surface. This sublayer, referred to as the *planetary boundary layer*, is that region of the atmosphere in which the surface influences temperature, moisture, and velocity through the turbulent transfer of mass. As a result of surface friction, winds in the planetary boundary layer are usually weaker than above that height, and tend to blow towards low pressure. For this reason, the planetary boundary layer has also been referred to as an *Ekman layer* after an originator of the relation between winds and height above the surface.

Under clear, sunny skies over land, the planetary boundary layer tends to be relatively deep as a result of the heating of the ground by the sun and resultant generation of convective turbulence. During the summer, the planetary boundary layer can reach heights of 1 km to 1.5 km, for example, in the eastern United States and up to 5 km in the desert southwest of the United States. Under this condition, the temperature decreases at the *dry adiabatic lapse rate* ($-9.8°$ C km^{-1}) throughout most of the boundary layer, with a *superadiabatic lapse rate* of a greater magnitude than this value near the heated surface. In contrast, during clear, calm nights turbulence tends to cease and radiational cooling from the surface results in a temperature that increases with height above the surface. An illustration of typical boundary layer structure is shown in Figure 4.2.

The gradient Richardson number, defined as

$$Ri = \frac{g}{T}\left[\frac{\Delta T}{\Delta z} + 9.8°\text{C km}^{-1}\right] \Big/ \left(\frac{\Delta \vec{V}}{\Delta z}\right)^2 \quad , \tag{4.1}$$

is a commonly used parameter to describe the tendency for the atmosphere to be turbulent. In this expression, $\Delta T/\Delta z$ is the temperature lapse rate, $\Delta \vec{V}/\Delta z$ is the velocity shear in the vertical, and g is the gravitation acceleration. The parameter Ri represents the ratio of the

Figure 4.1: Representative vertical temperature profile for the U.S. Standard Atmosphere [from Wallace, J.M. and P.V. Hobbs, 1977: *Atmospheric science: An introductory survey.* Academic Press, New York, NY, 467 pp].

Figure 4.2: Planetary boundary layer with typical clear sky temperature (T) lapse rates and wind speeds (|V|) with height for daytime (top) and night time (bottom).

generation or suppression of turbulence by buoyant production of energy to the mechanical generation of energy by wind shear.

When a region of the atmosphere has a temperature decrease with height, $\Delta T/\Delta z$, greater in magnitude than the adiabatic lapse rate, turbulence is generated by convective overturning as the warmer, lower-level air rises and mixes with the cooler air aloft. Since the environmental lapse rate is greater in magnitude than the adiabatic lapse rate, an ascending parcel of air remains warmer than the surrounding ambient air even though the parcel undergoes expansional cooling. This overturning occurs in the form of bubbles (eddies) of warmer air (e.g., see Figure 4.3). The larger bubbles often have sufficient buoyant energy to penetrate the top of the boundary layer, entrain air from aloft into the boundary layer, thereby deepening the layer. Since, generally, the air aloft has a lapse rate which is less in magnitude than the adiabatic lapse rate, compressional warming of this entrained air results in a heating of the boundary layer. The top of the daytime boundary layer is referred to as the *mixed-layer inversion.*

The ability of the convective bubbles to penetrate through the boundary layer top depends on the temperature lapse rate aloft. Since the numerator of Ri is usually positive at those heights, the turbulence of penetrative convective bubbles is rapidly eliminated as the parcel quickly becomes cooler than the ambient environment and negatively buoyant with additional ascent. The height that the boundary layer attains on a sunny day, therefore, is strongly influenced by the intensity of surface heating (which, with strong heating, results in large negative values of Ri near the surface) and the temperature lapse rate just above the boundary layer. The less negative the value of $\Delta T/\Delta z$ above the boundary layer, the greater is the suppression of turbulent bubble penetration.

On clear, calm nights, the value of Ri becomes large and positive since radiational cooling results in a temperature increase with height. For this situation, turbulence is suppressed by the strong thermal stratification and over flat terrain, nearly laminar flow can result. The depth of the radiationally cooled layer, referred to as the *nocturnal inversion*, depends on a variety of factors including the moisture content of the air, soil, and vegetation characteristics, and terrain configuration. In a dry, desert environment, for instance, the nocturnal inversion tends to be higher than in a moister environment. The inversion in the more humid environment is lower because more upward propagating longwave radiation is absorbed by the greater number of water molecules and re-emitted back downward, thereby preventing the lower levels from cooling as rapidly. If the air is moist, and sufficient near-surface cooling occurs, water vapor condenses resulting in what is called *radiation fog.*

During wind conditions, the mechanical production of turbulence, expressed by the denominator in Ri, becomes important. Turbulence eddies produced by wind shear tend to be smaller in size than the turbulence bubbles produced by buoyancy. Within a few tens of meters of the surface during wind conditions, the wind speed is very accurately represented as a logarithmic function of height. If the winds are sufficiently strong, even with a positive value of Ri, the generation of turbulence by wind shear can dominate the dissipation of turbulence by the stable temperature stratification. Theoretically, the wind shear has to

Figure 4.3: (a) Enhanced lidar PPI scan at 0846 CDT on 7 June. the bright areas represent enhanced aerosol scattering while the darker regions correspond to clear air between the structures. The x axis represents horizontal distance away from the liar while the y axis represents the distance away from the center shot. The dark sector near the center of the scan is due to missing data caused by the laser beam hitting a nearby utility pole. The elevation angle of this scan was 1.5 deg. (b) Same as (a) except for 0947 CDT. The elevation angle was 3.0 deg. (c) Same as (a) except for 1052 CDT. The elevation angle was 12.0 deg. [From Ferrare, R.A., J.L. Schols, and E.W. Eloranta, 1991: Lidar observations of banded convection during BLX83. *J. Appl. Meteor.*, **30**, 312-326.]

be such that $Ri < 0.25$ for this mechanical turbulence to exist, otherwise laminar flow will result.

Scientists who investigate atmospheric structure and dynamics within the boundary layer are referred to as *boundary layer meteorologists* or *micrometeorologists.*

Above the boundary layer in the troposphere, Ri tends to be greater than 0.25. The exceptions are near jet streams where large velocity shears exist, in and adjacent to cumuliform clouds where buoyant turbulence is being generated as a result of the release of latent heat, and at and just above cloud tops where radiational cooling from the clouds causes a destabilization and generation of buoyancy. Clear air turbulence, often referred to as CAT, is frequently reported when aircraft fly near one of these regions of turbulence generation.

The region above the boundary layer is commonly referred to as the *free atmosphere.* Winds in this volume are not directly retarded by surface friction. Clouds occur most frequently in this portion of the troposphere (exceptions are fog and clouds which impinge or develop over elevated terrain).

There are two basic types of clouds – *cumuliform* and *stratiform* clouds. Both cloud types develop when clear air ascends, cooling adiabatically as it expands until water begins to condense or deposition occurs. This change of state of water occurs because cooler air can hold less water as a gas than warmer air. For example, air at 20°C can contain almost four times as much water vapor as at 0°C before saturation occurs.

Stratiform clouds occur as saturated air is mechanically forced upward, remaining colder than ambient clear air at the same height. In the lower troposphere, such clouds are called *stratus. Advection fog* is stratus whose base is at the earth's surface.[1] In the middle troposphere, stratiform clouds are referred to as *altostratus,* while in the upper troposphere the terms *cirrostratus* and *cirrus* are used. The latter cloud type refers to thin, and often wispy cirrostratus. Precipitating, stratiform clouds that extend through a large fraction of the troposphere are called *nimbostratus.*

Cumuliform clouds occur when saturated air is turbulent. Such clouds, with their bubbly, turreted shapes, permit a visualization of small-scale up and down motions similar to what occurs, but is often visually unobservable, in the turbulent planetary boundary layer. Often such clouds are seen with bases near or at the top of the boundary layer as turbulent eddies generated near the earth's surface reach high enough for condensation to occur.

This type of cloud will occur in the free atmosphere if a parcel of air, upon saturation, is warmer than the surrounding ambient atmosphere. Since the parcel is warmer than its surroundings, it will accelerate upward, creating the saturated turbulent bubble which is the characteristic of a cumuliform cloud. Cumuliform clouds which extend no deeper than the lower troposphere are referred to as *cumulus humulus* when they are randomly distributed, and as *stratocumulus* when they are organized into lines. *Cumulus congestus* clouds extend into the middle troposphere, while the deep precipitating cumuliform clouds that extend throughout the troposphere are called *cumulonimbus.* Cumulonimbus clouds develop from cumulus humulus and cumulus congestus.

The different types of clouds are illustrated in Figure 4.5.

[1] Two different types of fogs are schematically illustrated in Figure 4.4.

Figure 4.4: Schematic of two different types of fogs.

Figure 4.5: (a) A stratus cloud over northern Illinois on 1 December 1974. (b) A stratocumulus cloud over Gogebic in the upper peninsula of Michigan in June of 1972. (c) A group of cumulus clouds over southern Florida at 0930 LST on 15 August 1978. (d) A cumulus congestus complex with layered clouds on its periphery located in southern Arizona at 1615 LST 23 October 1974 (photographed by Ron Holle). From Pielke, R.A. Sr., 2002: *Mesoscale Meteorological Modeling*, 2nd Edition, Academic Press, San Diego, CA, 676 pp.

The top of the troposphere, called the *tropopause*, corresponds to the level at which the general decrease of temperature within the troposphere ceases, and is replaced by an essentially isothermal layer. In the tropics and subtropics, the tropopause is high, often reaching to about 18 km as a result of the vigorous vertical mixing of the atmosphere by thunderstorms. In contrast, in polar regions where such deep atmospheric turbulence is much less frequent, the tropopause is often as low as 8 km. Temperatures at the tropopause height range from as low as $-80°$C in the tropics to $-50°$C in the polar regions.

The *stratosphere* is located above the troposphere and extends up to about 50 km. Above the isothermal layer in the lower stratosphere, temperature increases with height. Temperatures as high as 0°C are observed near the top of the stratosphere. This temperature increase is a result of solar heating as ultraviolet radiation in the wavelength range of 0.200 to 0.242 μm dissociates diatomic oxygen. The resultant attachment of single oxygen atoms to O_2 produces ozone. The observed increase of temperature with height results in strong thermodynamic stability (i.e., large and positive values of Ri) with little turbulence and vertical mixing. The warm temperatures and very dry air result in an almost cloud-free stratosphere. The infrequent clouds that do occur are called *nacreous*, or mother-of-pearl clouds, which appear to be composed of both ice and supercooled water. These clouds form up to heights of 30 km, and are associated with intense vertical motions that originate in the troposphere and propagate upward.

Ozone is produced mainly at tropical and midlatitudes in the stratosphere with a maximum destruction of ozone in the same locations through catalytic cycles of the nitrogen oxides. Ozone is also transported downward, primarily in the vicinity of the polar front, and poleward resulting in maximum vertical content in the chemically inactive polar region.

The top of the stratosphere is capped by the *stratopause*. Above this height, which occurs around levels near 45-50 km and pressures of 1 mb is the layer called the *mesosphere* in which temperatures again decrease with height. Unlike the stratosphere, vertical air currents are not strongly inhibited in this layer. Ice crystal clouds, called *noctilucent clouds* occasionally form in the upper mesosphere.

At a height of around 85 to 90 km, temperature again increases with height. Referred to as the *mesopause*, the layer above this height is called the *thermosphere*. Temperatures in the thermosphere range from around 500 K during quiet sun periods to up to 2000 K when the sun is active. The *thermopause*, defined as the level of transition to a more or less isothermal temperature profile at the top of the thermosphere occurs at heights of around 250 km during quiet sun periods to almost 500 km when the sun becomes active. Above 500 km molecular collisions are infrequent enough that temperature is difficult to define.

The portion of the thermosphere where charged particles, or ions are abundant is called the *ionosphere*. These ions result from the removal of electrons from gases by ultraviolet solar radiation. This layer, extending from about 80 km to 300 km in altitude, is an electrically conducting layer from which radio signals can be reflected. Maximums in ion density occur from 90 to 120 km (referred to as the lower E region) and from 150 km to 300 km (called the F region). The F region has two maxima during daylight called F_1 and F_2, with the ion density of the F_2 region reaching as high as 10^6 electrons cm^{-3}. These regions of high

ion density, and therefore efficiency of radio transmission, are strongly influenced by solar activity and time of day. The higher F_2 region is the most variable in terms of ion density. Shortwave radio transmissions which can reach around the world, take advantage of the ability of layers in the ionosphere to reflect certain wavelengths of electromagnetic radiation.

Above around 500 km, the motion of ions is strongly constrained by the presence of the earth's magnetic field. This region of the earth's atmosphere, called the *magnetosphere*, is compressed by the solar wind on the daylight side of the earth and stretched outward in a long tail on the night side. The colorful auroral displays often seen in polar latitudes are associated with the generation by solar energy outbursts of high energy particles in the magnetosphere which are subsequently injected into the lower ionosphere.

The layer above 500 km is also referred to as the *exosphere*. This is a region in which at least half of the upward moving molecules do not collide with one another, but follow long ballistic trajectories, exiting the atmosphere completely if their escape velocities are high enough. The rate of loss of molecules through the exosphere is critical in determining whether or not the earth, or other planetary body, retains an atmosphere.

The earth's atmosphere is also segmented into a lower layer, called the *homosphere*, in which turbulent mixing dominates molecular diffusion of gases. In this region, which occurs below 100 km or so, atmospheric composition tends to be independent of height. Above 100 km, however, in the layer called the *heterosphere*, the lighter gases are concentrated in the highest layers. Above 1000 km, helium and hydrogen are the dominant species. The relatively heavy gas, diatomic nitrogen (N_2) drops off rapidly with height and only traces remain at 500 km. This decrease in concentration of heavier gases with height is largest during periods of low sun activity when the temperatures in the heterosphere are relatively low. The transition zone at a height of around 100 km between the homosphere and heterosphere is called the *turbopause*.

Tides occur in the atmosphere, with greatest magnitudes in the upper atmosphere, as a result of direct diurnal heating of the air as the earth rotates, and due to sun and moon gravitational effects. In contrast to the ocean, the generation of tides by heating is much more important than the gravitational effect. A tidal period of 12 hours (called the *semi-diurnal solar atmospheric tide*) has the largest amplitude.

Methods to monitor the atmosphere are of two types – *in-situ* measurements and *remote sensing* observations. In-situ measurements require that instrumentation be located at the point of interest. Remote sensors include *passive systems* which receive information naturally emitted from a region in the atmosphere, and *active systems* in which the sensor apparatus emits acoustic or electromagnetic energy and records the characteristics of this energy which is backscattered to the sensor.

Within the planetary boundary layer, in-situ instrumentation includes towers, tethered balloons, and surface data collection platforms. A wide range of meteorological measurements are made from this equipment including temperature, dewpoint temperature, pressure, winds, longwave and shortwave radiative fluxes, and air chemistry. An example of results from in-situ measurements is presented in Figure 4.6. Active remote sensing observations are made using doppler and non-doppler radars, lidars, and acoustic sounders. Radars measure

Figure 4.6: Examples of several types of observational systems. These are types used at Colorado State University in their atmospheric science program (figure adapted from one prepared by S.K. Cox, 1993).

the backscattering of electromagnetic microwave radiation with wavelengths on the order of 3 cm to 10 cm. The non-doppler radars provide estimates of only precipitation intensity, while the doppler radars can also provide estimates of wind speed and direction, with the shorter wavelength radars of this type often able to measure winds even in clear air. Carbon dioxide infrared *lidars* (a type of laser) of a wavelength of 10.6 μm provide estimates of wind structure and turbulence within a few tens of kilometers of the instrument. Acoustic sounders are used primarily to monitor boundary layer depth and structure using echo return characteristics. Passive instrumentation include the pyranometer, which measures direct and diffuse solar radiation, and the pyrheliometer which samples only direct radiation from the sun.

Above the boundary layer, but within the troposphere, the primary standard observation platform is the *radiosonde*. Routinely released twice daily (at 0000 GMT and 1200 GMT) simultaneously around the world using helium balloons, a long period data archive of the status of the atmosphere has been achieved. Meteorological observations from radiosondes are also applied to initialize the numerical weather prediction models used to forecast day-to-day weather. Radiosondes measure temperature, dewpoint temperature, and pressure. The position of the radiosonde is monitored by radar tracking so that wind speed and direction as a function of height are routinely available – for this reason radiosondes are also referred to as *rawinsondes*. The radiosondes are designed to have a rise rate of about 200 m per minute.

Remote sensing systems called *profilers* have been developed to provide almost continuous measurements of wind, and somewhat less accurately, of moisture and temperature throughout the lowest 10 kms of the atmosphere. Winds are estimated by using an upward-looking doppler radar, while temperature and moisture profiles are evaluated by using a vertically pointing radiometer which measures electromagnetic emissions of selected wavelengths from various heights in the troposphere. Used in conjunction with earth-orbiting, satellite-based passive temperature and moisture radiometric soundings and active lidar wind measurements, profilers may make radiosonde soundings obsolete.

Aircraft (Figure 4.7 and 4.8) also provide detailed information concerning the structure of the atmosphere, particularly during meteorological field experiments. Airplanes such as the NOAA P-3, for example, are heavily instrumented, including doppler radar, turbulence sensors, and in-situ measurement devices for cloud water, and cloud ice content and structure. The NOAA P-3 has been used to fly through hurricanes and other types of deep precipitating cloud systems.

Lightning occurrences are currently monitored using ground-based detectors (Figure 4.9). Such systems measure time, location, flash polarity, and stroke count of the lightning strikes. When the observations from systems at different locations are combined, distribution maps of lightning strikes, and hence thunderstorm occurrences can be made.

Above the routine maximum height of the radiosonde data (above about 100 mb, $\sim$17 km), rocketsondes, and rocket-borne grenade and falling sphere experiments have been used to monitor the thermal structure at those heights. Since these measurements are much less frequent than radiosonde observations, however, less is known concerning meteorology above

Figure 4.7: Meteorological monitoring aircraft.

Figure 4.8: Meteorological monitoring aircraft.

Figure 4.9: Lightning data in a portion of central Alaska (adapted by John Yarie from Knowles, Captain John B., 1993, M.S. Thesis: The influence of forest fire induced albedo differences on the generation of mesoscale circulations. Department of Atmospheric Science, Colorado State University, 86 pp).

the tropopause than at lower heights. Satellite radiometric soundings have also been used to provide temperature structure down to 60 km or so, although of less vertical and spatial resolution than the in-situ measurements. Ground-based radar has also been used to measure atmospheric characteristics in the upper atmosphere.

Chapter 5

Horizontal Structure of the Atmosphere

The primary driving force for the horizontal structure of the earth's atmosphere is the amount and distribution of solar radiation which impinges on the planet. The orbit of the earth around the sun is an ellipse with an apogee (closest approach) of 1.47×10^8 km in early January, and a perigee (furthest distance) of 1.52×10^8 km in early July. The time between the *autumnal equinox* and following *vernal equinox* in the northern hemisphere (about September 22 to about March 21) is approximately one week shorter than the remainder of the year as a result of the earth's elliptical orbit, resulting in shorter winters in the northern hemisphere than south of the equator.

The earth rotates every 24 hours around an axis that is tilted at an angle of 23-1/2° with respect to the plane of its orbit. As a result of this tilt, during the summer season in either the northern or southern hemisphere, sunshine is more direct on a flat surface at a given latitude than it is during the winter season. Poleward of 66-1/2° of latitude, the tilt of the earth is such that for at least one complete day (at 66-1/2°) and as long as six months (at 90°), the sun is above the horizon during the summer season and below the horizon during the winter.

As a result of this asymmetric distribution of solar heating, during the winter season, high latitudes become very cold in the troposphere as a result of the long nights. In the summer at high latitudes, the troposphere warms significantly as a result of the long hours of daylight, although due to the oblique angle of the sunlight, the temperatures remain, in general, relatively cool compared to regions in the summer midlatitudes. Equatorward of 30° or so, however, substantial and similar radiational heating from the sun occurs during both winter and summer. The tropical troposphere, therefore, has comparatively little variation in the temperature during the year.

In the troposphere, the demarcation between the cold, polar air and warmer tropical atmosphere is usually well defined by the *polar front* – poleward of the front the air is of polar origin, equatorward it is of tropical origin. The colder, polar air is denser than the tropical air, with over a 30% difference in densities at the surface possible for extreme

wintertime contrasts. During the winter season, the polar front is generally located at lower latitudes and is stronger than in the summer. This frontal boundary is illustrated in Figure 5.1.

The region of greatest solar heating at the surface in the humid tropics results in areas of deep cumulonimbus convection. These cumulonimbus clouds occur because upon condensation the clouds are warmer than the surrounding ambient atmosphere. These clouds transport water substance, sensible heat, and the earth's rotational momentum to the upper portion of the troposphere. The tropopause in these latitudes is around 17 to 18 km as a result of the vigorous mixing of the atmosphere by convection.

Since motion upward into the stratosphere is inhibited by a very stable thermal stratification, the air transported upward by the convection diverges poleward in the upper troposphere. This divergence aloft results in a minimum of pressure at the surface, which is referred to as the *equatorial trough*. As the air is transported poleward it is deflected towards the right in the northern hemisphere and left in the southern hemisphere, since it tends to retain the angular momentum of the near equatorial region. At low latitudes, the angular momentum is large as a result of the earth's rotation.

Upon reaching around 30° of latitude poleward of its region of origin, the air is traveling primarily towards the east. Since motion upward is constrained by the stratosphere, the air must descend. The resultant compressional warming as the air descends creates vast regions of strong stable thermodynamic stability within the troposphere. The sparse precipitation in these regions, a result of stabilization and subsidence, is associated with the great arid regions of the world such as the Sahara, Atacama, Kalahari, and Sonoran deserts. The accumulation of air as a result of the convergence in the upper troposphere causes deep high pressure systems, referred to as *subtropical ridges*, to occur in these regions. Locally, these ridges or high pressure systems are given names such as the Bermuda High, the Azores High, and the North Pacific High.

Upon reaching the lower troposphere, the presence of the earth's surface requires that the air diverge, with some air moving poleward, the remainder equatorward. In either direction the air is deflected to the right in the northern hemisphere and to the left in the southern hemisphere. The tendency of an air parcel to conserve its momentum results in this horizontal deflection. This deflection occurs because according the Newton's first principle, a parcel in motion in a certain direction will retain the same motion unless acted on by an exterior force. With respect to a rotating earth, therefore, a moving parcel which is conserving its momentum (i.e., not acted on by an exterior force) will appear to be deflected with respect to fixed points on the rotating earth. As seen from a fixed point in space, a parcel which is conserving its momentum would be moving in a straight line. This apparent force on air motion is called the *Coriolis effect*. Air tends to rotate clockwise around large-scale low pressure systems, counter-clockwise around large-scale high pressure systems in the northern hemisphere as a result of the Coriolis effect. In the southern hemisphere, the flow direction is reversed. In the equatorward moving flow, this deflection results in northeast winds north of the equator and southeast winds south of that latitude. These low-level winds are called the *trade winds* since in the 17th and 18th centuries, sailing vessels used them to travel to

Figure 5.1: Schematic illustration of the different types of fronts. Fronts always move in the direction in which the more dense (i.e., colder) air mass is moving; $\bar{T}_1 < \bar{T}_3$ where $\bar{T}$ is the average temperature in the lower half of the troposphere.

the Americas. The low-level convergence region of the northeast and southeast trade winds from the two hemispheres is called the *Intertropical Convergence Zone* (ITCZ). The ITCZ corresponds to the equatorial trough and is the mechanism which helps generate the deep thunderstorms in this pressure trough.

The circulation of ascent in the equatorial trough, poleward movement in the upper troposphere, descent in the subtropical ridges, and equatorward movement in the trade winds is a *direct heat engine*, called the *Hadley cell*. It is a persistent circulation feature whereby heating from the latitudes of greatest solar insolation are transported to the latitudes of the subtropical ridges. The geographic location of the Hadley circulation moves north and south with the seasons with the equatorial trough lagging the latitude of greatest surface solar heating by about two months. This lag results because of the thermal inertia of the earth's surface – in which the highest daily temperatures are achieved after the time of greatest insolation since time is required to heat the ocean surface waters and the soil.

Poleward of the subtropical ridges in the lower troposphere, as a result of the tendency for air motions to conserve absolute angular momentum, southwesterlies in the northern hemisphere and northwesterlies in the southern hemisphere tend to occur.

Since warm air is being moved poleward at low levels, however, the wind flow is no longer associated with a direct heat engine. The transport of the heat which originally originated in the equatorial trough is consequentially transported further poleward by large, horizontal low pressure eddies which are called *extratropical cyclones*.

A schematic of the earth's circulation pattern is illustrated in Figure 5.2.

These extratropical cyclones develop on the polar front (which delineates air of polar origin from that of tropical sources) when a sufficiently large horizontal gradient of temperature in the lower troposphere develops across the front. The intensity of this temperature gradient is referred to as the *baroclinicity* of the front. Extratropical cyclones are found to have three stages of development – the *developing stage* in which an undulating wave develops along the front; the *mature stage* in which sinking cold air sweeps equatorward west of the surface low and ascending warm air moves poleward east of the cyclone; and the *occluded stage* in which the warm air has become entrained within and moved above the air of polar origin and cutoff from the source region of the tropical air. Cyclones which develop no further than the developing stage are referred to as *wave cyclones*, while extratropical lows that reach the mature and occluded stages are baroclinically unstable waves. Extratropical storm development is referred to as *cyclogenesis*, and is illustrated in Figure 5.3. Surface pressure falls of greater than about 24 mb day^{-1} which occasionally occur with rapid extratropical cyclone development is referred to as *explosive cyclogenesis*, and is often associated with major winter storms. Theoretical analysis has shown that the occurrence of baroclinically unstable waves is directly proportional to the magnitude of the temperature gradient, with maximum growth for wavelengths of 3000 to 5000 kms.

Cold fronts occur at the leading edge of the equatorward-moving polar air, while *warm fronts* are defined at the equatorward surface position of the polar air as it retreats poleward east of the extratropical cyclone. The equatorward-moving air behind the cold front occurs in pools of cold, dense polar and arctic surface high pressure systems. Arctic highs are

Figure 5.2: Schematic of the general circulation of the earth in the northern hemisphere winter. There is average subsidence in the subtropical ridge and arctic high, and average ascent in the intertropical convergence zone and polar front region. The polar front separates air from upper latitude origin from lower latitude origination. (From Pielke, R.A., M. Garstang, C. Lindsey, and J. Gusdorf, 1987: Use of a synoptic classification scheme to define seasons. *Theor. Appl. Climatol.*, **38**, 57-68.)

Figure 5.3: Schematic illustration of the evolution of an extratropical cyclone from a wave cyclone to a mature cyclone. The scalloped area represents cloud covered areas. Thickness is given by Δz where $\Delta_{z_3} > \Delta_{z_o}$. Pressure is in millibars. Examples of station observations as plotted on U.S. surface map analyses are shown.

defined to distinguish air of an origin even deeper within the high latitudes than are polar highs. When the polar air is neither retreating or advancing, the polar front is called a *stationary front*. In the occluded stage, where the cold air west of the surface low pressure center advances more rapidly eastward around the cyclonic circulation than the cold air east of the center moves poleward, the warm, less dense tropical air is forced aloft. The resultant frontal intersection is called an *occluded front*. Fronts of all types always move in the direction towards which the colder air is moving. The different types of fronts are shown in Figure 5.4.

Clouds and often precipitation occur poleward of the warm and stationary fronts whenever the poleward moving, less dense tropical air north of subtropical ridges reaches the latitude of the polar front, and is forced upward over the colder air near the surface. Such fronts are defined as *active fronts* and rain and snowfall from them form a major part of the precipitation received in mid and high latitudes particularly during the winter.

The position of the polar front slopes toward colder air with height. This occurs because cold air, being more dense, tends to undercut the warmer air of tropical origin. Since the cold air is more dense, pressure decreases more rapidly with height poleward of the polar front than on the warmer side. In the mid and upper troposphere, the resultant large horizontal pressure gradient between the polar and tropical air creates strong westerly winds as air circulates around the region of low pressure in the higher latitudes at these heights. The center of this low pressure region is called the *circumpolar vortex*. The region of strongest winds, which occurs at the juncture of the tropical and polar air masses, is called the *jet stream*. Since the temperature contrast between the tropics and the high latitudes is greatest in the winter, the jet stream is stronger during that season. In addition, since the midlatitudes also become colder during the winter, while tropical temperatures are relatively unchanged, the westerly jet stream tends to move equatorward during the colder season.

The jet stream reaches its greatest velocities at the tropopause. Above that level, lower tropopauses in the polar region than in the tropics result in a reversal of the horizontal temperature gradient in the stratosphere from that found in the troposphere, with relatively warmer temperatures at high latitudes. This causes a weakening of the westerlies with height. At intervals of 20 to 40 months, with a mean of 26 months, for reasons that are not completely understood, a reversal of wind direction occurs at low latitudes, so that easterly flow develops. This feature is called the *quasi-biennial oscillation* (QBO). Actual QBO data is presented in Figure 5.5. A phenomena called *sudden stratospheric warming*, apparently a result of strong downward motion, also occurs in the late winter and spring at high latitudes which can significantly influence the chemical balance of ozone and other reactive gases in the stratosphere.

Preferred geographic locations exist for the development, movement, and decay of extratropical cyclones, and for the presence of centers of the subtropical ridge. In the winter in mid and high latitudes, continents tend to become lower tropospheric high pressure reservoirs of cold air as heat is radiated out to space during the long nights. In contrast, oceans lose heat less rapidly as a result of the large thermal inertia of water, their ability to overturn as the surfaces cool and become negatively buoyant, and the existence of ocean currents

Figure 5.4: Schematic illustration of active and inactive cold, warm, and stationary fronts; where $\bar{T}_1 < \bar{T}_3$. $\bar{T}$ is the average temperature in the lower half of the troposphere.

Figure 5.5: The east-west winds over Singapore at two levels in the stratosphere as a function of time. [Figure courtesy of John Sheaffer, Colorado State University, Department of Atmospheric Science, Fort Collins, Colorado.]

such as the Gulf stream and Kuroshio Currents, which transport heat from lower latitudes poleward. The lower troposphere over the warmer oceanic areas, therefore, tends to be a region of relative low pressure. As a result of this juxtaposition of cold and warm air, east sides of continents and the western fringes of oceans in mid and high latitudes are preferred locations for extratropical storm development. Over the Asian continent, in particular, the cold high pressure system is sufficiently permanent that a persistent offshore flow called the *winter monsoon* occurs.

An inverse type of flow develops in the summer as the continents heat more than adjacent oceanic areas. Continental areas tend to become regions of relative low pressure, while high pressure in the lower troposphere becomes more prevalent offshore. Persistent lower tropospheric onshore flow that develops over large land masses as a result of the heating is referred to as the *summer monsoon.* The leading edge of this monsoon is associated with a trough of low pressure called the *monsoon trough.* Tropical moisture brought onshore by the monsoon often results in copious rainfall. Cherrapunji in India, for instance, recorded over 9 meters of rain in a month (July, 1861) due to the Indian summer monsoon. The lower tropospheric wind flow associated with the summer monsoon in the Indian subcontinent is shown in Figure 5.6.

The subtropical ridge is segmented into surface high pressure cells as a result of the continental effect. In the subtropics, large land masses tend to be relative centers of low pressure as a result of the strong solar heating. Persistent high pressure cells, therefore, such as the Bermuda and Azores Highs occur over the oceans. The oval shape of these high pressure cells cause different thermal structure in the lower troposphere on their eastern and western sides. On the east, subsidence from the Hadley circulation is enhanced as a result of the tendency for air to preserve its angular momentum on the rotating earth. As a result of the enhanced descent in the eastern oceans, land masses adjacent to these areas tend to be deserts such as found in northwest and southwest Africa and along western coastal Mexico. In contrast, despite being under the descending branch of the Hadley cell, western continental fringes of the subtropical oceans have precipitation since the stabilization effect of the subsidence portion of the Hadley cell is minimized by the upward vertical velocity associated with the circular subtropical high pressure cells.

The aridity found along the west coasts of continents in subtropical latitudes is further enhanced by the influence of the equatorward surface flow around the high pressure cells on the ocean currents. This flow exerts a shearing stress on the ocean surface which results in the deflection to the right in the northern hemisphere and to the left in the southern hemisphere of the layer of water above the oceanic thermocline. This deflection is a result of the tendency for the water to conserve its angular momentum and therefore to move westward when displaced toward the equator. Cold, lower-level water from below the thermocline rises to the surface to replace this offshore ocean flow. Called *upwelling* (Figure 5.7), these areas of cold, coastal surface waters result in enhanced atmospheric stability in the lower troposphere and an even further reduction in the likelihood for precipitation, although fogs and low stratus clouds are common. Upwelling regions are also associated with enriched sea

Figure 5.6: Seasonal average winds for 1980-1981 at 150 mb for (a) 1 December to 28 February. For wind arrows, the distance between two vertical lines corresponds to 14 m s^{-1} (from Pielke, R.A., 1990: *The Hurricane*. Routledge Press, London, England, 228 pp).

Figure 5.6: Cont. Seasonal average winds for 1980-1981 at 150 mb for (b) 1 March to 31 May. For wind arrows, the distance between two vertical lines corresponds to 14 m s^{-1} (from Pielke, R.A., 1990: *The Hurricane*. Routledge Press, London, England, 228 pp).

Figure 5.6: Cont. Seasonal average winds for 1980-1981 at 150 mb for (c) 1 June to 31 August. For wind arrows, the distance between two vertical lines corresponds to 14 m s^{-1} (from Pielke, R.A., 1990: *The Hurricane*. Routledge Press, London, England, 228 pp).

Figure 5.6: Cont. Seasonal average winds for 1980-1981 at 150 mb for (d) 1 September to 30 November. For wind arrows, the distance between two vertical lines corresponds to 14 m s^{-1} (from Pielke, R.A., 1990: *The Hurricane*. Routledge Press, London, England, 228 pp).

life as the cold, oxygen and nutrient rich bottom ocean waters are transported up to near the surface.

North-south oriented mountain barriers, and large massifs, such as the Rocky Mountains, Scandanavian Mountains, and Tibetan Plateau also influence the atmospheric flow. By imposing a barrier to the general westerly flow in midlatitudes, air tends to be blocked and transported poleward west of the terrain and equatorward east of the obstacle (see Figure 5.8). Air that is forced up the barrier often is sufficiently moist to produce considerable precipitation on windward mountain slopes, while subsidence on the lee slopes produces more arid conditions. The elevated terrain affects the atmosphere as if it were an anticyclone, with the result that warm air is transported further towards the pole west of the terrain. It is also difficult for cold air in the interior to move westward of the terrain, therefore, relatively mild weather for the latitude exists, for example, along the west coast of North America. East-west mountain barriers, such as the Alps, in contrast, offer little impediment to the general westerly flow, resulting in maritime conditions extending far inland.

A major focus of weather forecasting in the mid and high latitudes is to forecast the movement and development of extratropical cyclones, polar and arctic highs, and the location and intensity of subtropical ridges. Spring and fall frosts, for example, are associated with the equatorward movement of polar highs behind a cold front, while droughts and heat waves in the summer are associated with unusually strong subtropical ridges.

Scientists who investigate the physics associated with atmospheric flow are called *dynamic meteorologists* (also dynamicists). When the investigation procedure involves the application of large computer models of atmospheric structure and dynamics, the scientists are called *numerical modelers*. Scientists and technicians who specifically investigate procedures of weather forecasting are called *synoptic meteorologists*.

Figure 5.7: The "local" upwelling solution. Upwelling at a steady rate is caused by offshore Ekman transport. A coastal jet is generated in the upper layer, this being in the same direction as that of the wind. An undercurrent in the opposite direction is also generated. Directions are for an eastern boundary (from Gill, A.E., 1982: *Atmosphere-ocean dynamics.* Academic Press, Inc., Orlando. Florida, 662 pp.).

Figure 5.8: Isotherms (solid, °C), inversion layers (tops and bases dashed), and stable layers (dash-dot) for a cross section normal to the Appalachians. Location of the traveling synoptic-scale pressure ridge axis is shown by an H. Cold and warm pockets are shown by C and W, respectively. (a) Temperatures at 0000 UTC 13 January 1980, shortly prior to onset of damming. (b) Temperatures at 1200 UTC 13 January 1980, in the early stage of damming. (c) 12-h temperature change ending at 1200 UTC on 13 January 1980. (d) Temperatures at 0000 UTC 14 January 1980, following the onset of onshore warming. (e) 12-h temperature change ending at 0000 UTC on 14 January 1980. [From Forbes, G.S. Forbes, R. A. Anthes, and D.W. Thomson, 1987: Synoptic and mesoscale aspects of an Appalachian ice storm associated with cold-air damming. *Mon. Wea. Rev.*, **115**, 564-591.]

Figure 5.8: Continued

Chapter 6

Cloud Processes

The formation of cloud droplets and cloud ice crystals occurs associated with suspended aerosols of natural and anthropogenic origin which are ubiquitous in the earth's atmosphere. In the absence of such aerosols, relative humidities much greater than 100% with respect to a flat surface of H_2O are required for water vapor to spontaneously condense into liquid water or deposit into ice. The development of clouds in such a fashion, which only occurs in a controlled laboratory environment, is referred to as *homogeneous nucleation*. Air containing water vapor with the relative humidity greater than 100% with respect to a flat surface is referred to as being *supersaturated*. In the atmosphere, aerosols serve as initiation sites for the condensation or deposition of water vapor. By having a discrete size, they reduce the amount of supersaturation required for water vapor to change its phase. Aerosols which are effective as embryonic sites for the conversion of water vapor to liquid water are referred to as *cloud condensation nuclei*. The larger the aerosol and the greater its solubility, the lower will be the supersaturation required for the aerosol to serve as cloud condensation nuclei. Cloud condensation nuclei in the atmosphere become effective at supersaturations of around 0.1% to 1%. The concentration of cloud condensation nuclei in the lower troposphere at a supersaturation of 1% range from around 100 per cm^3 in oceanic air to 500 per cm^3 in a continental atmosphere.

Aerosols which are effective for the conversion of water vapor to ice crystals are referred to as *ice nuclei*. In contrast to cloud condensation nuclei, the most effective ice nuclei are hydrophobic with molecular spacings and a crystallographic structure which is close to that of ice.

While cloud condensation nuclei are always readily available in the atmosphere, ice nuclei are often deficient. As a result, liquid water which is elevated and cooled below 0°C can often remain liquid at subfreezing temperatures because of the absence of effective ice nuclei. Except for ice crystals which are effective at 0°C, all other ice nuclei become effective only at temperatures lower than freezing. Liquid water at temperatures less than 0°C is referred to as *supercooled water*. In the absence of any ice nuclei, freezing of supercooled water droplets of a few micrometers in radius (called *homogeneous ice nucleation*) requires temperatures at or lower than –39°C. While a raindrop will freeze near 0°C, small cloud droplets have too

few molecules to create an ice crystal by random chance until the molecular motion is slowed to its values as the temperature reaches –39°C. When ice nuclei are present, *heterogeneous ice nucleation* can occur at warmer temperatures.

Ice nuclei are of three types – *deposition nuclei, contact nuclei,* and *freezing nuclei.* Deposition nuclei act analogously to condensation nuclei in that water vapor directly deposits as ice crystals on the aerosol. Contact and freezing nuclei, in contrast, are associated with the conversion of supercooled water to ice. Contact nuclei act to convert liquid water to ice by the touching of the contact nuclei aerosol to the supercooled water droplet. Freezing nuclei are absorbed into the liquid water and convert the supercooled water to ice from the inside out.

Examples of cloud condensation nuclei are sodium chloride (NaCl), (salt) particles and ammonium sulfate $[(NH_4)_2SO_4]$, while the clay mineral, kaolinite, represents an example of an ice nuclei. Recently, it has been found that naturally occurring bacterium found in decayed leaf litter can act as an ice nuclei at temperatures of less than about $-4°$ C. Silver iodide, with effective ice nucleating temperatures at less that $-4°$ C, has been used for years to attempt to augment the conversion of supercooled water to ice crystals in regions with a scarcity of natural ice nuclei.

The subsequent evolution of clouds after cloud droplets or ice crystals form depends on which phase of water occurs. A cloud in which only liquid water occurs (even at temperatures less than 0° C) is referred to as a *warm cloud* and precipitation which results from such a cloud is said to be due to *warm cloud processes.* In such a cloud, the growth of liquid water from a cloud droplet to a raindrop occurs first as continued condensational growth due to additional water vapor condensing in a supersaturated atmosphere. This process is effective, however, only until the droplet attains a radius of around 10 μm. Above this size, since the mass of the droplet increases as the cube of its radius, further increases in its radius by condensational growth is very slow. Subsequent growth, therefore, occurs only when the cloud droplets develop at slightly different rates due to spatial variations in the initial aerosol sizes and solubilities, and magnitudes of supersaturation. Cloud droplets with different sizes will fall at different velocities such that cloud droplets of different radii will collide. If the collision is hard enough to overcome the surface tension between the two colliding droplets, coalescence will occur with a new larger single droplet resulting. This process of cloud droplet growth is referred to as *collision-coalescence. Warm cloud* rain results when the droplets attain a sufficient size to fall to the ground. Such a raindrop (perhaps about 1 mm in radius) contains on the order of one million 10 μm cloud droplets. Typical sizes of raindrops resulting from this type of precipitation process range up to several mm in radius with fall velocities of around 3 to 4 m s^{-1}. This type of precipitation is very common from shallow cumulus clouds over tropical oceans where the concentration of cloud condensation nuclei is small such that there is only limited competition for the available water vapor.

A cloud that contains ice crystals is referred to as a *cold cloud*, and precipitation which results from such a cloud is said to be a result of *cold cloud processes.* Traditionally, this process has also been referred to as the Bergeron-Findeisen mechanism. In this type of cloud, ice crystals can grow by deposition directly from water vapor, which is supersaturated

with respect to ice, or as a result of the evaporation of supercooled water and subsequent deposition onto the ice crystal. Since the saturation vapor pressure of liquid water is always greater than or equal to the saturation vapor pressure of ice, ice crystals will grow at the expense of the liquid water. For example, air which is saturated with respect to liquid water is supersaturated with respect to ice by 10% at –10° C and by 21% at –20° C. This results in a rapid conversion of liquid water to ice. This substantial and rapid change of phase permits large ice crystals in a cloud with a large number of supercooled cloud droplets to grow quickly (often in less than 15 minutes) from tiny ice crystals to large precipitation snowflake sizes by depositional growth alone. Clouds which are converted to only ice crystals are referred to as *glaciated clouds*. Ice crystals which grow by deposition have much lower densities than solid ice because of the air pockets which occur within the volume of the crystal. This lower density differentiates snow from ice. Fall velocities of snow range up to about 2 m s^{-1}.

The specific form of the ice crystals that form depend on the temperature and the degree of supersaturation with respect to ice. At –14° C and a relatively large supersaturation with respect to liquid water, for example, dendritic ice crystals form. This type of ice crystal, the one usually used to represent snowflakes in books, has growth at the end of radial arms on one or more planes of the crystal. At –40° C and a supersaturation with respect to liquid water of close to zero, hollow ice columns form. A number of different crystalline shapes of snow are presented in Figure 6.1 and their relation to temperature and humidity is shown in Figure 6.2.

Ice crystals can also grow to precipitation size through *aggregation*, or by *riming*. Aggregation occurs when the arms of the ice crystals interlock resulting in a clump. This collection of intermingled ice crystals can occasionally attain sizes of several centimeters in diameter. Ice crystals can also grow when supercooled water directly freezes onto the crystal. Referred to as riming, the accumulation of dense ice on the crystal increases its fall velocity. When the riming is substantial enough, the crystal form of the snowflake is lost and a more-or-less spherical precipitation-sized particle called *graupel* results. Smaller-sized graupel is generally referred to as *snow grains*. In cumulonimbus clouds in which the graupel is repeatedly wetted and then injected back towards high altitudes as a result of strong updrafts, very large graupel referred to as *hail* results. Hail has been observed on the ground at sizes larger than grapefruits.

The repeated collision of ice crystals and graupel in clouds is associated with the buildup of electrical charge. This electrification is particularly large in cumulonimbus as a result of vigorous vertical mixing and collisions. On the average, positive charges accumulate in the upper regions, negative charges lower down but above the 0°isotherm, and a much smaller pocket of positive charge near the melting level. Electrical discharges (*lightning* – see Figure 6.3) occur when the electric potential gradient becomes large enough between different regions of the cloud (*cloud-to-cloud lightning*) and between the cloud and the generally positively charged ground (*cloud-to-ground lightning*). The passage of the lightning through the air heats it to above 30,000 K causing a large pressure increase, and a resultant powerful shock soundwave which is called *thunder*.

Figure 6.1: Schematic of different types of snow (from Magono, C. and C.W. Lee, 1966: Meteorological classification of natural snow crystals. *J. Fac. Sci.*, Hokkaido University, Japan, 321-335.)

Figure 6.1: Cont. Schematic of different types of snow (from Magono, C. and C.W. Lee, 1966: Meteorological classification of natural snow crystals. *J. Fac. Sci.*, Hokkaido University, Japan, 321-335.)

Figure 6.2: The shape of a crystal is related to environmental conditions in a complicated manner: temperature, supersaturation of the atmosphere with water vapor, and speed of falling all have an effect. Most crystals grow under natural conditions not far removed from the line (color) representing water saturation. The dotted lines to the left of dendrites and needles show how the speed of falling extends the zones in which those elongated forms grow. (After Keller and Hallett, 1982; from Peterson et al., 1988: Manual for snowflake observation, identification, and replication. Department of Atmospheric Science, Colorado State University, Fort Collins, CO, 29 pp.)

Figure 6.3: (a) Lightning photo

Figure 6.3: (b) Lightning photo.

Frozen precipitation which falls to levels much warmer than 0° C reaches the ground as rain. Such cold cloud rain at the ground is usually distinguished from warm cloud rain by its larger size. Melted hailstones, in particular, make a large radius impact when they strike the ground.

Cold cloud rain occasionally refreezes if a layer of subfreezing air exists near the surface. If the freezing occurs in the free atmosphere, the frozen raindrops are referred to as *sleet* or *ice pellets*. When the freezing occurs only at impact on the ground, *freezing rain* results (see Figure 6.4). Heavy accumulations of ice due to freezing rain can result in *ice storms* in which large trees and electrical lines are broken by the weight of the ice.

The study of cloud and precipitation processes in clouds is performed by *cloud physicists*. The presence of cloud condensation and ice nuclei in air parcels are tested using *cloud chambers* in which controlled temperatures and relative humidities are specified. In the actual atmosphere, aircraft fly through clouds and collect droplets and ice on collection plates or photograph their presence in the airstream. Identification of the different sizes of droplets and the various types of ice crystals in the past have been tediously performed subjectively by a researcher, although new computer-image assessment procedures are automating this analysis. At the ground, rainfall impaction molds and snow crystal impressions are made. Hailstones are also collected since an analysis of their structure often helps define the ambient environment in which they formed. Chemical analyses of the cloud droplets, ice crystals, and precipitation is also frequently performed in order to identify natural and manmade pollutants within the different forms of water.

Sunlight which propagates through clouds and precipitation produces fascinating optical images (Figure 6.5). *Rainbows* are produced when the sun's electromagnetic radiation is diffracted into its component colors by water droplets. *Halos* are produced by the refraction and reflection of sunlight or moonlight by ice crystals, while *coronas* are formed when sunlight or moonlight passes through water droplets.

Atmospheric scientists who investigate the physical mechanisms associated with cloud droplet and ice crystal growth are called *cloud physicists*. Researchers who study atmospheric optical effects are referred to as *physical meteorologists*.

Figure 6.4: Schematic of the temperature profile associated with freezing rain and sleet.

Figure 6.5: (a) Rainbow with dramatic background light inside the primary bow (photographed in California by Allen L. Laws). (b) Complete 22-degree halo (photographed in Wisconsin by Robert Greenler). (c) Corona aureole around the moon (photographed in New Zealand by Robert Greenler). From Greenler, R., 1991: *Rainbows, Halos, and Glories.* Cambridge University Press, New York, NY, 195 pp.

Chapter 7

Climatology and Climate Change

There are two definitions of the term *climate*. Climate is defined as the expected weather conditions for specific geographic locations. Such weather conditions have a major impact on the expected vegetation, as illustrated in Figure 7.1. Climate is defined in terms of averages and as standard deviations around the average.

Primary influences on climate include latitude, degree of continentality, character of the surface, and elevation of a location. Latitude directly influences the intensity of sunlight reaching the ground. In the polar regions, for example, little or no solar radiation reaches the surface in mid-winter, while at the equator the annual variation of solar intensity is small.

The degree of continentality determines the extent to which nearby marine areas moderate temperature variations. Terrestrial areas heat and cool relatively rapidly because of the low thermal conductivity of ground surfaces. In contrast, water bodies have a much larger thermal inertia as a result of the ability for sunlight to penetrate to significant depths and of the capability for water to vertically mix. Consequently, diurnal and annual temperature variations over marine areas tend to be much smaller than over continental sites at the same latitude. Observing sites over land, but near water bodies tend to have climates which are moderated by the marine influence, particularly when the average wind flow is from the water towards the land. Areas with a large continentality tend to be drier than marine areas since such regions are removed from the oceanic source of water vapor to the atmosphere.

The character of the surface also directly influences local climate. Ground which is heavily vegetated tends to have smaller temperature variations than bare ground (e.g., see Figure 7.2). Ground without vegetation converts a relatively large fraction of solar radiation into sensible heating of the air. In contrast, solar radiation onto vegetation also produces evapotranspiration which reduces the magnitude of sensible heating as illustrated in Figure 7.2a and b. At night, bare soil radiates heat to space effectively thereby producing substantial cooling, whereas vegetation helps insulate the ground to this heat loss. Snow-covered ground produces a cooler climate than would otherwise occur as a result of its greater reflection of incident sunlight. Evapotranspiration from vegetation moistens the atmosphere making precipitation more likely.

Figure 7.1: Chart that differentiates the vegetation of dry land areas of the world into 100 closely equivalent formations separated by temperature, precipitation, and evaporation lines of equal value (from Holdridge, L.R., 1947: Determination of world plant formations from simple climatic data. *Science*, **105**, 367-368).

Figure 7.2: (a) Schematic illustration of the surface moisture budget over bare soil and vegetated land. The roughness of the surface (and for the vegetation, its displacement height) will influence the magnitude of the moisture flux. Dew and frost formation and removal will also influence the moisture budget (from Pielke and Avissar, 1990: Influence of landscape structure on local and regional climate. *Landscape Ecology*, **4**, 133-155).

Figure 7.2: Cont. (b) Schematic illustration of the surface heat budget over bare soil and vegetated land. The roughness of the surface (and for the vegetation, its displacement height) will influence the magnitude of the heat flux. Dew and frost formation and removal will also influence the heat budget (from Pielke and Avissar, 1990: Influence of landscape structure on local and regional climate. *Landscape Ecology*, **4**, 133-155).

Elevation directly influences climate, and therefore vegetation, since temperature normally decreases with height in the troposphere. Elevated areas, therefore, tend to have cooler temperatures than lower sites at the same latitude as well as more mosaic and cooler vegetation types (see Figure 7.3). In addition, solar intensity during daylight and longwave radiative loss at night to space tend to be larger at higher altitudes since the overlying atmosphere is thinner. This often results in larger diurnal variations in temperature at higher elevations than occurs closer to sea level.

The climatic distribution of precipitation can be related to the major general circulation features of the earth. Air ascends on the average in the Intertropical Convergence Zone and along the polar front (see Chapter 5). The Intertropical Convergence Zone, which separates air of northern and southern hemispheric origin, is associated with deep thunderstorms, while migratory extratropical cyclones propagate along the polar front producing large-scale organized areas of precipitation. Locations in proximity to these major weather features throughout the year tend to have substantial precipitation evenly distributed through the seasons. Western Europe and the northeast United States represent examples of regions near the polar front while the Amazon basin is one location which is usually in close proximity to the Intertropical Convergence Zone.

In contrast, descending motion (subsidence) is associated with the subtropical ridge and the circumpolar arctic high pressure region. A tendency toward little precipitation exists in those areas which are dominated by these weather features. Such arid climatic regions as the Sahara, Kalahari, Atacama, and Sonoran deserts directly result from the persistence of subtropical ridges over these areas throughout the year. Regions which are influenced by the subtropical ridge only during the summer, such as southern California, southwest Australia and the Mediterranean region, but are often in the vicinity of the polar front during the winter have a dry summer, wet winter climate pattern. The Antarctic continent is very dry because of its location relative to the subsidence of the circumpolar Antarctic high pressure region.

Climatologists have designed typing definitions for climate (Figure 7.4). These are based on temperature and precipitation patterns plus locations of mountains and ice caps. The University of Wisconsin geographer G.T. Trewartha defines the major climatic groups as tropical humid, dry, subtropical, temperate, boreal, polar, and highland. The current global distribution vegetation biomass, as related to these climates is presented in Figure 7.5a, while the vegetation distribution in the 48 states of the United States is shown in Figure 7.5b. .

Agricultural and other activities of man have adjusted to the current climatic configuration of the earth. Climatic conditions, however, change with time, for example, from the apparent humid warm global conditions 325 million years ago during the Carboniferous Period to the widespread continental glaciation of the Pleistocene Epoch of 20 thousand years before the present. The periodic occurrence of extensive glaciation separated by long periods of a warm global climate is a recurrent characteristic of the earth. The causes of these climatic changes have been attributed to a variety of mechanisms, including enhanced volcanic emissions which have been associated with shielding of the sun and a resultant cooling at

Figure 7.3: Vegetation chart for the Santa Catalina Mountains, southeastern Arizona. The pattern above 9000 feet is for the nearby Pinaleno Mountains. 400 vegetation samples were plotted on the chart by their positions in relation to the elevation gradient on the left, and the topographic moisture gradient on the bottom. Boundary lines were drawn to connect the mean positions at which one community-type, as these had been defined in this study, gave way to another. Dominant species are indicated in the parts of the pattern where they are most important (from Whittaker, R.H., 1975: *Communities and Ecosystems.* MacMillan Publishing Co., Inc., New York, N.Y., 385 pp.).

Figure 7.4: Groups and types of climate (from Trewartha, G.T., and L.H. Horn, 1980: *An Introduction to Climate*, Fifth Edition, McGraw-Hill Book Company, New York, N.Y., 416 pp.).

Figure 7.5: (a) Global vegetation index (from *EOS*, **70**, No. 41, October 10, 1989).

Figure 7.5: (b) Map of 1990 vegetation greenness classes.

the surface. Periodic reductions in solar output have been suggested as also causing global cooling.

Over long time periods, the movement of continents over the surface of the earth has caused different global climatic patterns. Large continental areas in the polar regions have been associated with particularly cold temperatures in high latitudes, as contrasted with the situation of a large oceanic area at those latitudes in which the marine environment mitigates large temperature variations. This movement of the continents, called *continental drift*, has been used to explain geologic evidence of tropical fauna in Antarctica and of glaciers at low altitudes in Africa.

Variations over time of the *obliquity* of the earth's axis with respect to its orbital plane, the *eccentricity* of the orbit, and the *precession* of the axis directly influence the distribution of solar radiation over the earth, and therefore the climate (Figure 7.6). The obliquity of the earth varies between $24°36'$ and $21°39'$ with a period of around 40,000 years from its current value of 23-1/2°. The eccentricity ranges between about 0 to 0.05 over a time period of about 92,000 years from its current value of 0.016, while the precession of the axis requires from 16,000 to 26,000 years to turn a complete circle. The most pronounced difference between winter and summer seasons occur with a large obliquity and a large eccentricity such that winter occurs when the earth is farthest from the sun. Enhanced glaciation is felt to occur when the earth is farther from the sun during the summer and the obliquity is small such that the difference in incident solar radiation between winter and summer is minimized resulting in less glacier melt during the warm season.

Over the last couple of hundred years, man has been directly influencing global and local climate. The construction of urban areas has created different ground characteristics resulting in *urban heat islands* (Figure 7.7) in which cities are warmer, particularly at night, than the surrounding countryside. The input of carbon dioxide (CO_2) through industrial activities has been suggested to be associated with warming near the surface as additional longwave radiation emitted at the surface is absorbed by the CO_2 and re-radiated back towards the surface. This absorption and re-emission of radiation by CO_2 is erroneously referred to as the *greenhouse effect*[1]. In the period 1958-1975, for example, the average CO_2 in the atmosphere increased at a rate of about 1.7 parts per million per year. By 2100, there is concern that the enhanced CO_2 levels resulting from industrial activity will increase the average global temperatures by up to 5°C with the greatest impact at high altitudes.

Aerosols are also emitted by industrial and other human activities. Climatologists have suggested that anthropogenic-generated aerosols could alter the earth's radiation budget, perhaps even counteracting the warming effect of CO_2. The ability of additional aerosols to heat or to cool the earth's atmosphere depends on their vertical and horizontal distribution, and their concentration, size, and chemistry.

The addition of anthropogenic aerosols to the atmosphere which serve as additional cloud condensation and ice nuclei could also alter the percentage of the earth covered by clouds. Increased concentrations of cloud condensation nuclei, for example, would reduce the average cloud droplet size within the cloud making them more colloidally stable, and therefore less

[1] A greenhouse primarily heats because vertical air currents are constrained by plate glass.

Figure 7.6: An illustration of the angles used in Eq. 11-40 in Pielke, 1984. [From Pielke, R.A., 1984: *Mesoscale meteorological modeling.* Academic Press, New York, N.Y., 612 pp.]

Figure 7.7: The predicted winds at 1 km at 1100 LST on 18 July 1975 over St. Louis, Missouri. The urban land use areas are located within the stippled area. The wind arrows are drawn to a scale of 8 m s^{-1} per grid interval, and the isotachs are contoured at 1 m s^{-1} intervals (from Hjelmfelt, M., 1980: Numerical simulation of the effects of St. Louis on boundary layer airflow and convection. Ph.D. Dissertation, University of Chicago, Chicago, Illinois.).

likely to precipitate. Such clouds are likely to persist longer, resulting in enhanced reflection of sunlight during the daylight (i.e., a cooling effect), but a reduction of longwave radiational cooling at night, if the clouds are in the low to middle troposphere. The net effect on global climate is not clear.

Recently, the ejection of aerosols from a volcanic eruption (and sulphur dioxide gases which convert to sulfate) into the upper troposphere and stratosphere has apparently cooled the global temperature (Figure 7.8).

Scientists who investigate the dynamics and observations of climate are called *climatologists*. Researchers who concentrate on ancient climate patterns are referred to as *paleoclimatologists*.

Figure 7.8: Global temperature anomalies as derived from satellite data (from http://www.ghcc.msfc.nasa.gov/temperature/).

Chapter 8

The Atmospheres of Other Planets

There are nine planets and over 44 moons in the solar system Of these, the planets Venus, Earth, Mars, Jupiter, Saturn, Uranus, and Neptune have significant atmospheres (Table 8.1). Pluto may have an appreciable atmosphere, but perhaps only when its highly elliptic orbit is closest to the sun. Of the moons, only Titan of Saturn is known to have a thick atmosphere. Much of what is known of these planets and moons has resulted from the Pioneer, Viking, Mariner, Voyager, and Venera rocket missions. Astronomical bodies retain an atmosphere when their escape velocity is significantly larger than the average molecular velocity of the gases present in the atmosphere.

The atmosphere of Venus is almost 98% carbon dioxide, with surface temperatures around 750 K. Clouds on Venus are made of sulfuric acid (H_2SO_4) rather than predominantly water as they are on earth. Venusian clouds move in a westerly circulation of about 100 m s^{-1}. Venus itself rotates only once every 243 days. Surface pressures on Venus are around 90,000 mb (the earth, in contrast, has a sea level pressure of around 1,000 mb).

Mars, in contrast, has only a thin atmosphere composed of about 85% diatomic nitrogen with most of the remainder in the form of carbon dioxide. Traces of water vapor occur. Surface pressures are around 6 mb. Both water and carbon dioxide clouds are observed on Mars. Mars has well defined seasons with surface air temperatures estimated to range from below 148 K at the south pole during the winter to above 275 K during summer days in the mid latitudes. Cyclonic storms and clouds associated with the boundary between cold polar cap air and warmer mid latitude air have been observed on Mars, as well as periodic regional or global dust storms. The rotation rate of Mars is close to the rotation rate of earth. Evidence of river channels on Mars indicate that liquid water was present and atmospheric air density were much higher in the prehistoric past than they are now.

Along with the earth, Mars and Venus have atmospheres which are primarily formed as a result of volcanic gas emissions, although the evolution of these gases for each planet has been very different. On Venus, for example, its closer proximity to the sun and resultant higher temperatures may have resulted in the loss of most of its water as a result of the dissociation of H_2O into hydrogen and oxygen. The light gas hydrogen was lost to space, and the oxygen oxidized into compounds. Carbon dioxide produced by volcanic emissions accumulated to

Table 8.1: Table

high concentrations on Venus, in contrast to the earth where much of this gas became part of the crustal materials. On Mars, temperatures are currently so low that most of the water vapor emitted by volcanos has apparently been deposited as ice (i.e., *permafrost*) within the crustal soils. The occurrence of substantial oxygen in the earth's atmosphere is a result of photosynthesis by plants. The development of earth's habitable atmosphere as contrasted with the torrid climate of Venus appears to be directly related to the distance of the earth from the sun. Current analysis suggests that the earth's atmosphere would have evolved to the form found on Venus if the planet had been only 5% closer during the evolution of the atmosphere.

The remainder of the planets with atmospheres appear to have retained the primordial atmospheres associated with their formation. The air on Jupiter and Saturn, for example, are constituted of almost 100% diatomic hydrogen (H_2) and helium (He) with small contributions of methane (CH_4) and other chemical compounds. These Jovian planets, in fact, have an atmosphere not unlike the sun and would be stars if their densities and mass were larger. Much less is known regarding the atmospheres of the somewhat smaller Jovian planets Uranus and Neptune, although both are felt to be similar to that of Saturn and Jupiter.

Colorful cloud bands and areas located at different altitudes and latitudes circulate at speeds up to several hundreds of meters per second relative to each other on Jupiter and Saturn. The large velocity shears associated with this motion creates turbulent eddies including Jupiter's Great Red Spot. The bright zones on these planets correspond to the tops of high, upwelling clouds in the cold, upper atmosphere, while the more colorful bands are lower and warmer. An explanation for the colorful clouds is uncertain but may be associated with the occurrence of sulfur and phosphorus compounds. Both aurora and intense lightning have been observed on these planets.

Chapter 9

Practical Applications

The prediction of the future distribution of winds, temperature, water content, and pressure over the globe within the troposphere is called *weather forecasting*. A necessary condition to perform such predictions is an adequate characterization of the current pattern of these meteorological variables. Referred to as *meteorological analyses*, twice daily rawinsonde balloon ascents at 00 GMT and 12 GMT are made around the world (Figure 9.1, top) in order to prepare global analyses of temperature, moisture, and winds. These analyses are routinely prepared for the surface from the data sites shown in Figure 9.1 (bottom), and for the standard pressure levels of 850 mb, 700 mb, 500 mb, 300 mb, and 200 mb. Weather information is shared worldwide via the Global Telecommunications System (GTS).

The tools used to predict the future weather include *numerical weather prediction models* (Table 9.1). Using mathematical representations of the physical conservation laws of motion, heat, mass, and water substance in the form of a set of nonlinear, partial differential equations, the relations are approximated for solution on a three-dimensional grid mesh and integrated forward in time. The grid mesh corresponds to the domain of interest, which can represent the entire earth (such a model is referred to as a *global model*) or to local regions such as North America (with a model called a *limited area model*). Exact solutions of these nonlinear equations are not possible, in general, which necessitates their evaluation on a grid. An example of a numerical model prediction for the great blizzard of 1993 in the eastern United States is shown in Figure 9.2. Large, fast supercomputers of the United States National Meteorological Center and the British Meteorological Office, and the CRAY computers of the National Center for Atmospheric Research (NCAR) and the European Centre for Medium Range Forecasting (ECMWF) are required to perform the vast number of calculations associated with the integration of the models forward in time. The CRAY XM-P/48 installed at ECMWF in early 1986 has four central processors and 8 million words of memory.

Forecast skill in predicting pressure fields and temperature anomalies, and to a lesser extent precipitation using models of the atmosphere integrated on these large computers, appears to be possible out to at least five to seven days in the future. Public forecasts of

Figure 9.1: Surface and rawinsonde locations.

Figure 9.2: An example of a numerical model prediction for the great blizzard of 1993 in the eastern United States.

Figure 9.2: Continued.

Figure 9.2: Continued.

Figure 9.2: Continued.

Figure 9.2: Continued.

Table 9.1: List of operational United States weather forecast models.

weather beyond 12 hours are almost exclusively based on the predictions and statistically derived products of these models.

For time periods less than 12 hours, radar, satellite, and surface observations are used extensively to characterize details of local weather and its short term extrapolation into the future. Referred to as *nowcasting*, these sources of information are also used to fill in spatial variations in weather which are both unobservable and incapable of being predicted in the large-scale weather forecasting models, with their horizontal grid mesh distances of 80 km or larger. The monitoring of hurricane track and intensity, and of squall line evolution are examples in which high resolution observation platforms are used to monitor the systems. Recently, numerical prediction models with much smaller grid meshes (on the order of 1 km to 20 km) have been applied over several hundred kilometer by several hundred kilometer areas to give predictions of weather out to 12 to 18 hours. This scale of atmospheric motion is defined as the *mesoscale*, as contrasted with the global and continental domain simulations which are referred to as *synoptic scale*. Atmospheric scientists who investigate these smaller scale weather systems are called *mesoscale meteorologists*.

Along with predicting weather, man is seeking to deliberately alter atmospheric conditions. Called *weather modification*, most past and current efforts involve attempts to augment precipitation, suppress hail and fog, and weaken hurricanes.

Precipitation increases have been sought by both *static* and *dynamic cloud seeding*, as illustrated in Figure 9.3. One technique of static cloud modification involves the introduction of modest amounts of silver iodide or dry ice, usually from aircraft or surface-based rockets, into subfreezing levels of a liquid water cloud in which natural ice nuclei are deficient. Silver iodide crystals, as a result of its close correspondence to the crystal lattice structure of ice, provides artificial ice nuclei, while dry ice directly freezes the liquid water. Since snow crystals can grow rapidly in such a subfreezing liquid water environment, precipitation results. This mechanism of cloud seeding is used often in stratiform clouds upwind of mountainous areas in order to increase snowpack. It is also used to dissipate subfreezing fog at airports through the conversion of the fog droplets to snow crystals which precipitate to the ground.

Dynamic cloud seeding involves the massive injection of silver iodide into a subfreezing layer of a liquid water, growing cumulus cloud. The rapid conversion of the supercooled water to ice, and associated release of the latent heat of fusion, causes enhanced buoyancy and growth of the cumulus cloud into a larger system than it otherwise would be. Greater precipitation is generally associated with deeper cumulus clouds. In addition, by judiciously seeding adjacent cumulus clouds, it may be possible to promote their merger into large, organized cumulonimbus systems.

In hurricanes (Figure 9.4), dynamic cloud seeding outside of the circle of intense, deep cumulonimbus convection surrounding the eye, called the *eye wall*, has been applied in areas of cumulus cloud convection which reach to subfreezing heights and contain liquid water. The hypothesis is that seeding-enhanced cumulonimbus activity at a greater radius will expand the radius of maximum winds, and therefore by conservation of angular momentum, result in a reduction in the wind speed in a newly created greater radius eye wall. The validity of this seeding hypothesis, however, has not yet been firmly established.

Figure 9.3: Schematic of weather modification.

Figure 9.4: Satellite image of Hurricane Andrew at landfall in south Florida on 24 August 1992 (courtesy of Ray Zehr).

The injection of large quantities of silver iodide into potential hailstorms has also been pursued. The hypothesis is that a larger number of ice crystals from which hailstorms develop will result in smaller, more numerous hail as the competition for the available water among the ice particles is greater. Since the hail is smaller it is more likely to melt before reaching the surface and doing damage to crops.

Man is also inadvertently modifying weather and climate. Alterations in ground surface characteristics by urbanization, agriculture, clear-cutting, etc., have altered the heat and moisture budget at the surface. Clearing of the forests in the Amazon, for example, is thought to be causing an increase in the carbon dioxide content of the atmosphere as a result of the loss of this photosynthetic biomass. The burning of fossil fuels also releases carbon dioxide. Carbon dioxide is an effective absorber and emitter of longwave radiation emitted from the earth so that higher levels of CO_2 are thought to cause global warming, possibly to the extent of melting substantial portions of the Greenland and Antarctic icecaps. The burning of fossil fuels and other industrial activity, however, also releases vast quantities of airborne particulates. As a result of tropospheric wind circulation and cumulus cloud venting, and the continuous emission of these air pollutants, more solar radiation may be reflected back into space than would otherwise occur, resulting in a tendency for global cooling. This is particularly true if the material reaches into the upper troposphere and stratosphere where its residence time would be long.

Cooling associated with enhanced turbidity from industrial particulates within the earth's atmosphere could balance the warming which is suggested to result from enhanced CO_2 concentrations within the atmosphere. Unfortunately, both effects are expected to become much larger during the next century as the underdeveloped countries industrialize. Should either effect become dominant over the other, a rapid deterioration of climate from what we currently have could result.

Selected Additional Reading

Evolution of the Atmosphere

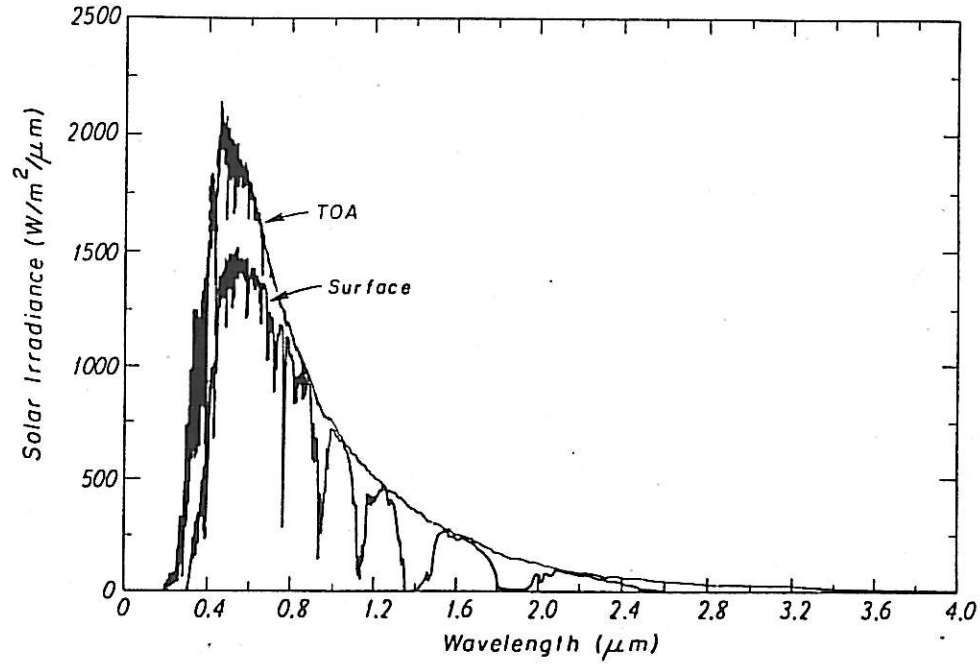

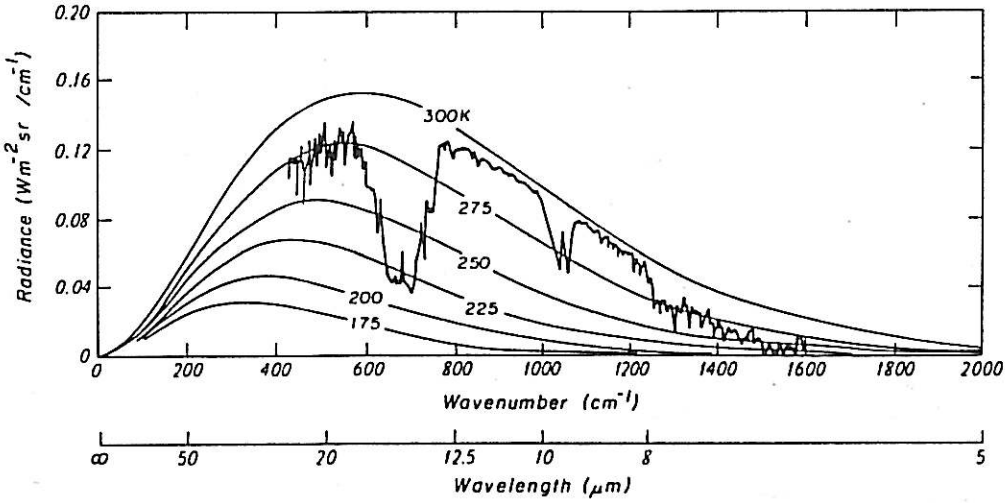

Figure 3.1: (a) Solar irradiance at the top of the atmosphere (TOA) and at the surface for a clear atmosphere as a function of wavelength. The sun has an elevation of 30° above the horizon (from Kneizys et al., 1988 as reproduced by Liou, K.N., 1992: Radiation and cloud processes in the atmosphere. Oxford Monographs on Geology and Geophysics No. 20, 487 pp.) (b) Earth's radiation as observed by an earth-orbiting satellite (from Kunde et al., 1974 as reproduced by Liou, K.N., 1992).

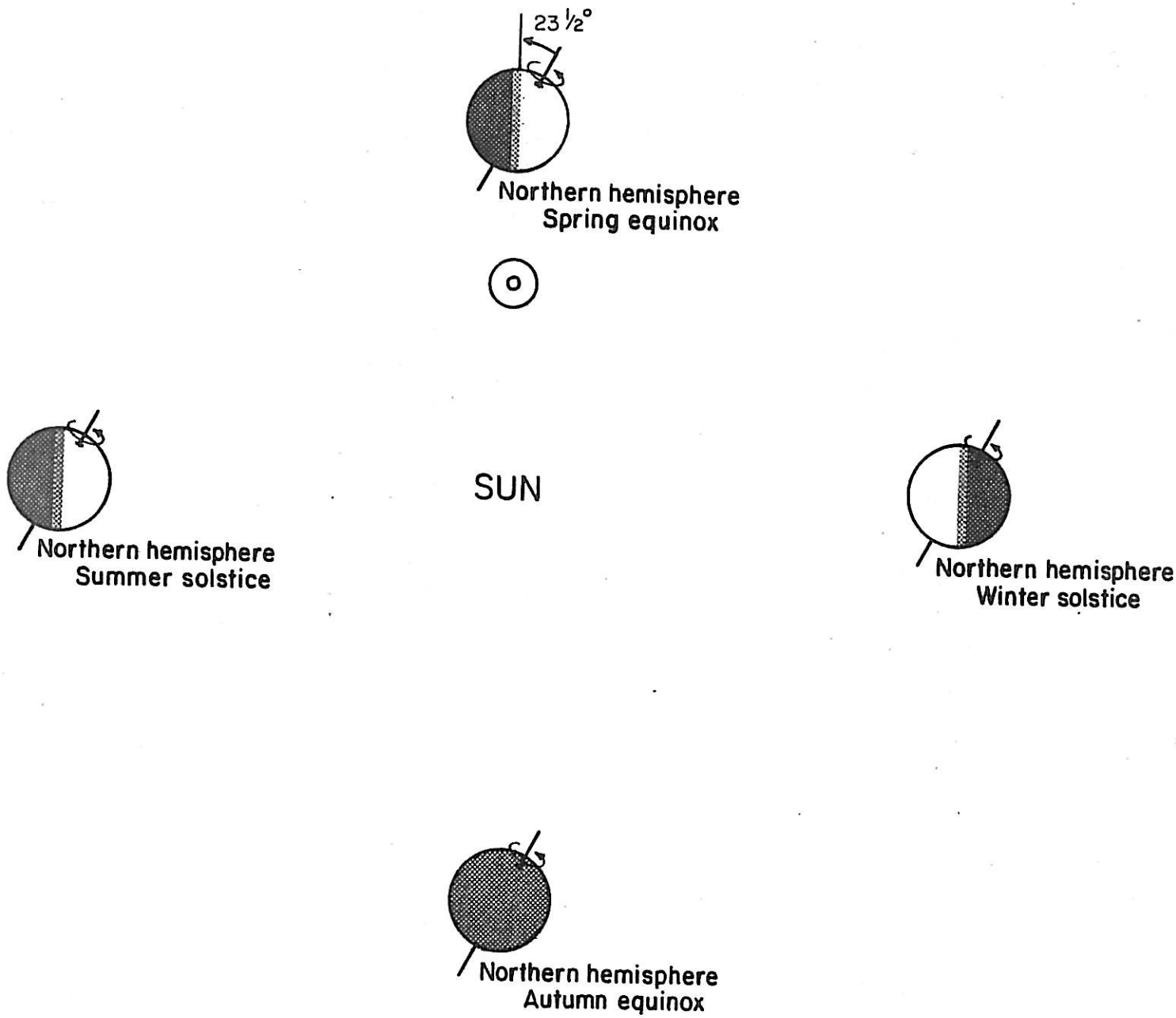

Figure 3.2: A schematic illustration of the orbit of the earth around the sun to illustrate the annual progression of seasons.

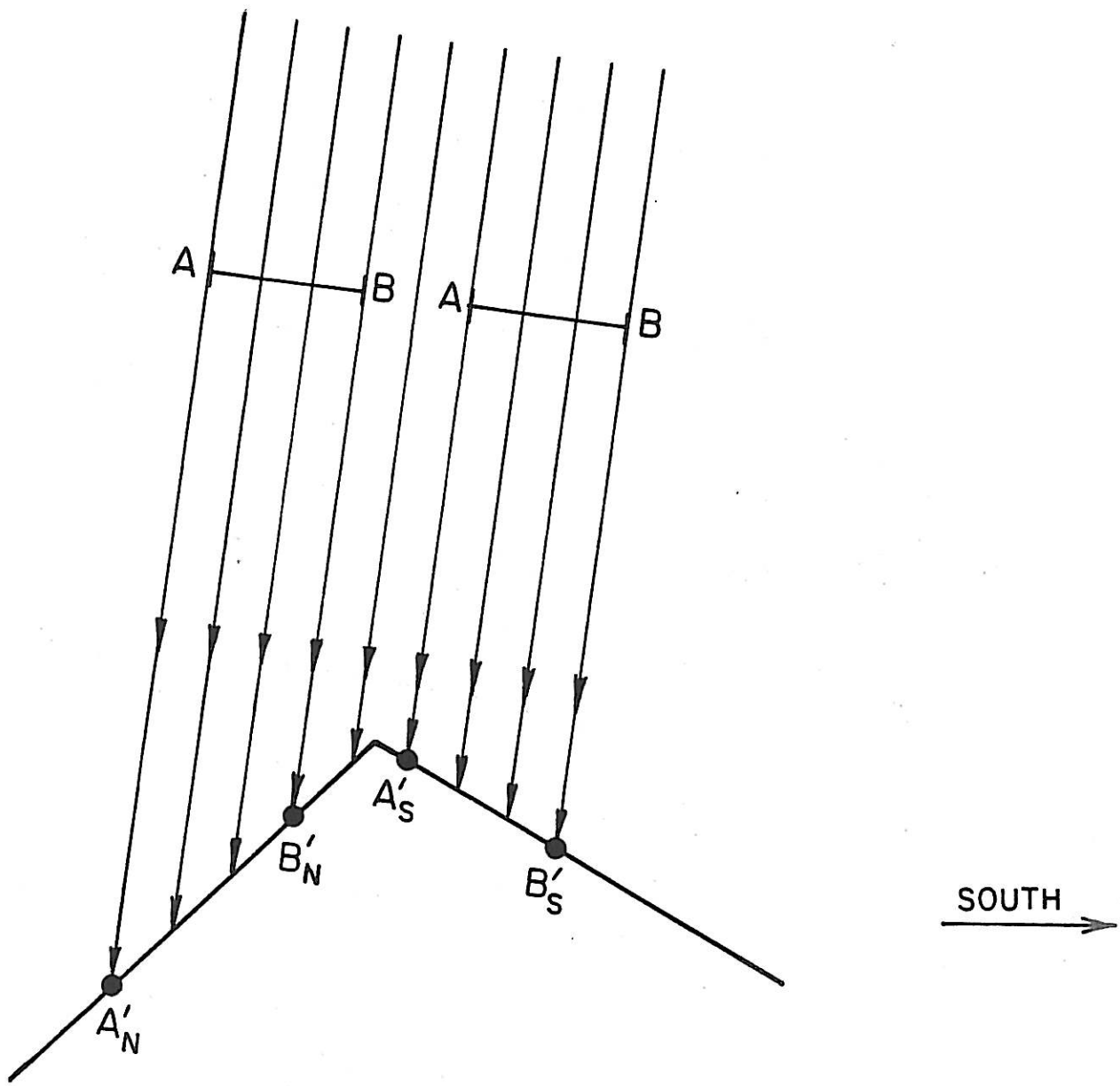

Figure 3.3: Relation of direct solar insolation to slope orientation with respect to the sun. The solar irradiance is perpendicular to the line segment A-B. Because of the angle of incidence of the insolation with respect to the slope angle, the north facing slope receives this insolation along the slope distance $A'_N - B'_N$, while this insolation is received across the distance $A'_S - B'_S$ on the south facing slope. Since the $A'_N - B'_N$ distance is larger than the distance $A'_S - B'_S$, there would be less insolation per unit distance on the north facing slope.

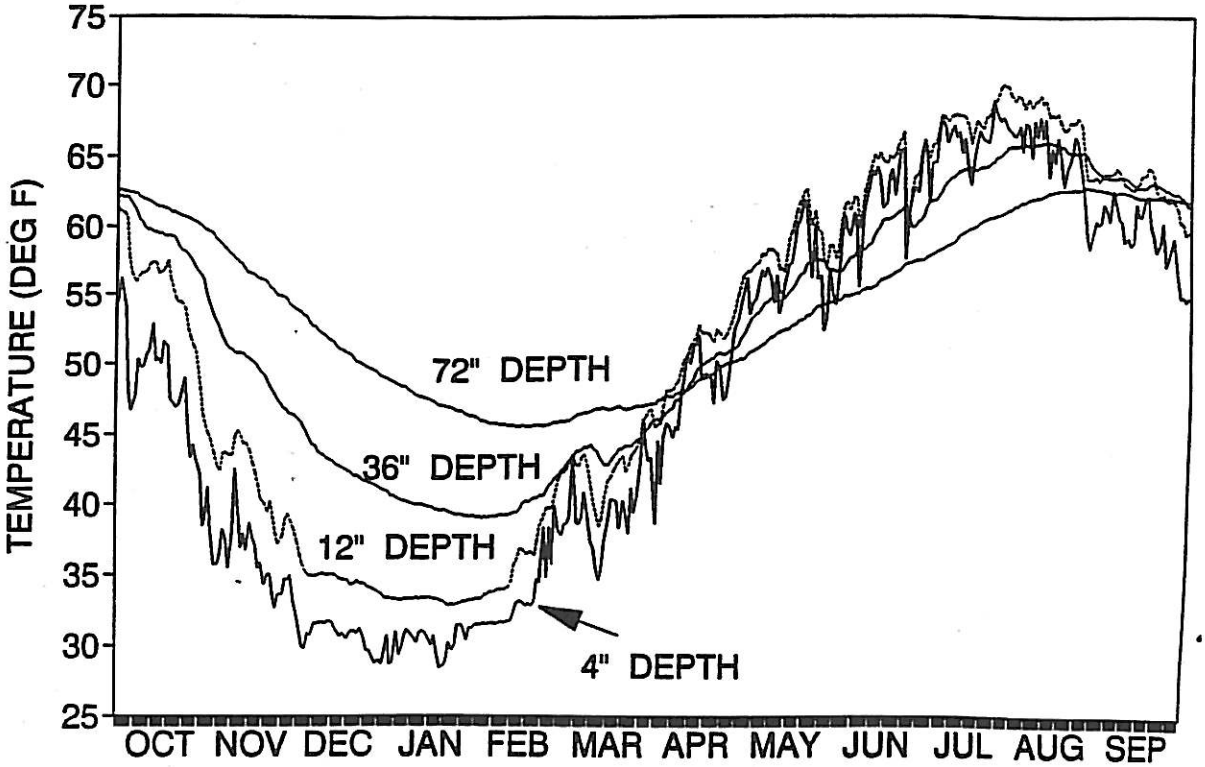

Figure 3.5: Soil temperatures at 0700 MST for Fort Collins, Colorado for October 1, 1991 – September 30, 1992 (courtesy of Nolan Doesken, Assistant State Climatologist, Colorado Climate Center, Colorado State University, Fort Collins, Colorado).

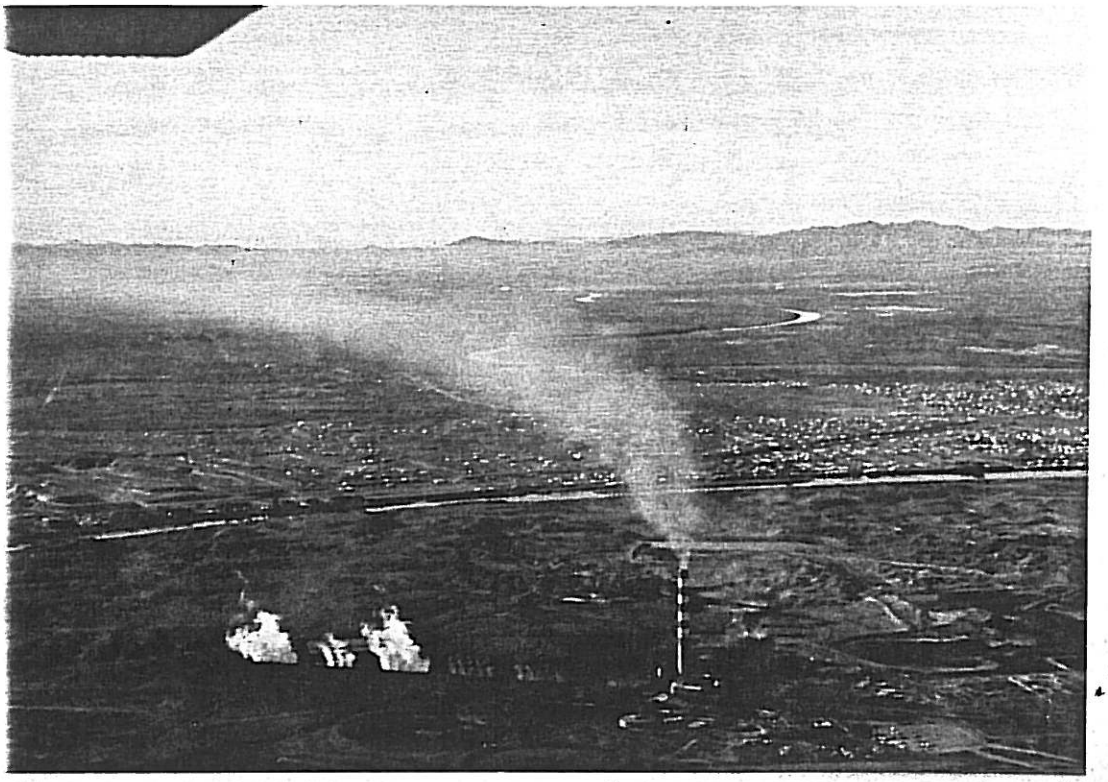

Figure 3.6: Photo of smoke plume from a power plant which rises into a region without substantial vertical mixing (courtesy of Douglas A. Latimer, Latimer and Associates, Inc., Boulder, Colorado).

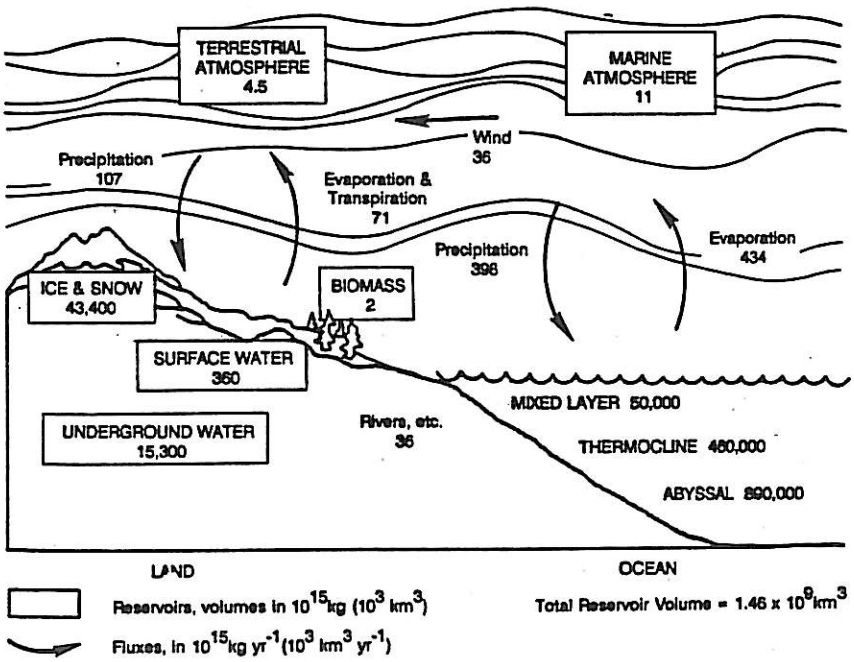

Figure 3.7: The hydrologic cycle at global scale. [From National Research Council, 1991: *Opportunities in the Hydrologic Sciences*, National Academy Press, Washington, D.C., 348 pp.]

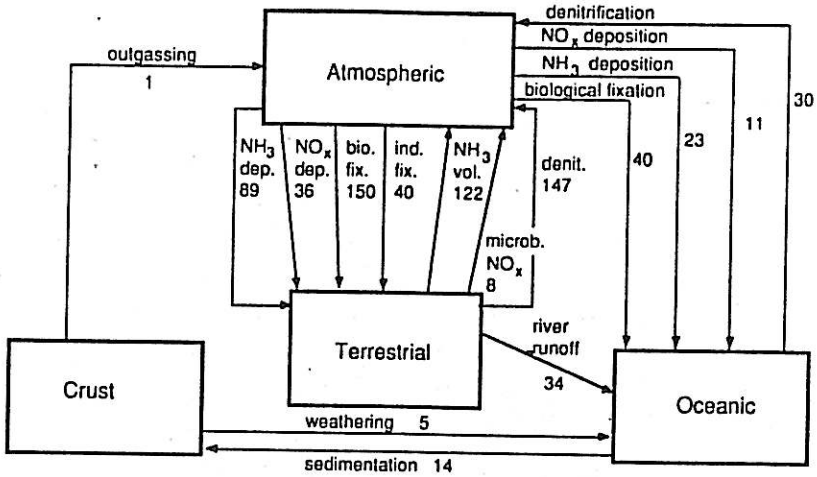

Figure 3.8: The nitrogen cycle (10^{12} grams N/year) (from Jaffe, D.A., 1992: The nitrogen cycle. In: *Global Biogeochemical Cycles*, Academic Press, San Diego, CA, 261-284).

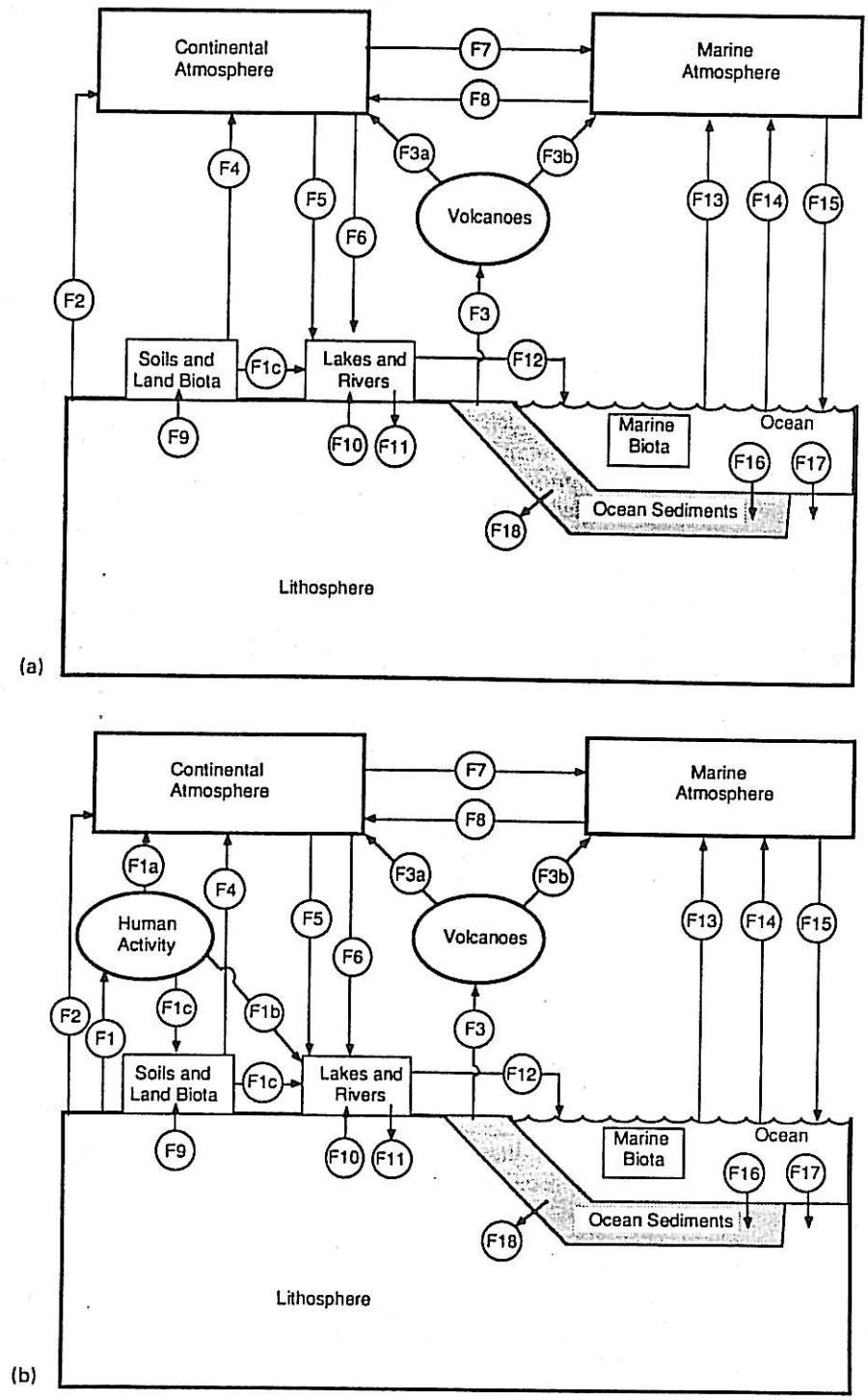

Figure 3.9: Major fluxes of the global biogeochemical sulfur cycle (a) excluding, and (b) including human activity (from Charlson, R.J., T.L. Anderson, and R.E. McDuff, 1992: The sulfur cycle. Chapter 13 in: *Global Biogeochemical Cycles*, Butcher, Charlson, Orians, and Wolfe, Editors, Academic Press, San Diego, CA, 285-300).

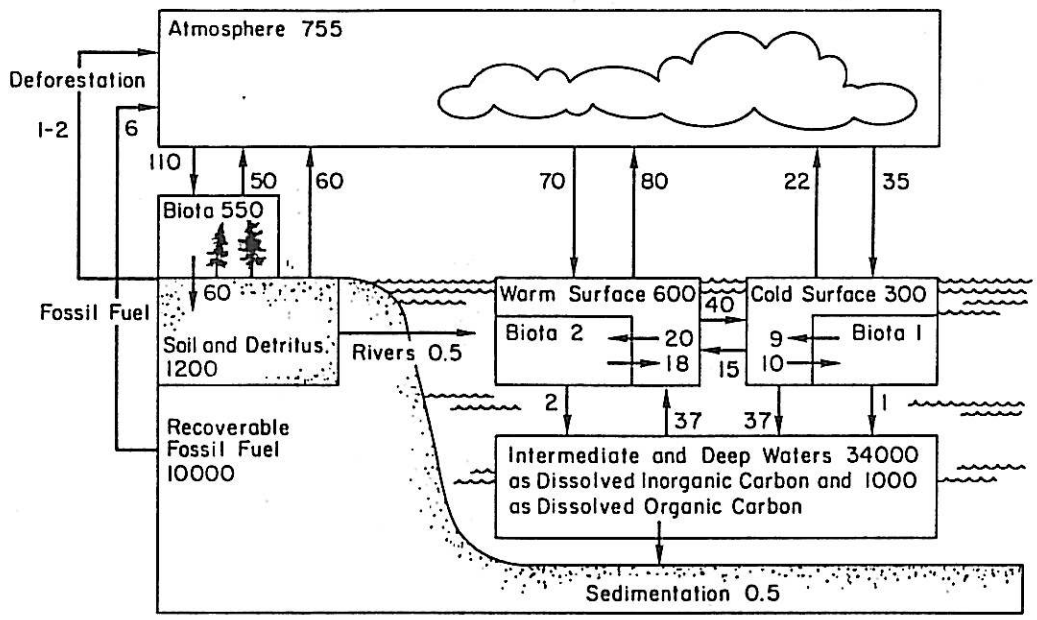

Figure 3.10: The global carbon cycle. The boxes are in Pg C, and the fluxes (arrows) are in 10^{15} grams of carbon per year of CO_2 (from Moore, B. III, 1992: Four simple ocean carbon models. In: *Modeling the Earth System*, UCAR/Office for Interdisciplinary Earth Sciences, Boulder, CO, 197-224).

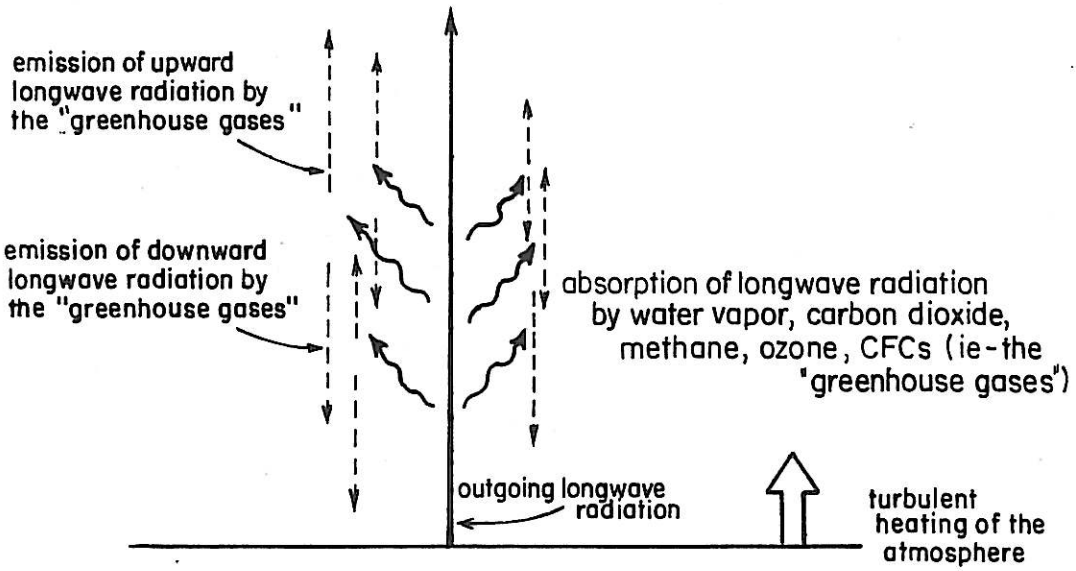

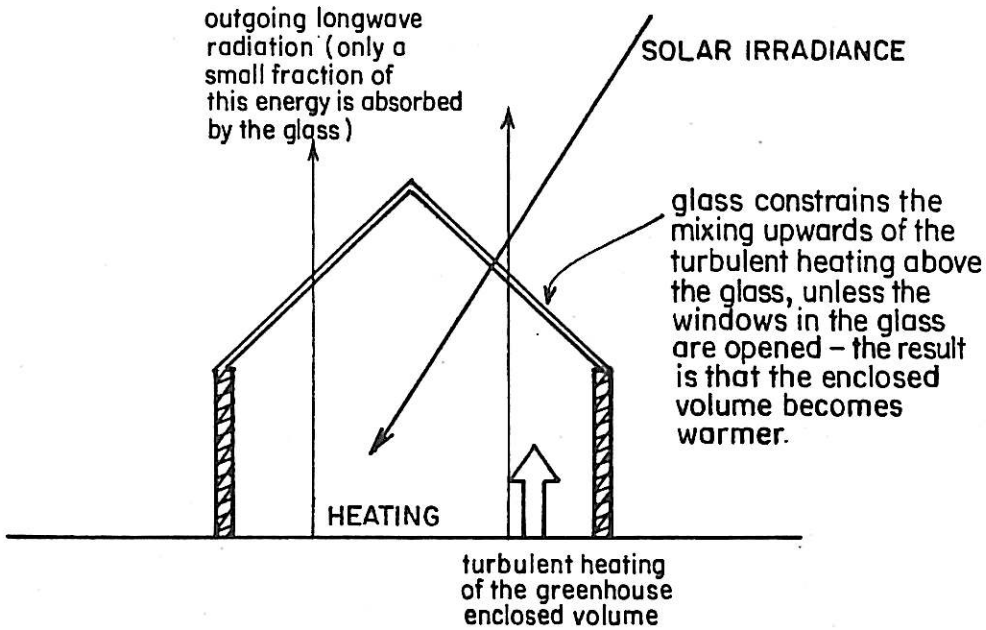

Figure 3.11: Schematic of (a) actual greenhouse, and (b) atmospheric greenhouse (see also Figure 7.2b).

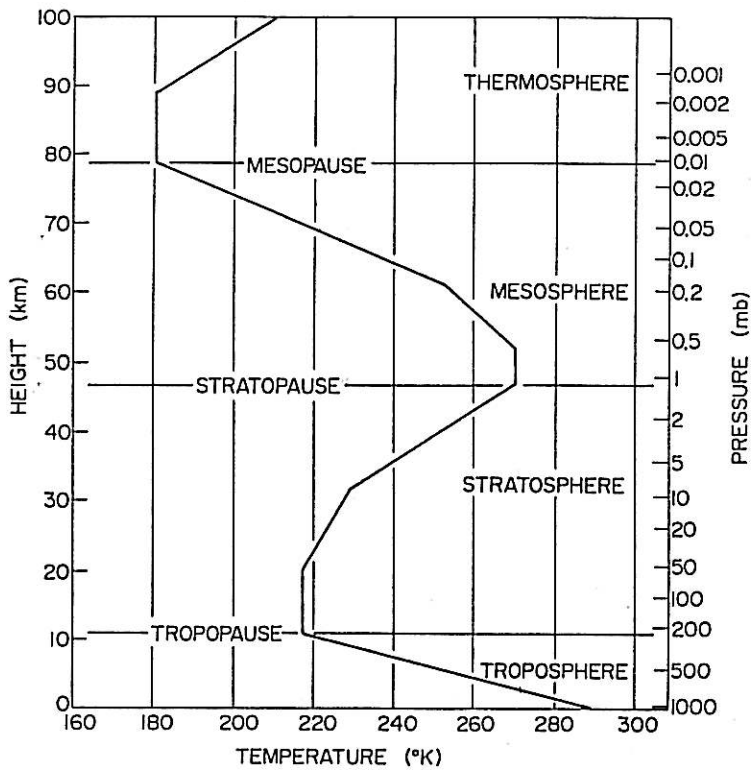

Figure 4.1: Representative vertical temperature profile for the U.S. Standard Atmosphere [from Wallace, J.M. and P.V. Hobbs, 1977: *Atmospheric science: An introductory survey.* Academic Press, New York, NY, 467 pp].

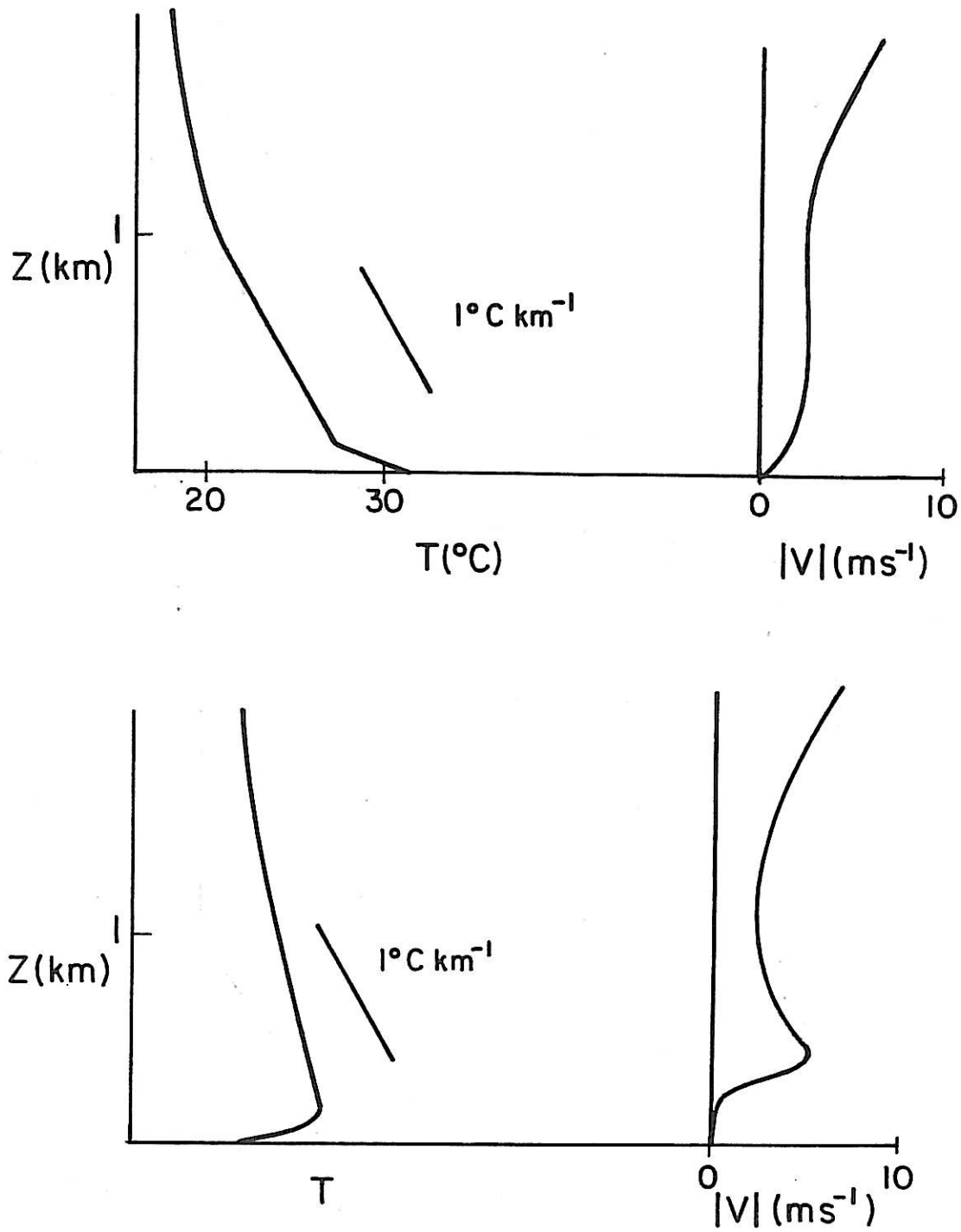

Figure 4.2: Planetary boundary layer with typical clear sky temperature (T) lapse rates and wind speeds (|V|) with height for daytime (top) and night time (bottom).

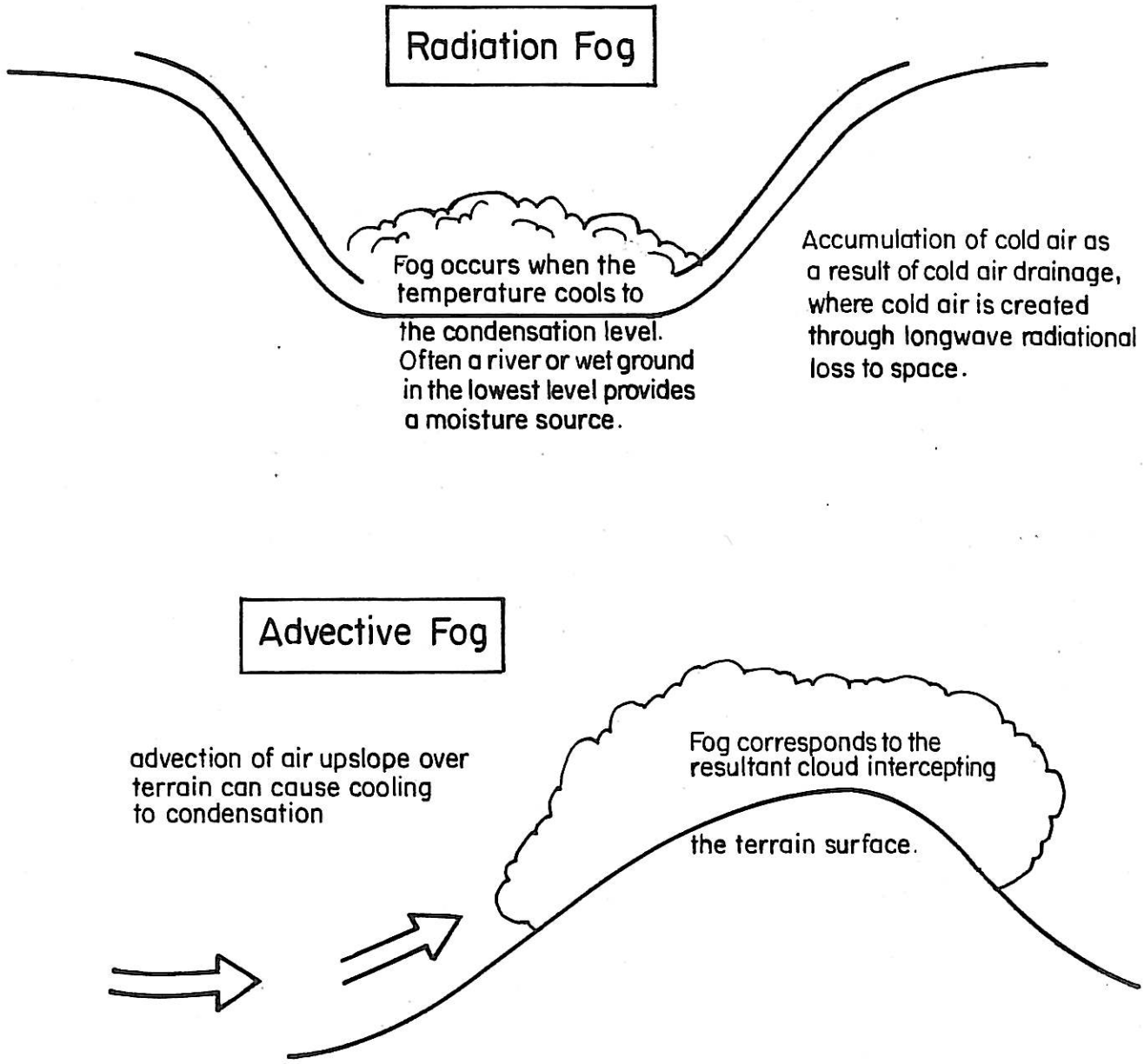

Figure 4.4: Schematic of two different types of fogs.

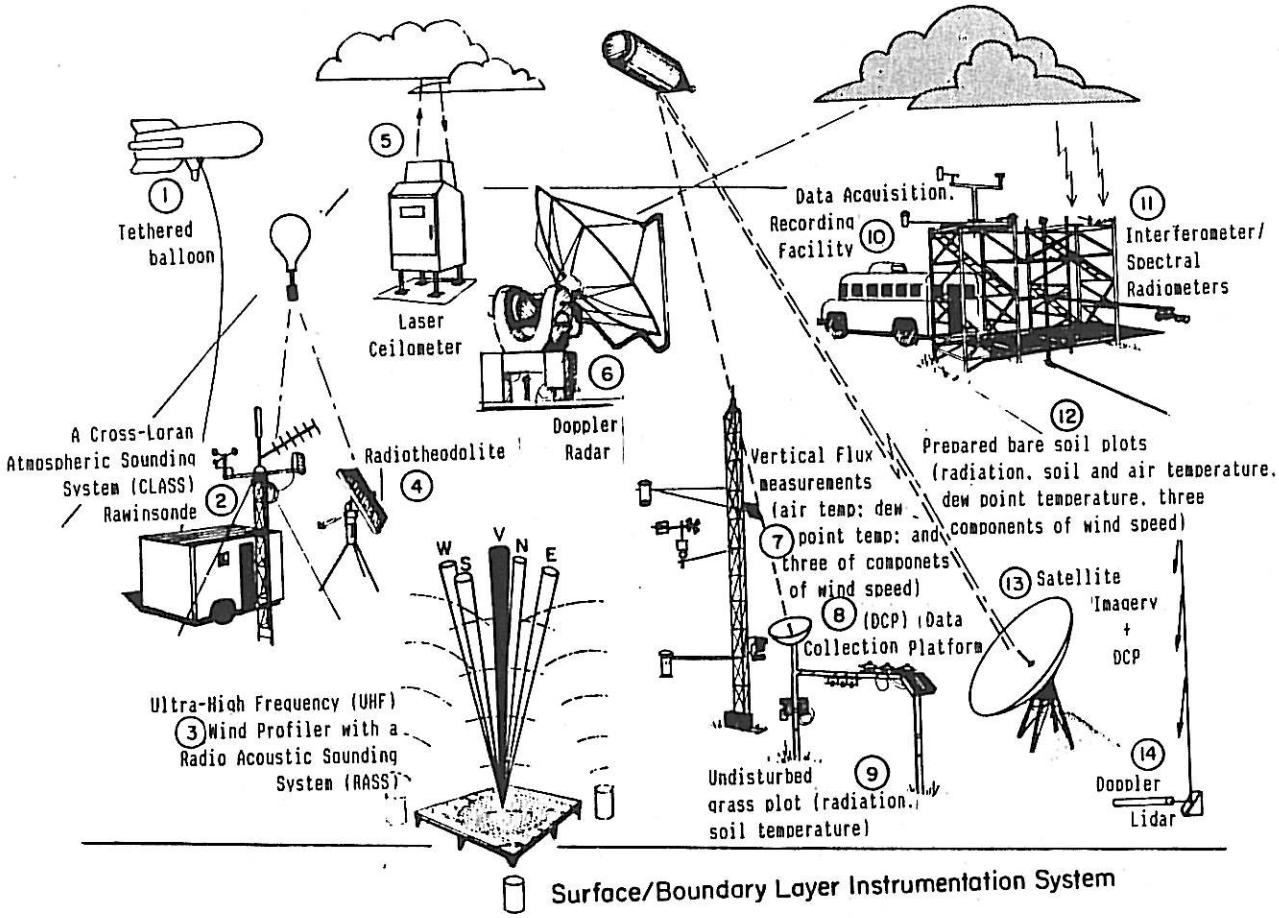

Figure 4.6: Examples of several types of observational systems. These are types used at Colorado State University in their atmospheric science program (figure adapted from one prepared by S.K. Cox, 1993).

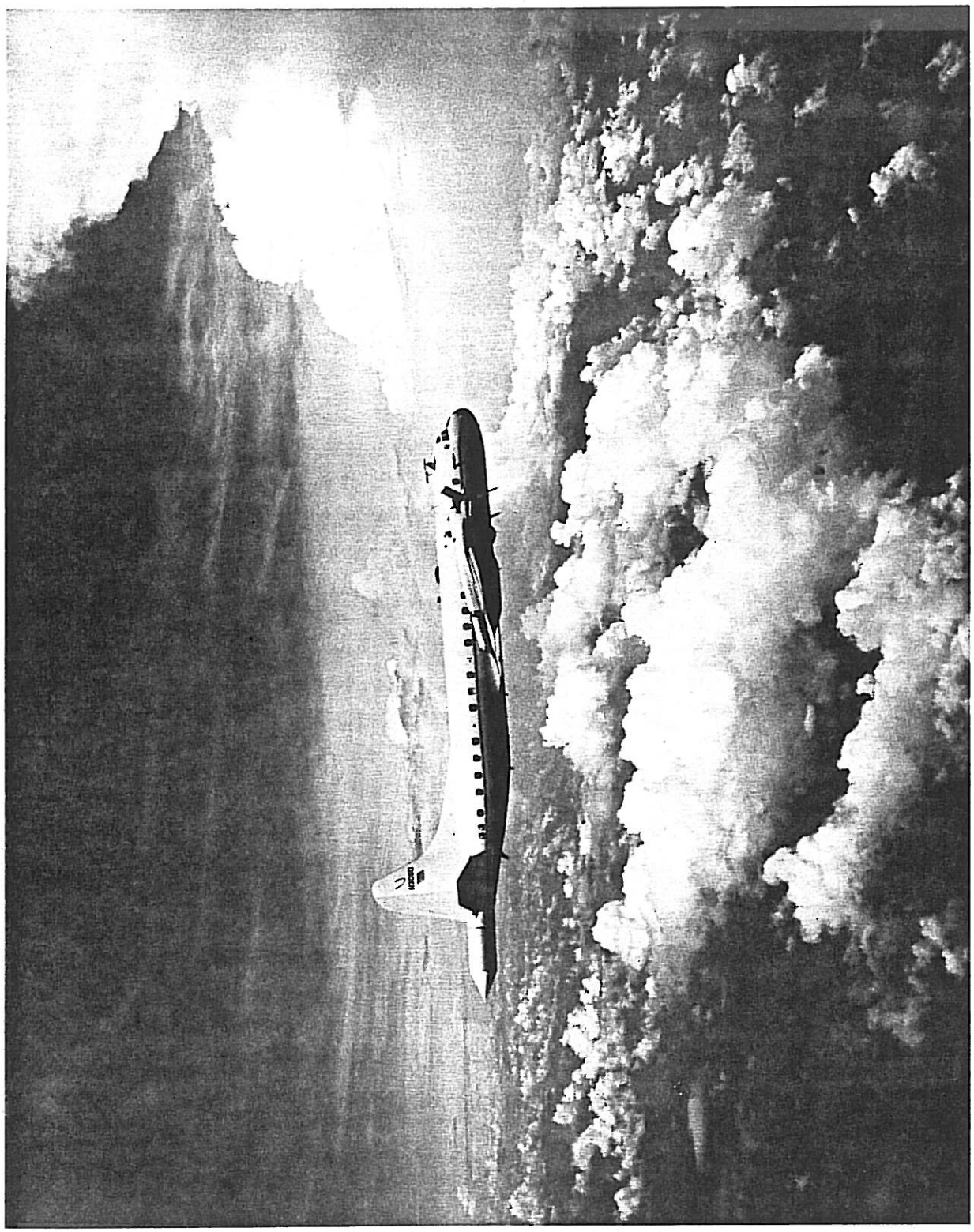

Figure 4.7: Meteorological monitoring aircraft.

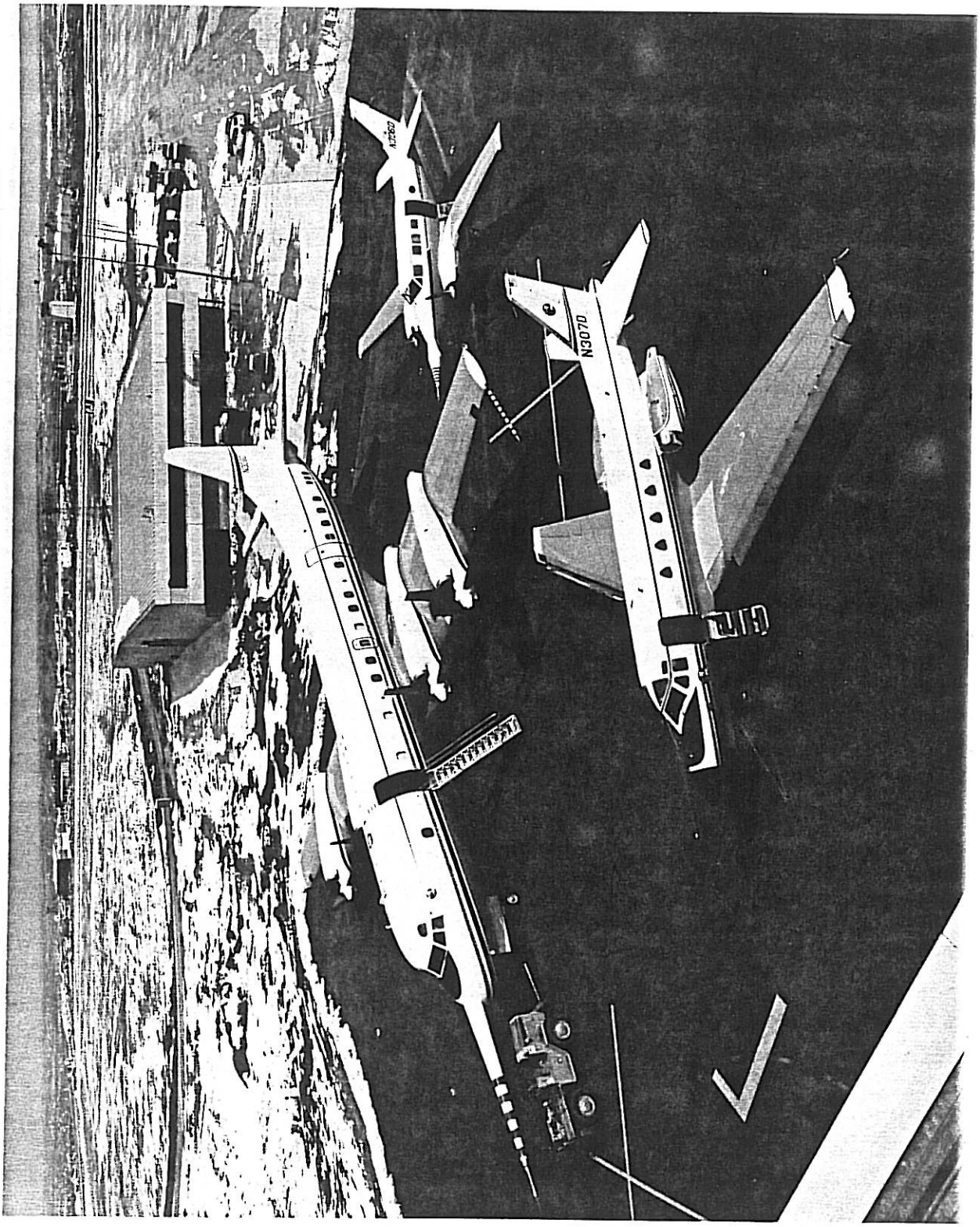

Figure 4.8: Meteorological monitoring aircraft.

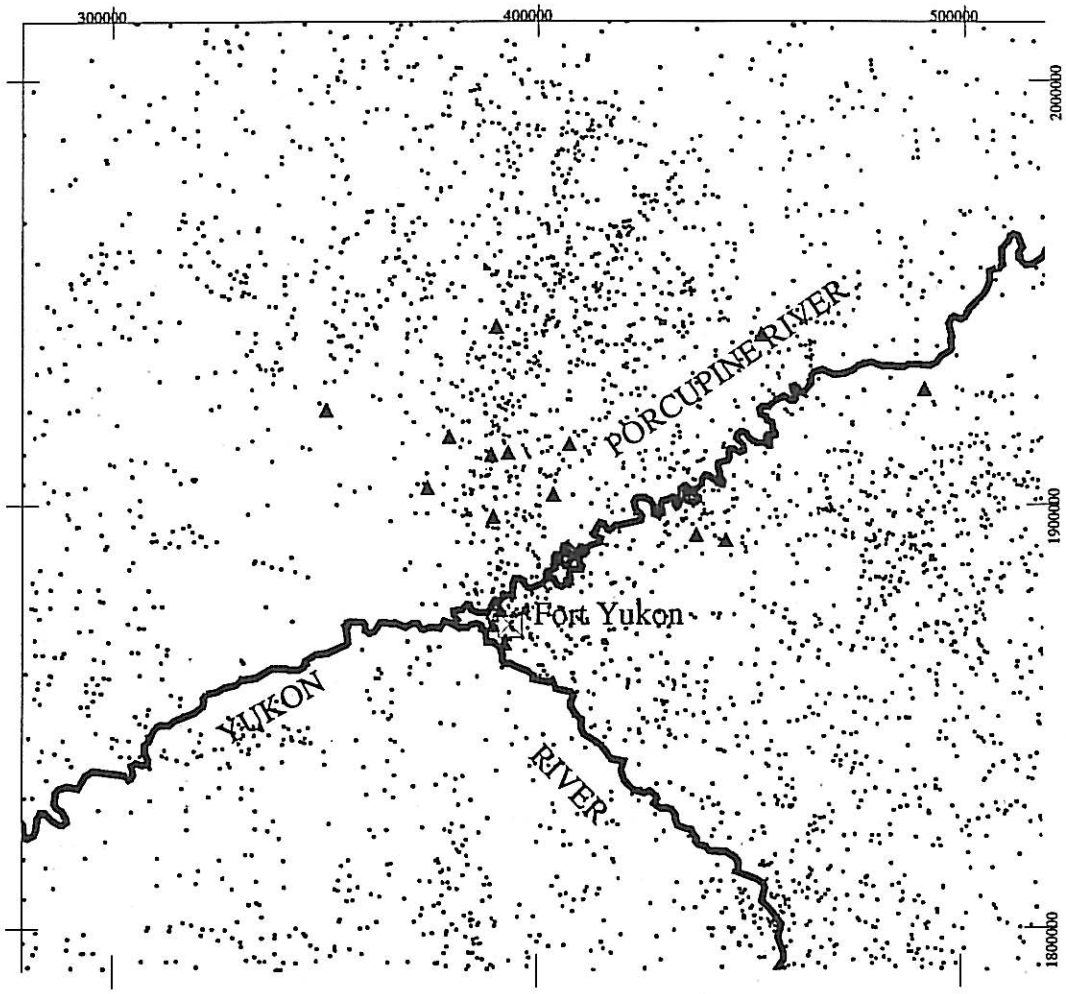

KEY

· lightning strike location

▲ fire start locations

N

SCALE

1:1,500,000

Projection = Albers equal area (units meters)

Figure 4.9: Lightning data in a portion of central Alaska (adapted by John Yarie from Knowles, Captain John B., 1993, M.S. Thesis: The influence of forest fire induced albedo differences on the generation of mesoscale circulations. Department of Atmospheric Science, Colorado State University, 86 pp).

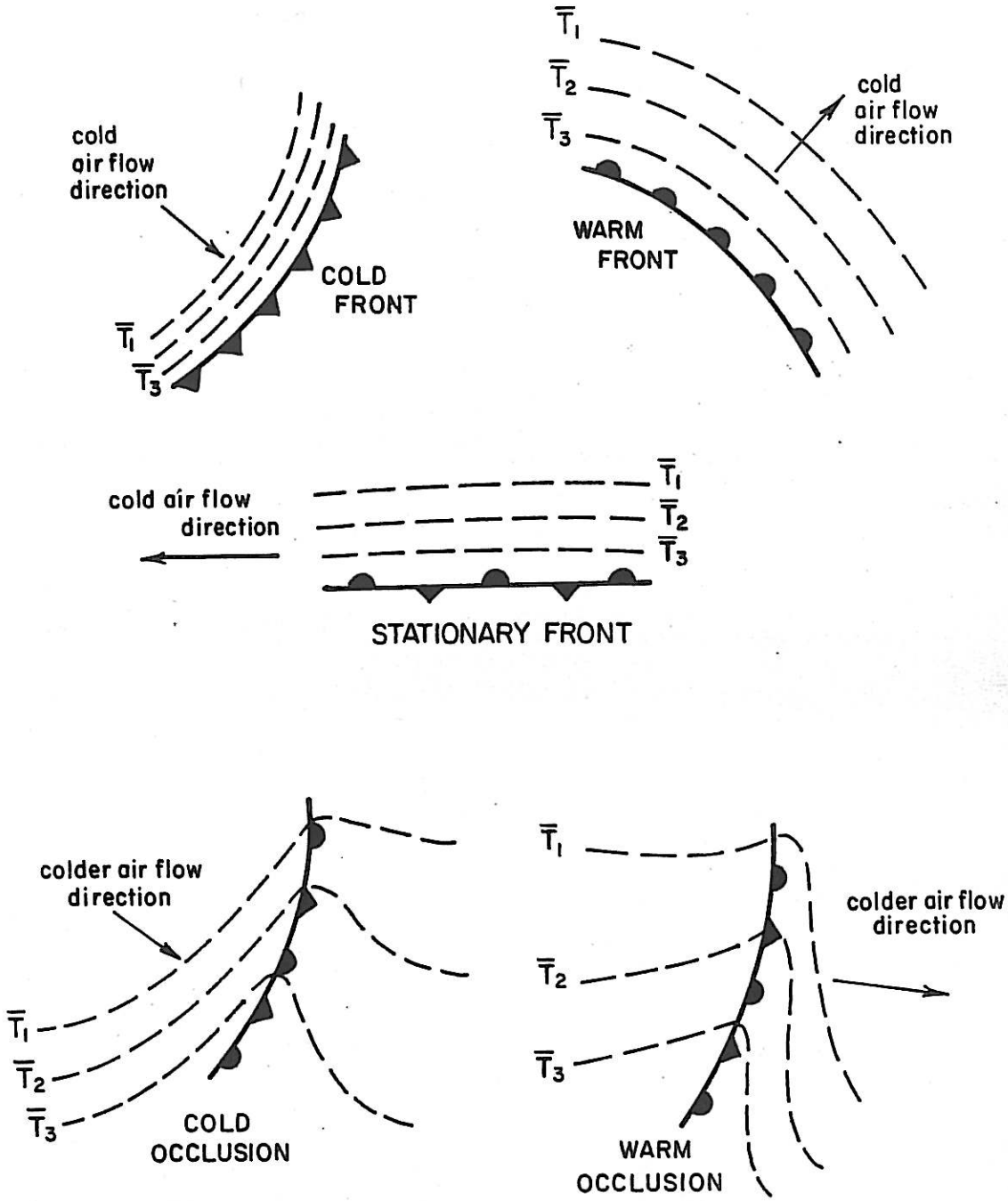

Figure 5.1: Schematic illustration of the different types of fronts. Fronts always move in the direction in which the more dense (i.e., colder) air mass is moving; $\bar{T}_1 < \bar{T}_3$ where $\bar{T}$ is the average temperature in the lower half of the troposphere.

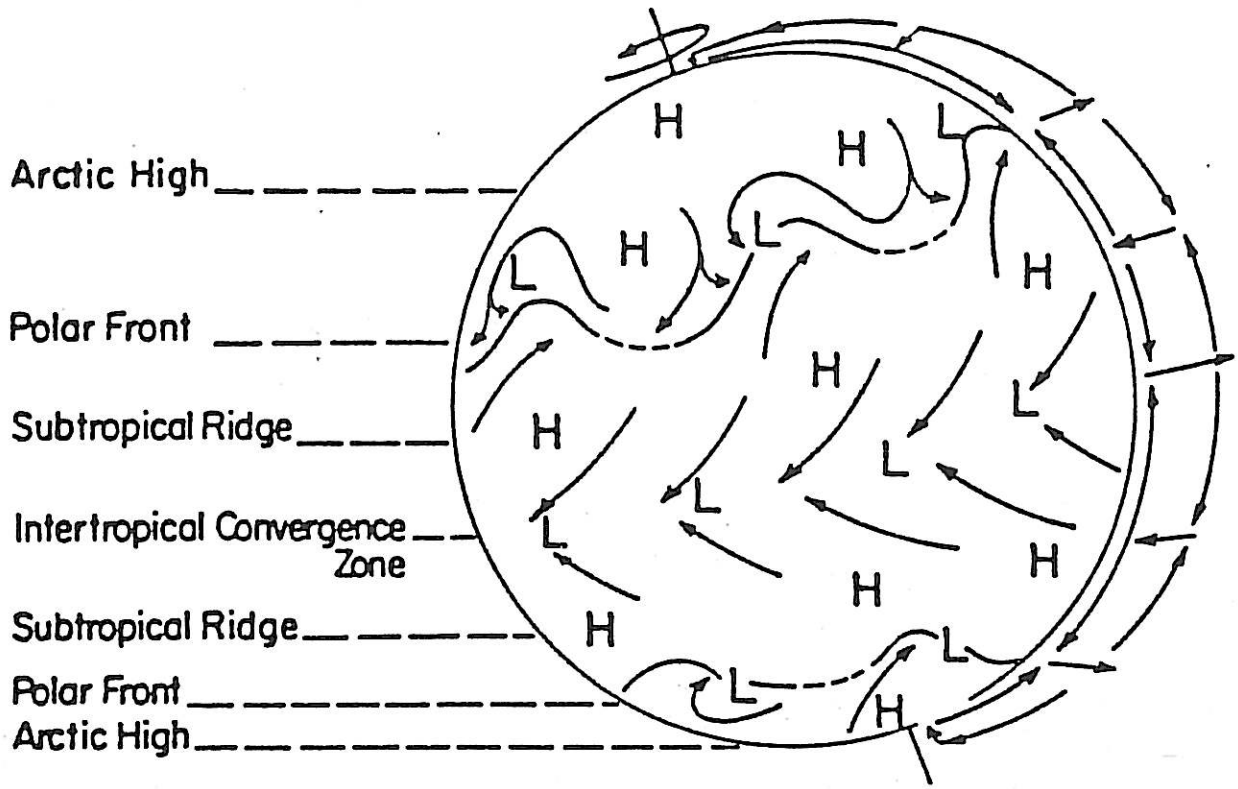

Figure 5.2: Schematic of the general circulation of the earth in the northern hemisphere winter. There is average subsidence in the subtropical ridge and arctic high, and average ascent in the intertropical convergence zone and polar front region. The polar front separates air from upper latitude origin from lower latitude origination. (From Pielke, R.A., M. Garstang, C. Lindsey, and J. Gusdorf, 1987: Use of a synoptic classification scheme to define seasons. *Theor. Appl. Climatol.*, **38**, 57-68.)

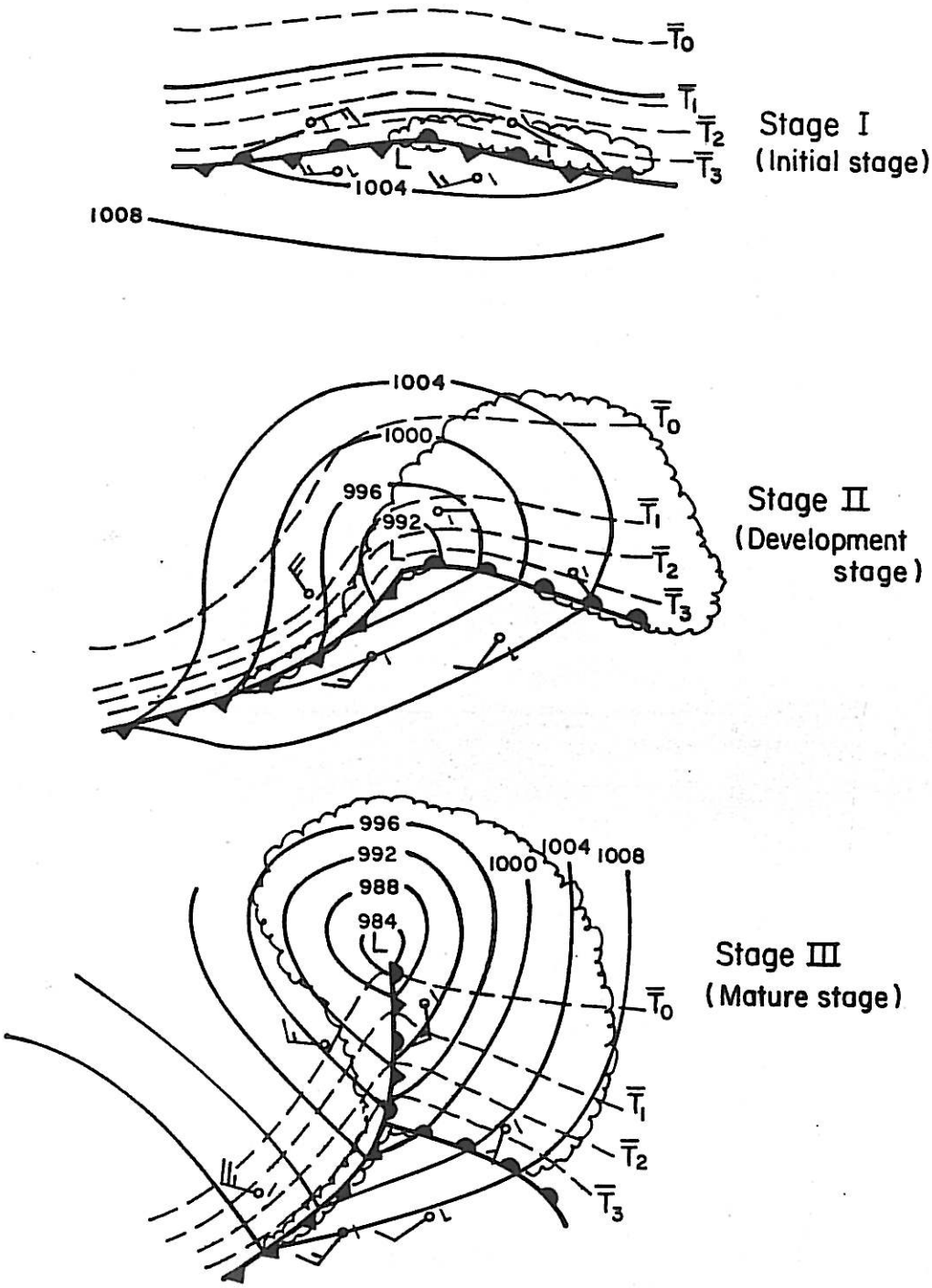

Figure 5.3: Schematic illustration of the evolution of an extratropical cyclone from a wave cyclone to a mature cyclone. The scalloped area represents cloud covered areas; $\bar{T}_0 < \bar{T}_3$ where $\bar{T}$ is the average temperature in the lower half of the troposphere. Pressure is in millibars. Examples of station observations as plotted on U.S. surface map analyses are shown.

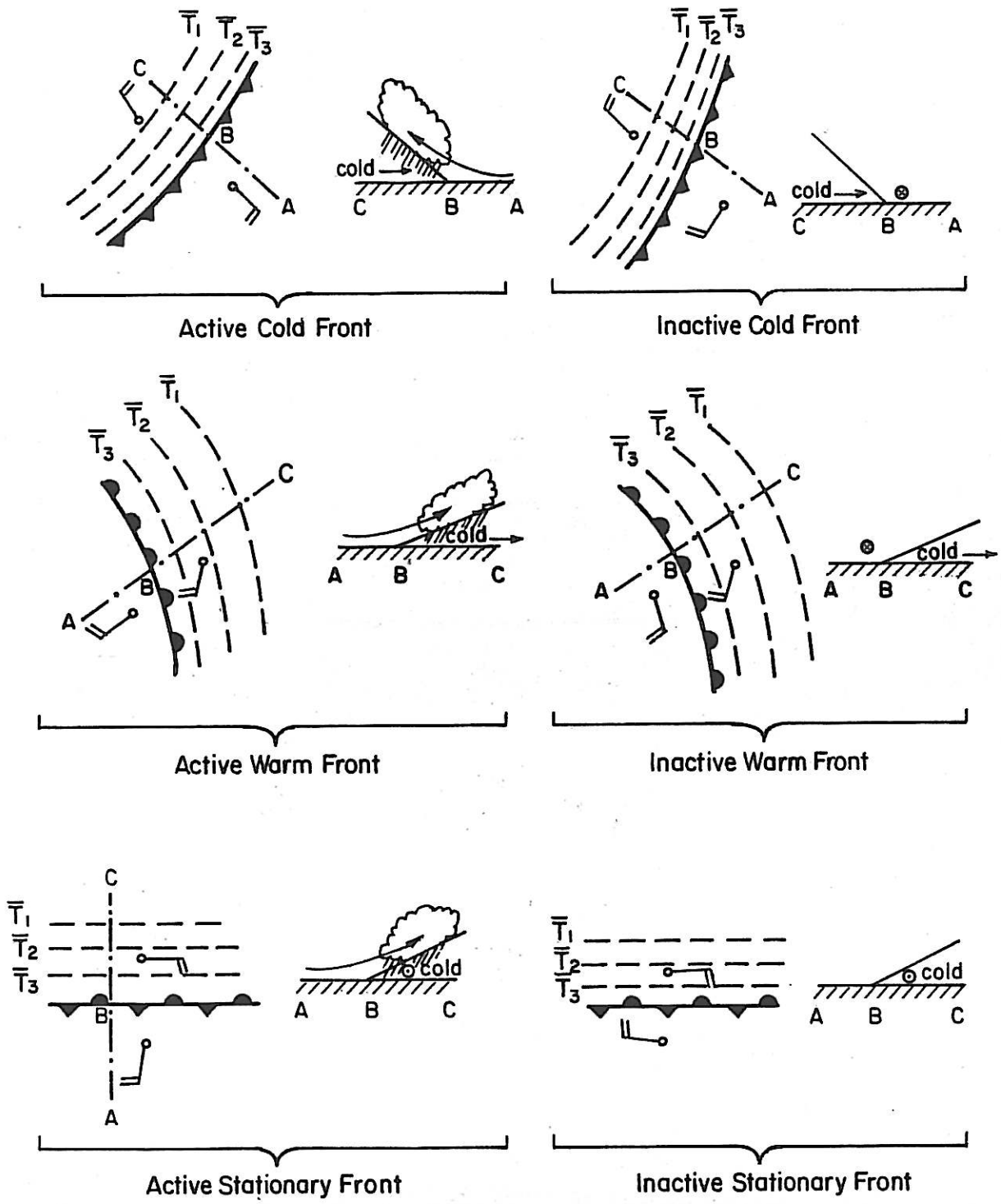

Figure 5.4: Schematic illustration of active and inactive cold, warm, and stationary fronts; where $\bar{T}_1 < \bar{T}_3$. $\bar{T}$ is the average temperature in the lower half of the troposphere.

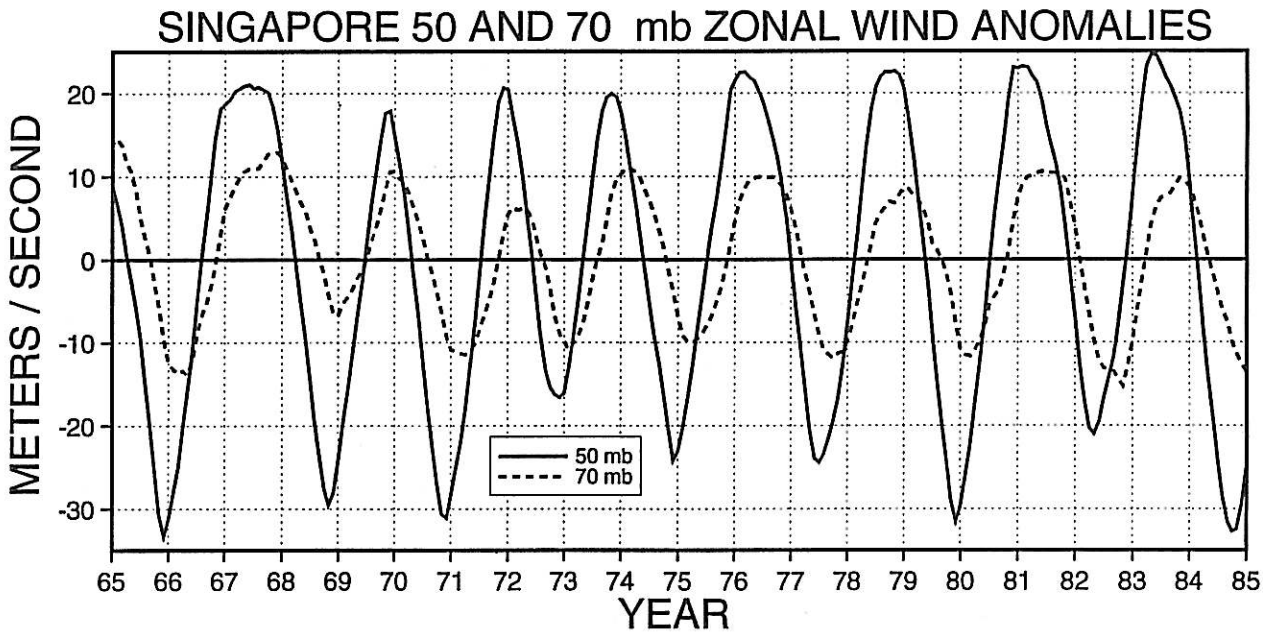

Figure 5.5: The east-west winds over Singapore at two levels in the stratosphere as a function of time. [Figure courtesy of John Sheaffer, Colorado State University, Department of Atmospheric Science, Fort Collins, Colorado.]

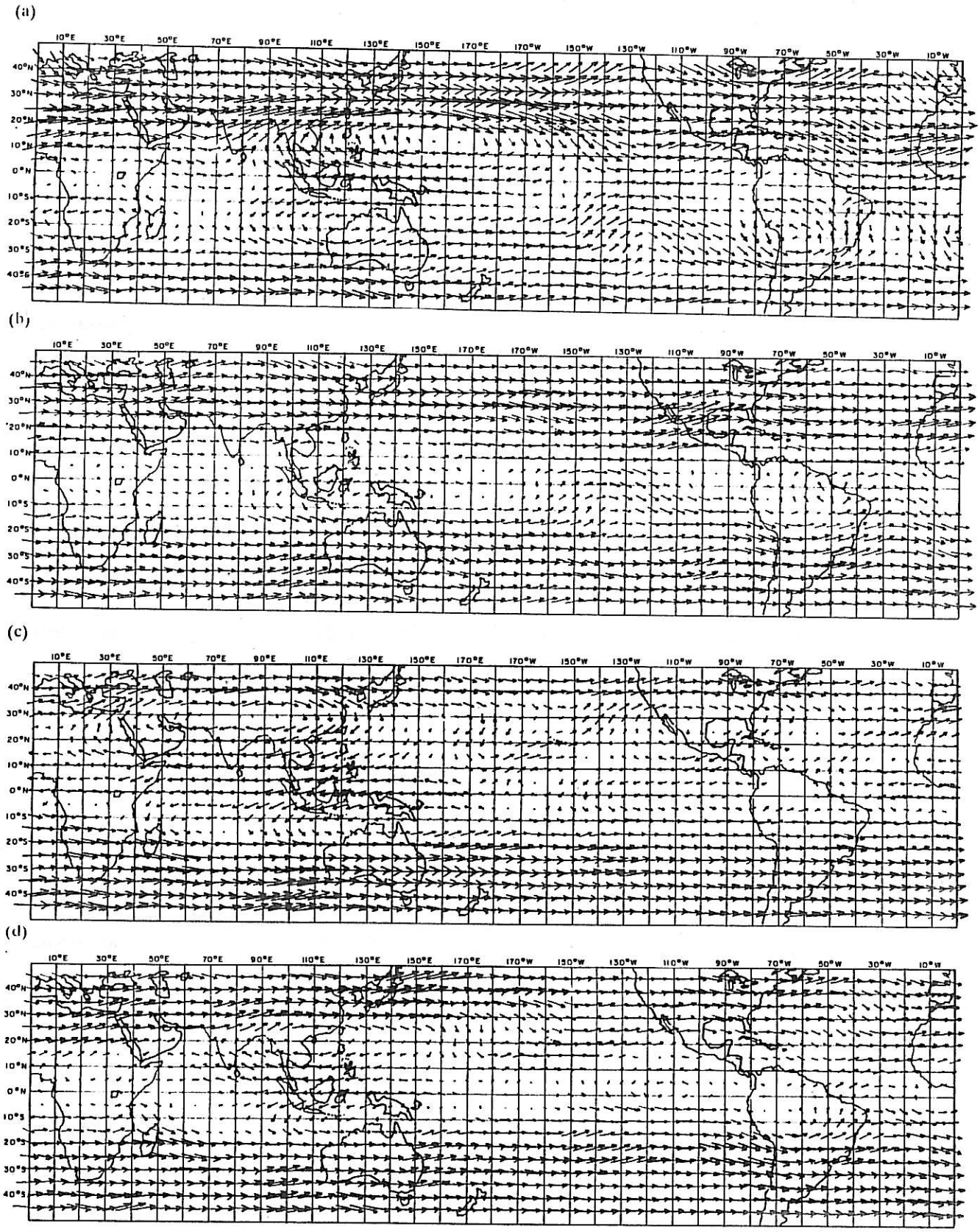

Figure 5.6: Seasonal average winds for 1980-1981 at 150 mb during the periods (a) 1 December to 28 February, (b) 1 March to 31 May, (c) 1 June to 31 August, and (d) 1 September to 30 November. For wind arrows, the distance between two vertical lines corresponds to 14 m s^{-1} (from Pielke, R.A., 1990: *The Hurricane*. Routledge Press, London, England, 228 pp).

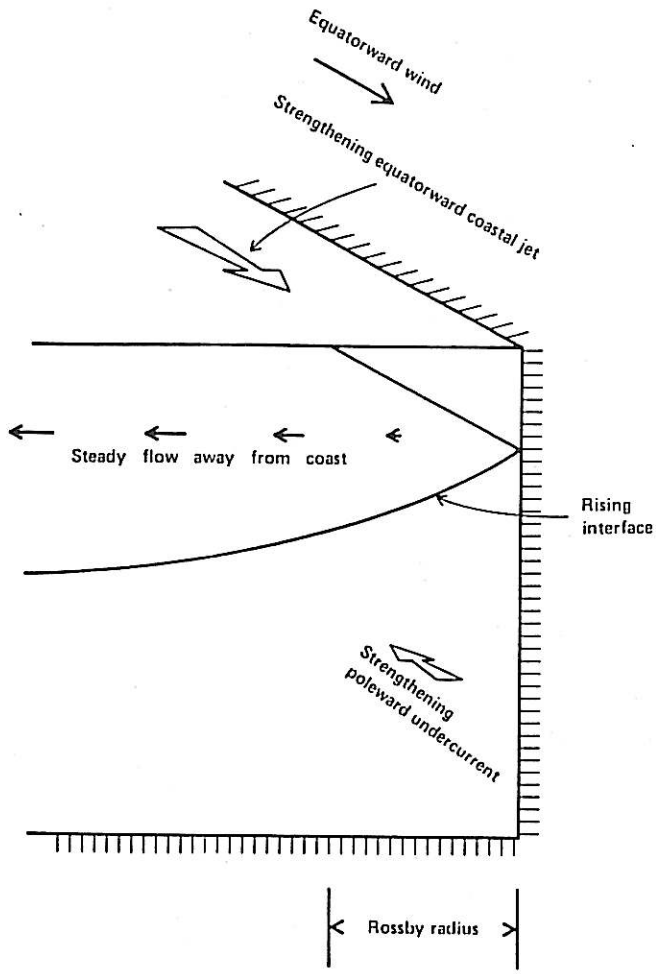

Figure 5.7: The "local" upwelling solution. Upwelling at a steady rate is caused by offshore Ekman transport. A coastal jet is generated in the upper layer, this being in the same direction as that of the wind. An undercurrent in the opposite direction is also generated. Directions are for an eastern boundary (from Gill, A.E., 1982: *Atmosphere-ocean dynamics*. Academic Press, Inc., Orlando. Florida, 662 pp.).

Figure 6.1

6.1

	N1a Elementary needle		C1f Hollow column		P2b Stellar crystal with sectorlike ends
	N1b Bundle of elementary needles		C1g Solid thick plate		P2c Dendritic crystal with plates at ends
	N1c Elementary sheath		C1h Thick plate of skeleton form		P2d Dendritic crystal with sectorlike ends
	N1d Bundle of elementary sheaths		C1i Scroll		P2e Plate with simple extensions
	N1e Long solid column		C2a Combination of bullets		P2f Plate with sectorlike extensions
	N2a Combination of needles		C2b Combination of columns		P2g Plate with dendritic extensions
	N2b Combination of sheaths		P1a Hexagonal plate		P3a Two-branched crystal
	N2c Combination of long solid columns		P1b Crystal with Sectorlike branches		P3b Three-branched crystal
	C1a Pyramid		P1c Crystal with broad branches		P3c Four-branched crystal
	C1b Cup		P1d Stellar crystal		P4a Broad branch crystal with 12 branches
	C1c Solid bullet		P1e Ordinary dendritic crystal		P4b Dendritic crystal with 12 branches
	C1d Hollow bullet		P1f Fernlike crystal		P5 Malformed crystal
	C1e Solid column		P2a Stellar crystal with plates at ends		P6a Plate with spatial plates

Figure 6.1

	P6b Plate with spatial dendrites		CP3d Plate with scrolls at ends		R3c Graupel-like snow with nonrimed extensions
	P6c Stellar crystal with spatial plates		S1 Side planes		R4a Hexagonal graupel
	P6d Stellar crystal with spatial dendrites		S2 Scalelike side planes		R4b Lump graupel
	P7a Radiating assemblage of plates		S3 Combination of side planes, bullets, and columns		R4c Conelike graupel
	P7b Radiating assemblage of dendrites		R1a Rimed needle crystal		I1 Ice particle
	CP1a Column with plates		R1b Rimed columnar crystal		I2 Rimed particle
	CP1b Column with dendrites		R1c Rimed plate or sector		I3a Broken branch
	CP1c Multiple capped column		R1d Rimed stellar crystal		I3b Rimed broken branch
	CP2a Bullet with plates		R2a Densely rimed plate or sector		I4 Miscellaneous
	CP2b Bullet with dendrites		R2b Densely rimed stellar crystal		G1 Minute column
					G2 Germ of skeleton form
	CP3a Stellar crystal with needles		R2c Stellar crystal with rimed spatial branches		G3 Minute hexagonal plate
	CP3b Stellar crystal with columns		R3a Graupel-like snow of hexagonal type		G4 Minute stellar crystal
					G5 Minute assemblage of plates
	CP3c Stellar crystal with scrolls at ends		R3b Graupel-like snow of lump type		G6 Irregular germ

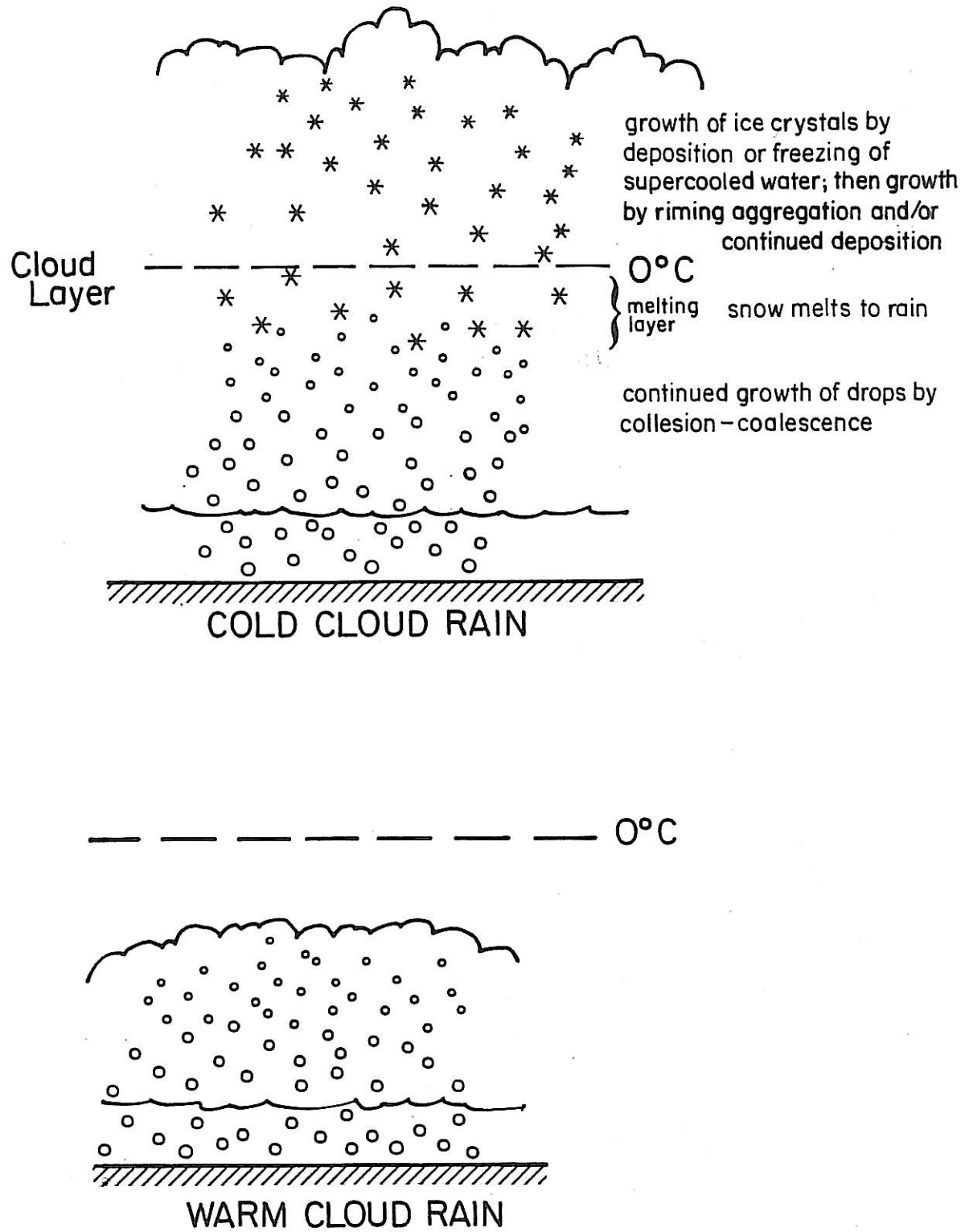

Figure 6.3: Schematic of 2 types of rainfall mechanisms.

6.5a

6.5b

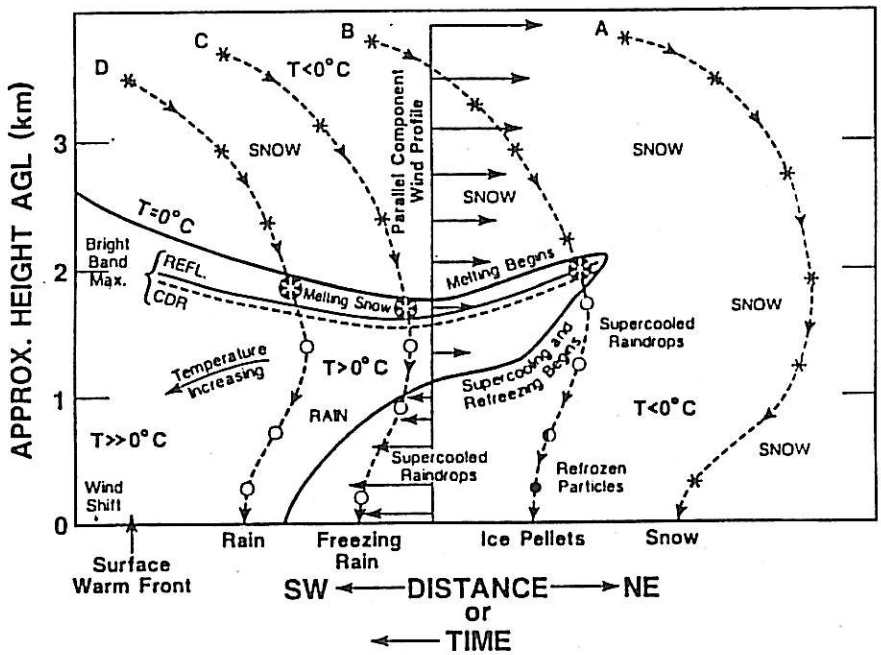

Figure 6.6: Schematic of the temperature profile associated with (a) freezing rain, and (b) sleet.

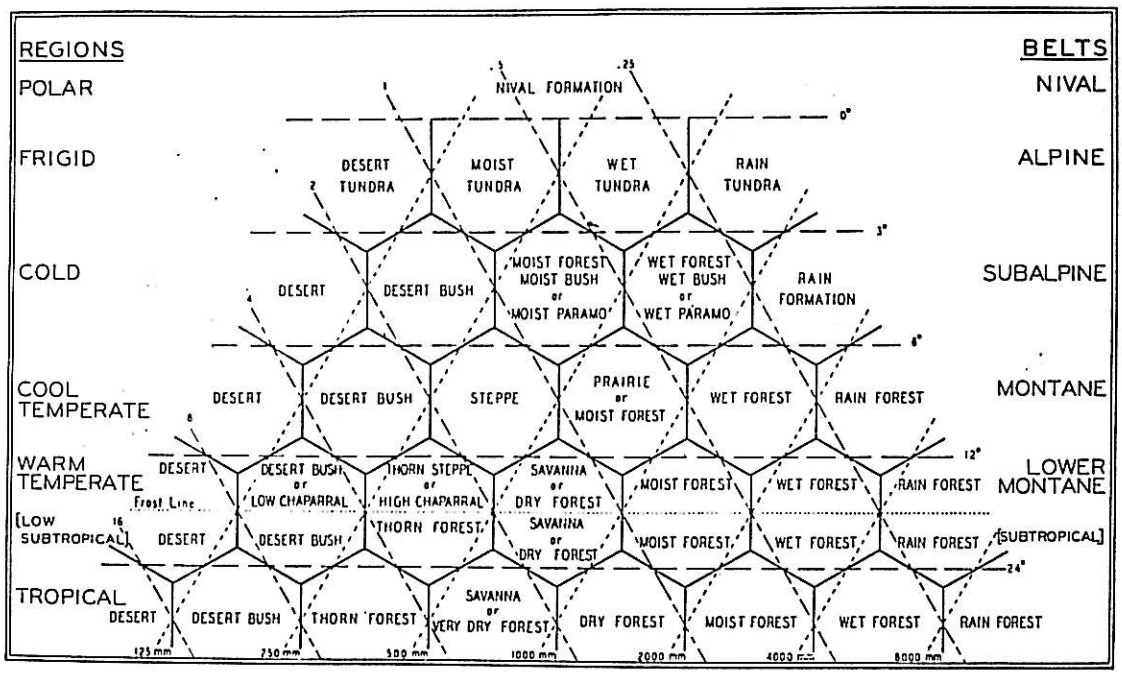

Figure 7.1: Chart that differentiates the vegetation of dry land areas of the world into 100 closely equivalent formations separated by temperature, precipitation, and evaporation lines of equal value (from Holdridge, L.R., 1947: Determination of world plant formations from simple climatic data. *Science*, **105**, 367-368).

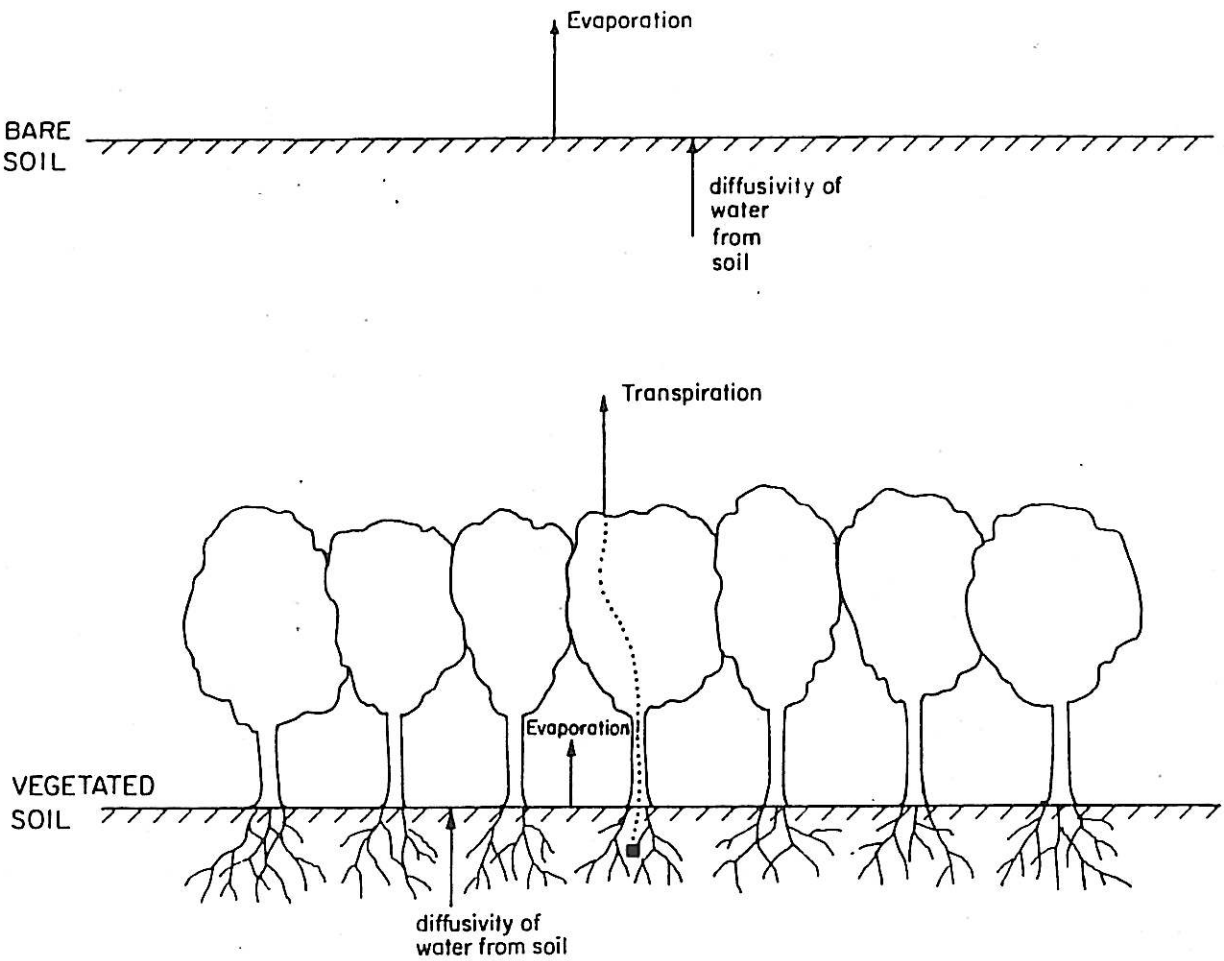

Figure 7.2: (a) Schematic illustration of the surface moisture budget over bare soil and vegetated land. The roughness of the surface (and for the vegetation, its displacement height) will influence the magnitude of the moisture flux. Dew and frost formation and removal will also influence the moisture budget. (b) Schematic illustration of the surface heat budget over bare soil and vegetated land. The roughness of the surface (and for the vegetation, its displacements height) will influence the magnitude of the heat flux. Dew and frost formation and removal will also influence the heat budget (from Pielke and Avissar, 1990: Influence of landscape structure on local and regional climate. *Landscape Ecology*, **4**, 133-155).

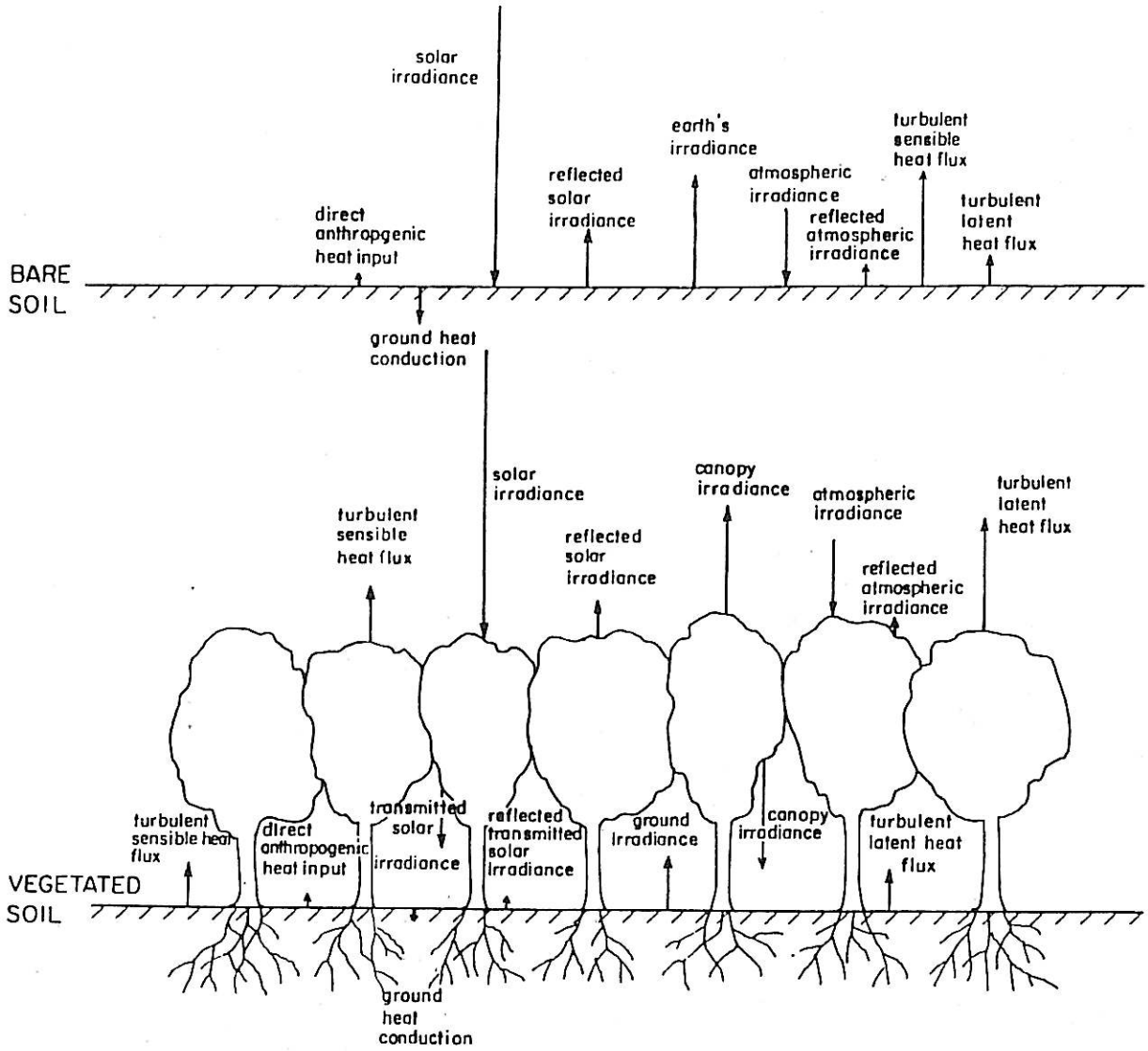
solar irradiance
earth's irradiance
turbulent sensible heat flux
reflected solar irradiance
atmospheric irradiance
reflected atmospheric irradiance
turbulent latent heat flux
direct anthropgenic heat input
BARE SOIL
ground heat conduction
solar irradiance
canopy irradiance
atmospheric irradiance
turbulent latent heat flux
turbulent sensible heat flux
reflected solar irradiance
reflected atmospheric irradiance
turbulent sensible heat flux
direct anthropogenic heat input
transmitted solar irradiance
reflected transmitted solar irradiance
ground irradiance
canopy irradiance
turbulent latent heat flux
VEGETATED SOIL
ground heat conduction

Figure 7.2b

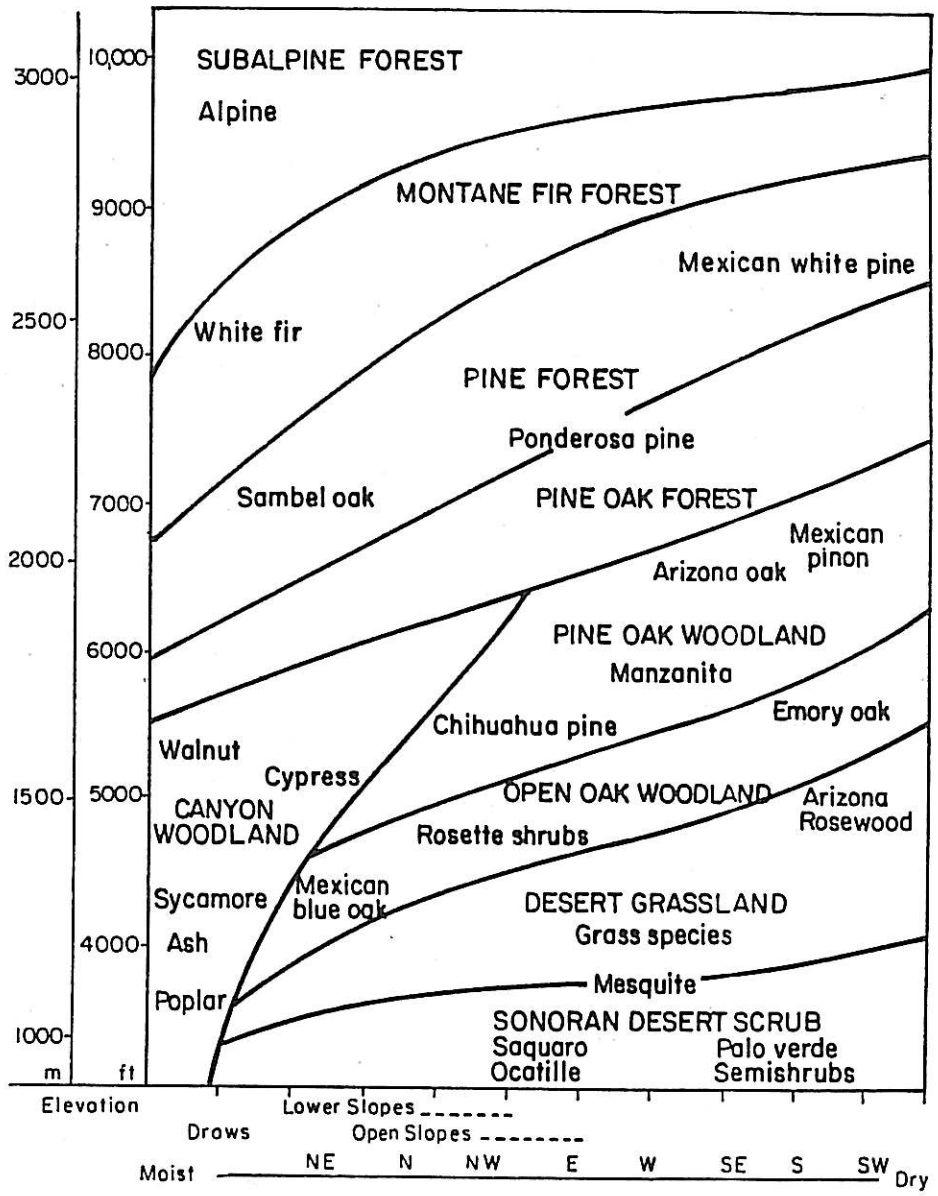

Figure 7.3: Vegetation chart for the Santa Catalina Mountains, southeastern Arizona. The pattern above 9000 feet is for the nearby Pinaleno Mountains. 400 vegetation samples were plotted on the chart by their positions in relation to the elevation gradient on the left, and the topographic moisture gradient on the bottom. Boundary lines were drawn to connect the mean positions at which one community-type, as these had been defined in this study, gave way to another. Dominant species are indicated in the parts of the pattern where they are most important (from Whittaker, R.H., 1975: *Communities and Ecosystems.* MacMillan Publishing Co., Inc., New York, N.Y., 385 pp.).

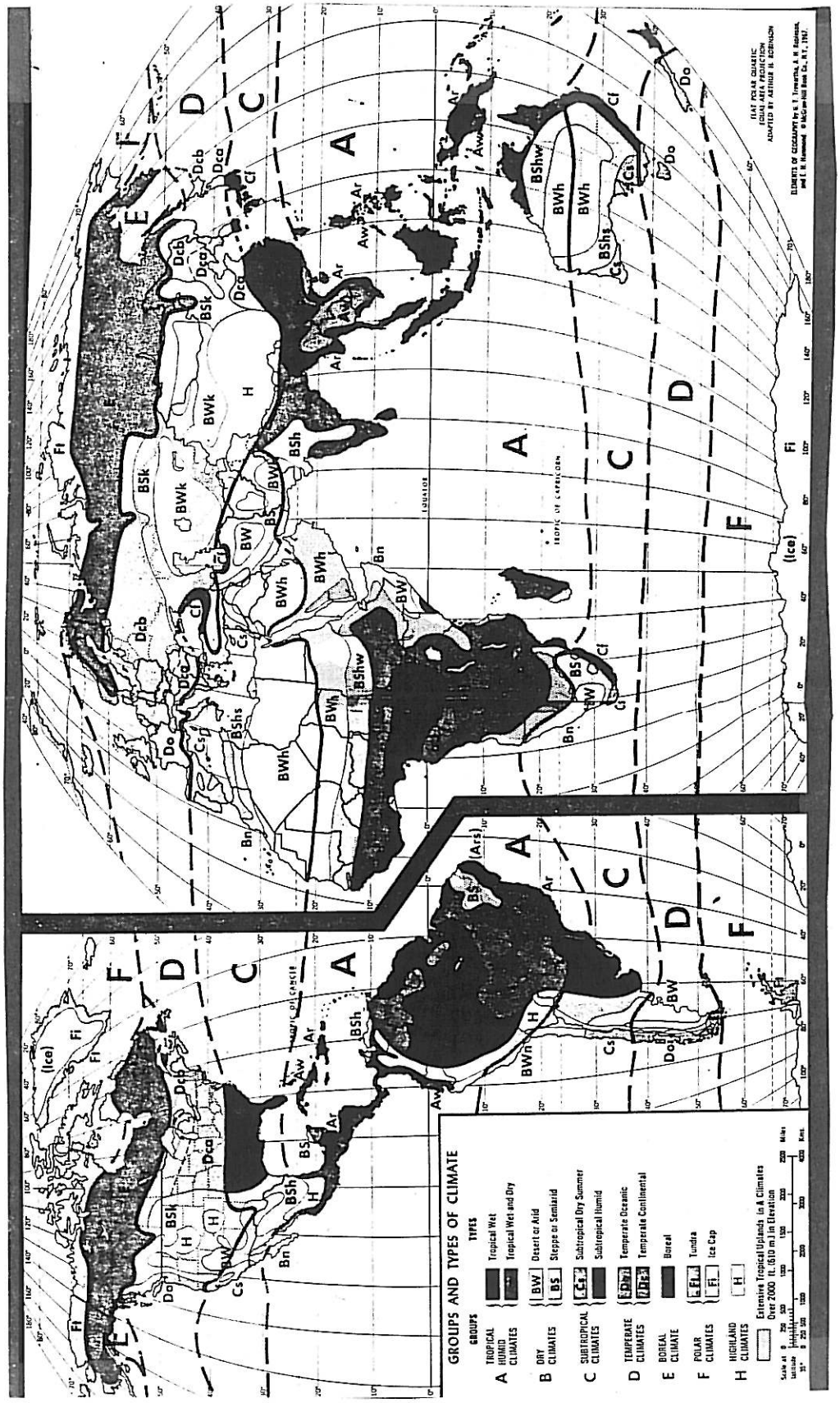

Figure 7.4: Groups and types of climate (from Trewartha, G.T., and L.H. Horn, 1980: *An Introduction to Climate*, Fifth Edition, McGraw-Hill Book Company, New York, N.Y., 416 pp.).

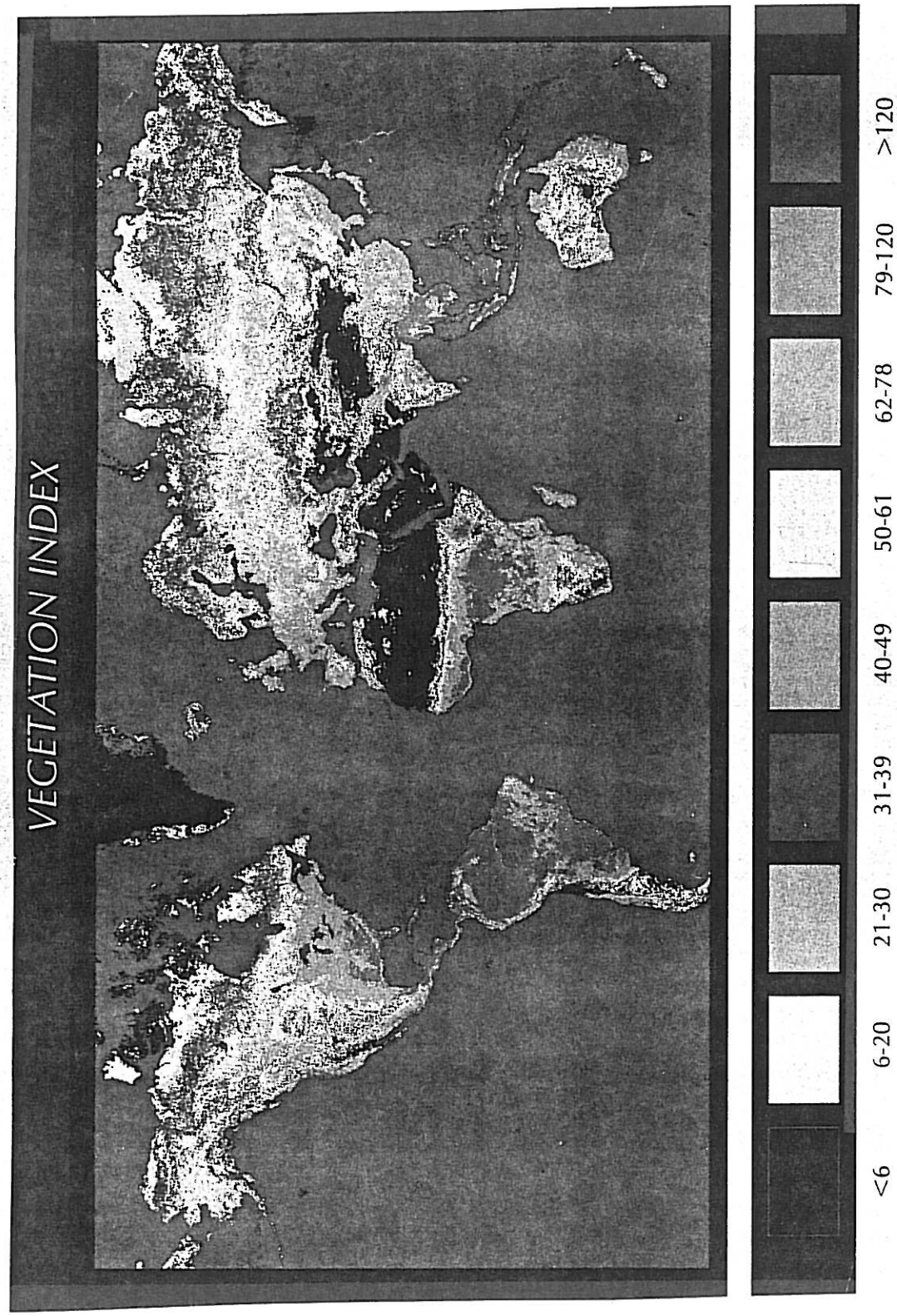

Figure 7.5: (a) Global vegetation index (from *EOS*, **70**, No. 41, October 10, 1989).

PRELIMINARY MAP OF 1990 VEGETATION GREENNESS CLASSES

CLASS #

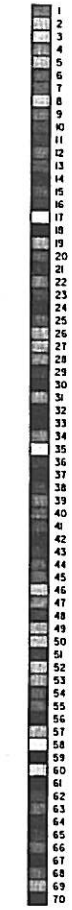

U.S. STATE BOUNDARIES DERIVED
FROM USGS 1:2,000,000 DLG

INTERNATIONAL AND STATE/PROVINCIAL
BOUNDARIES FROM WORLD DATA BANK II

LAMBERT AZIMUTHAL EQUAL AREA PROJECTION
CENTER: 100°W, 45°N

EROS DATA CENTER
NATIONAL MAPPING DIVISION
U.S. GEOLOGICAL SURVEY
SIOUX FALLS, SD

1:15,000,000

100 0 200 500 KILOMETERS

100 0 300 MILES

STATE/PROVINCIAL BOUNDARY

INTERNATIONAL BOUNDARY

AREA SCALES

1,000,000 HECTARES
10,000 SQ KM

1,000,000 ACRES
1,562.5 SQ MI

1 HECTARE = 2.471 ACRES

THESE SPECTRAL CLASSES REPRESENTING CLUSTERED TIME SERIES VEGETATION CONDITION DATA, WERE PRODUCED USING UNSUPERVISED IMAGE CLASSIFICATION TECHNIQUES. THE VEGETATION CONDITION DATA WERE NORMALIZED DIFFERENCE VEGETATION INDEX (NDVI) VALUES TRANSFORMED FROM NOAA-11 AVHRR IMAGERY. EIGHT CONSECUTIVE REPORTING PERIODS WITH EACH REPRESENTING MAXIMUM NDVI DURING A FOUR WEEK INTERVAL WERE USED IN THE ANALYSIS.

FIG 7.5b

7.5b

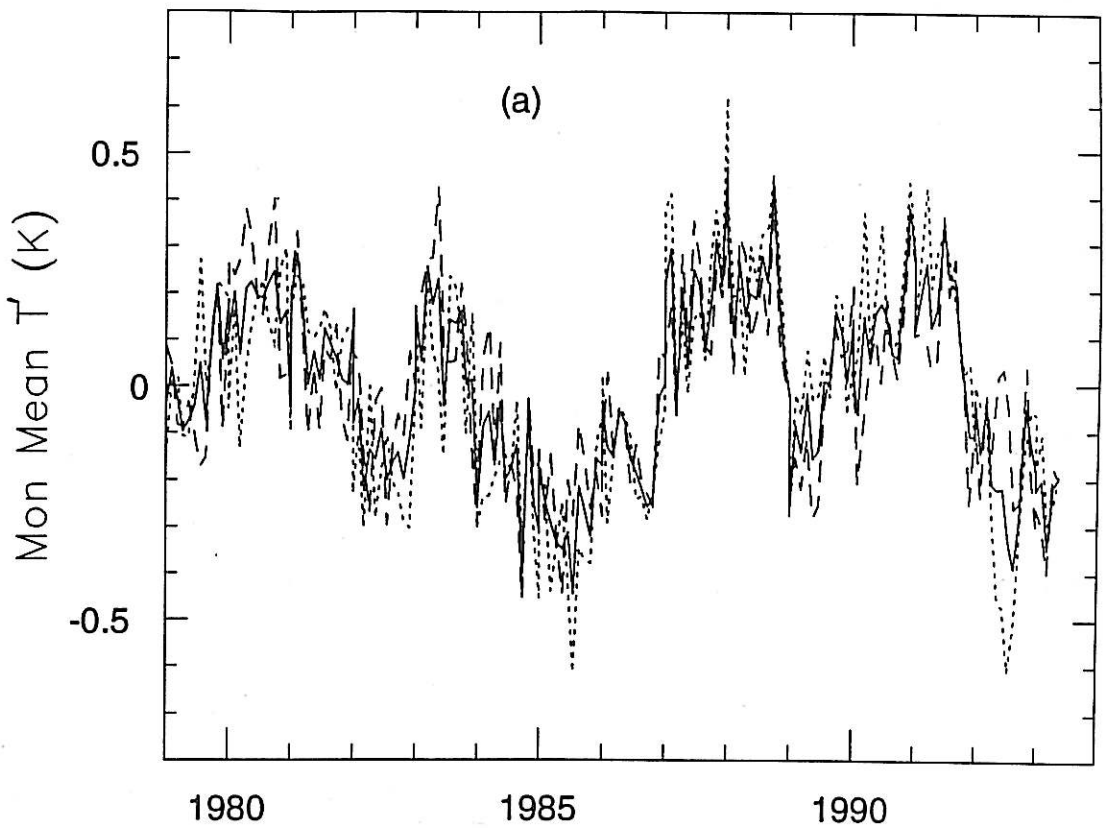

Figure 7.8: Lower tropospheric temperature as derived from satellite data for the period 1980 to mid 1993. Data provided by ??, and plotted by Xubin Zeng.

9.2

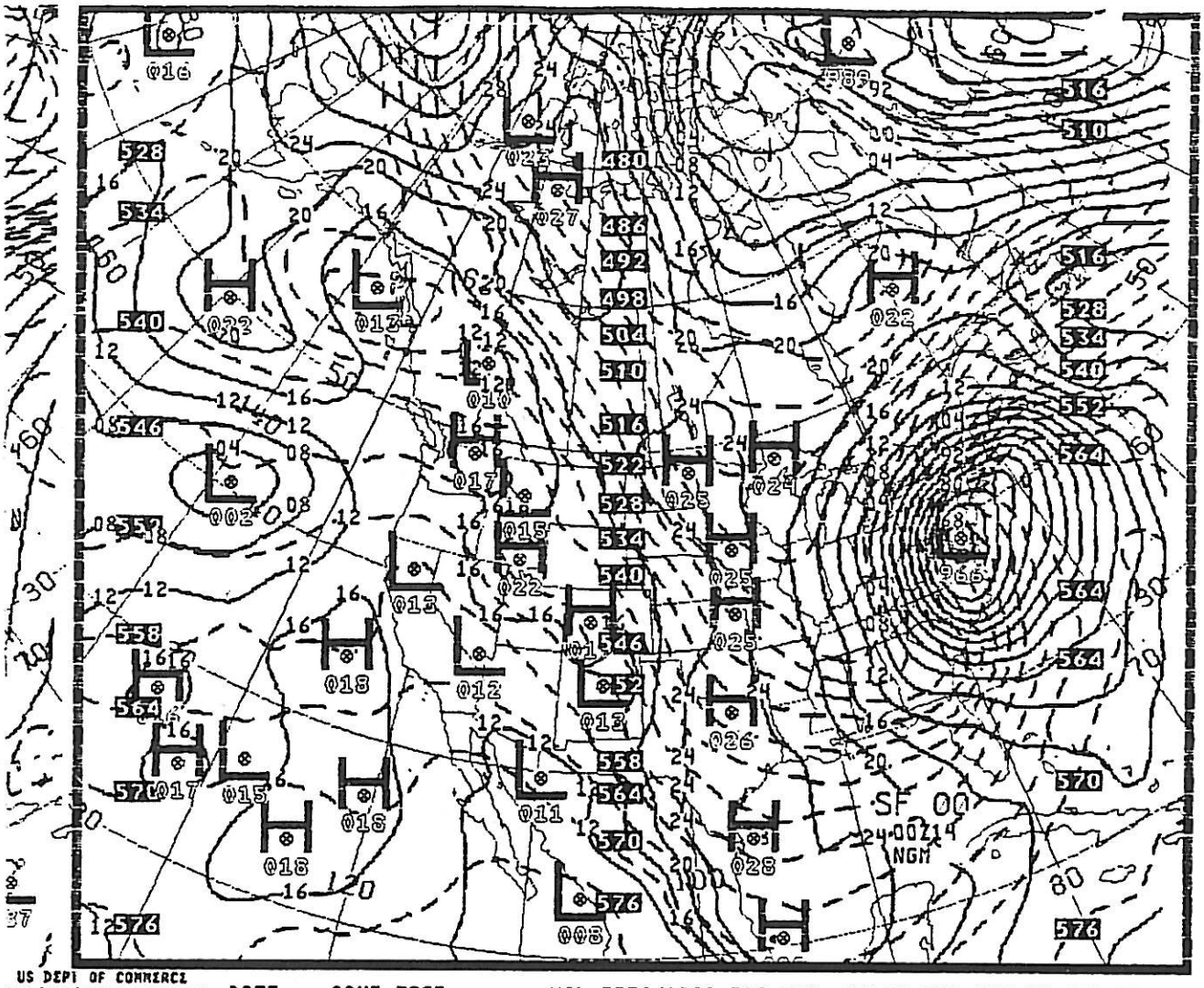

US DEPT OF COMMERCE
OAA/NWS/NMC WASHINGTON D033 .. 00HR FCST MSL PRES/1000-500 THK VALID 00Z SUN 14 MAR 93

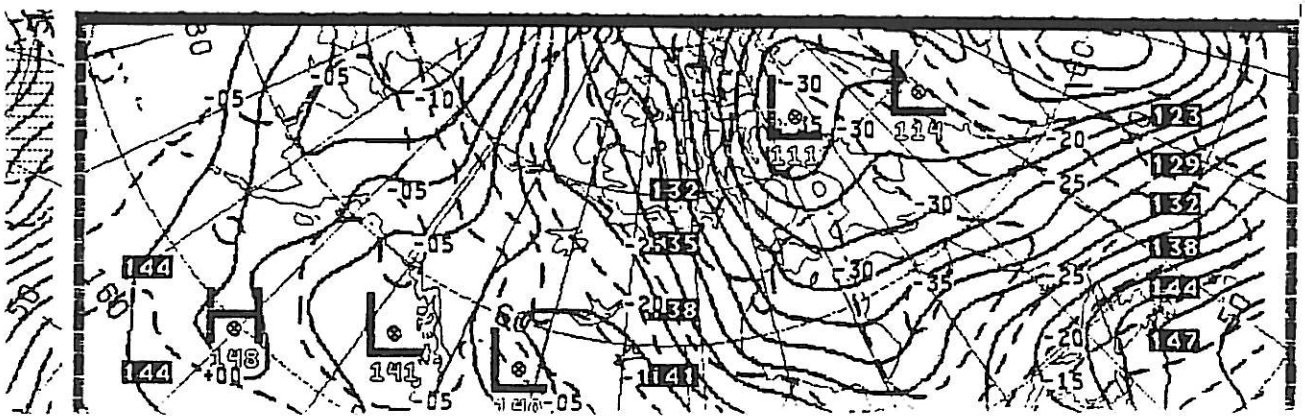

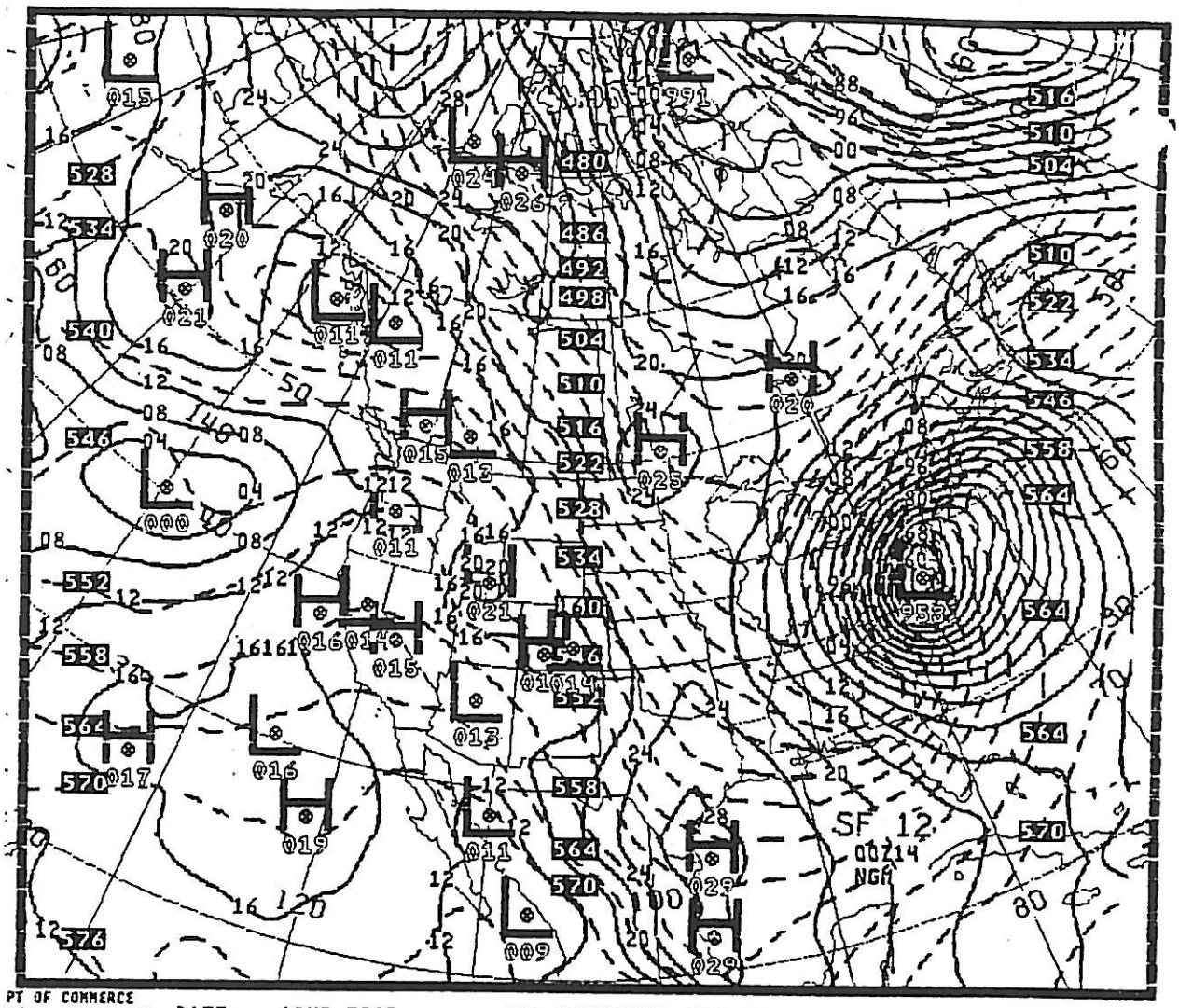

PT OF COMMERCE
S/WMC WASHINGTON D177 .. 12HR FCST MSL PRES/1000-500 THK VALID 00Z SUN 14 MAR 93

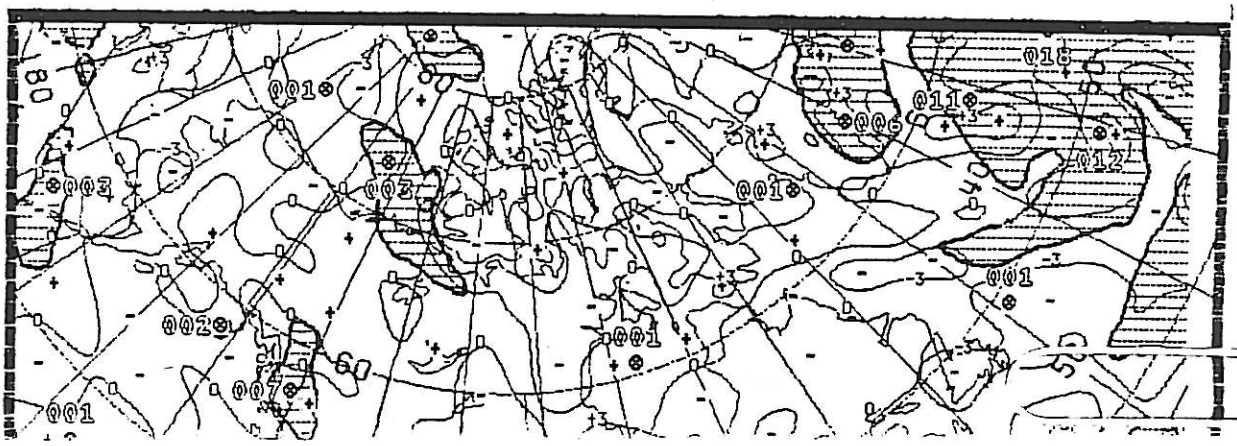

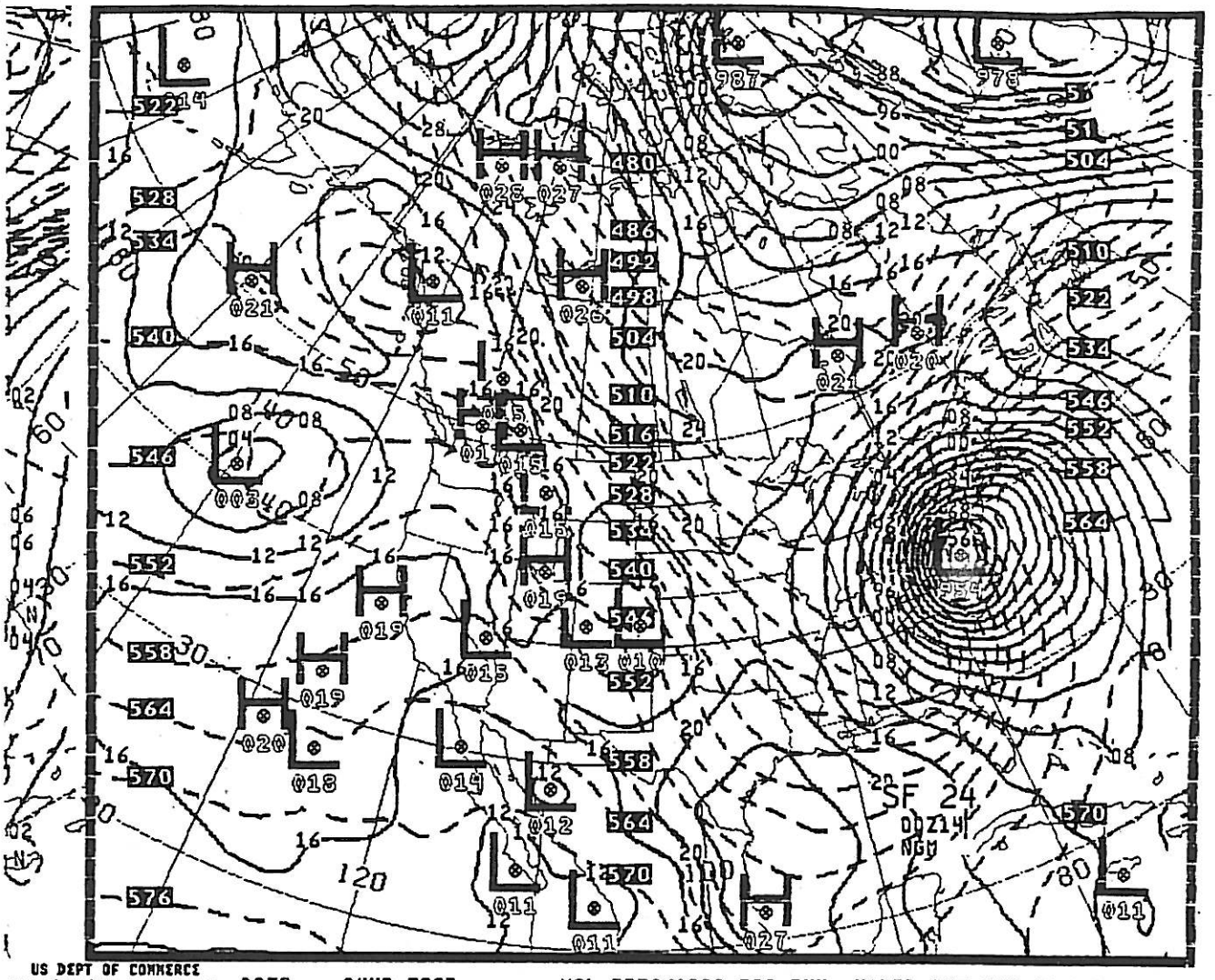

US DEPT OF COMMERCE
NOAA/NWS/WMC WASHINGTON D039 .. 24HR FCST MSL PRES/1000-500 THK VALID 00Z SUN 14 MAR 93

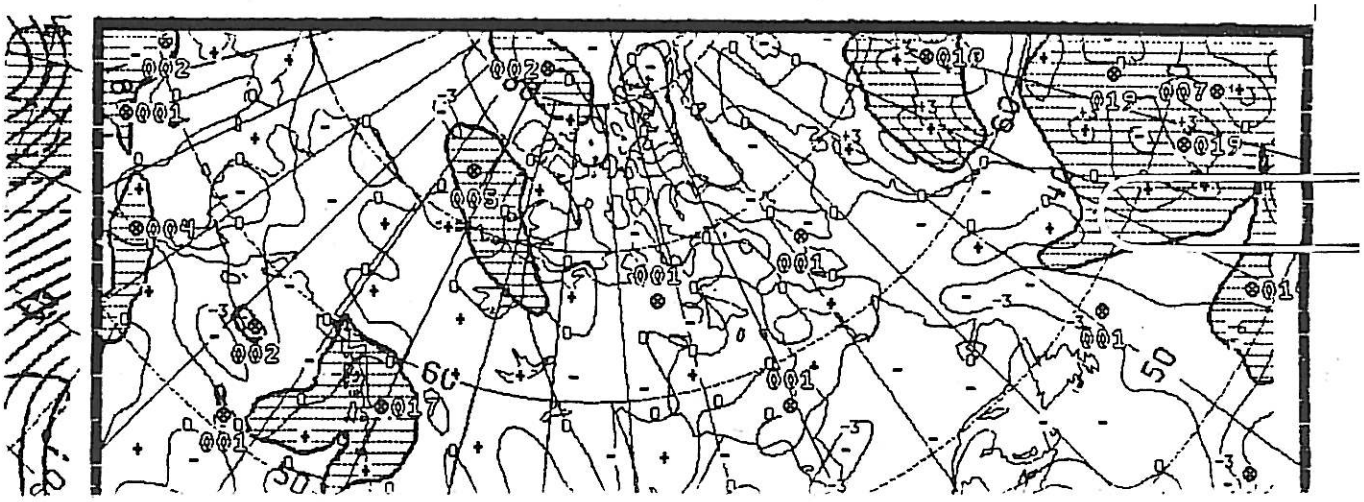

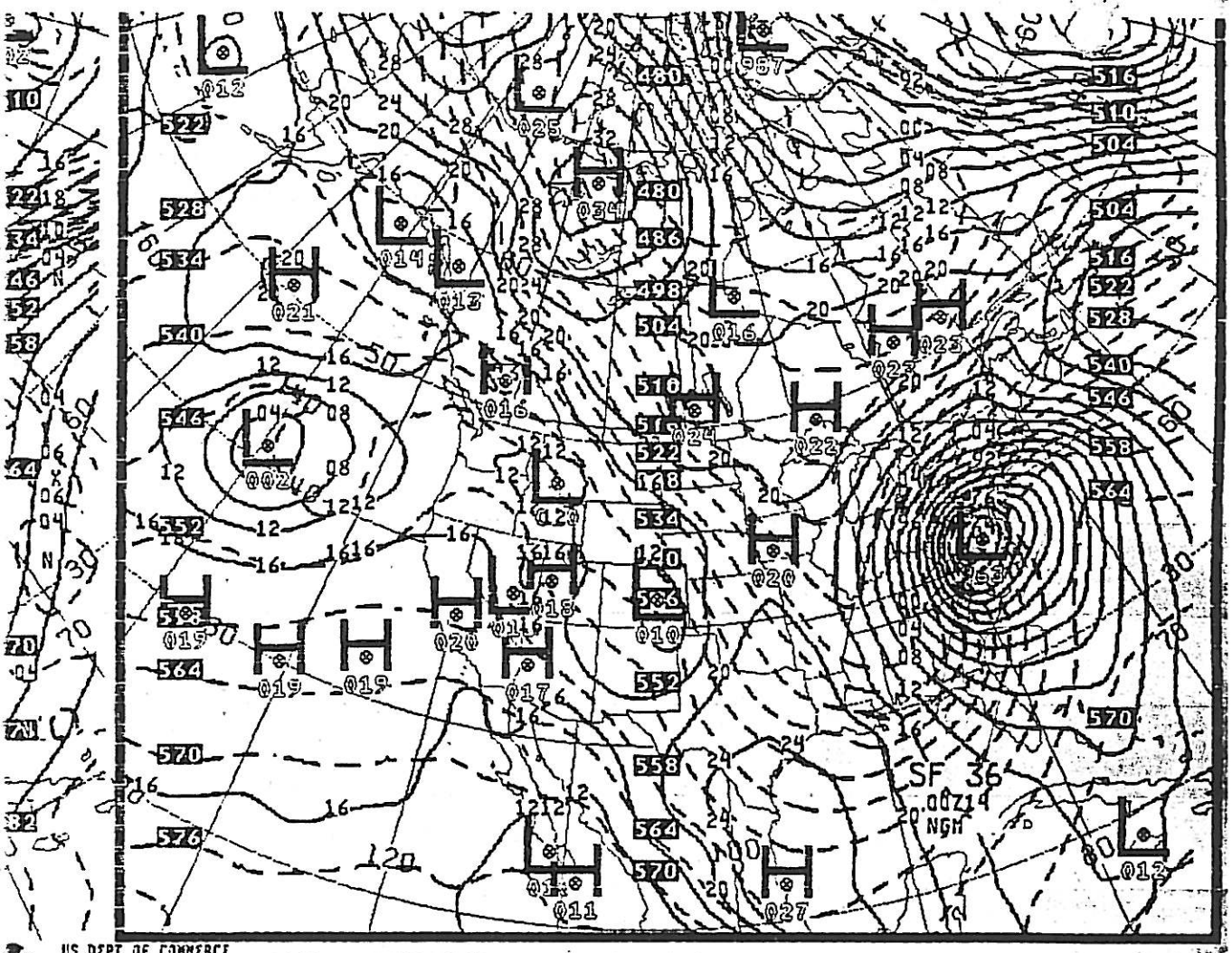

US DEPT OF COMMERCE
NOAA/NWS/NMC WASHINGTON D182 .. 36HR FCST MSL PRES/1000-500 THK VALID 00Z SUN 14 MAR 93

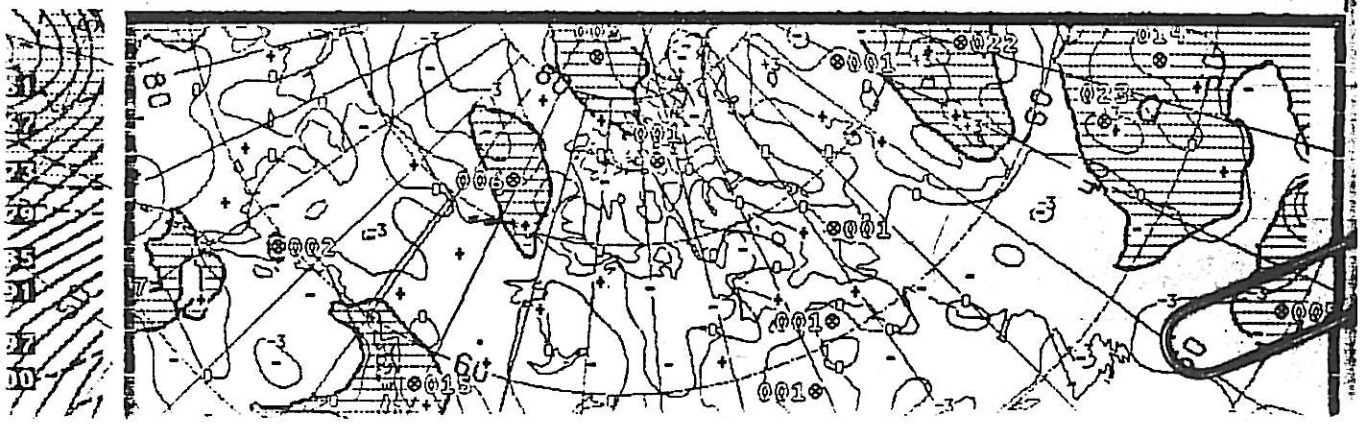

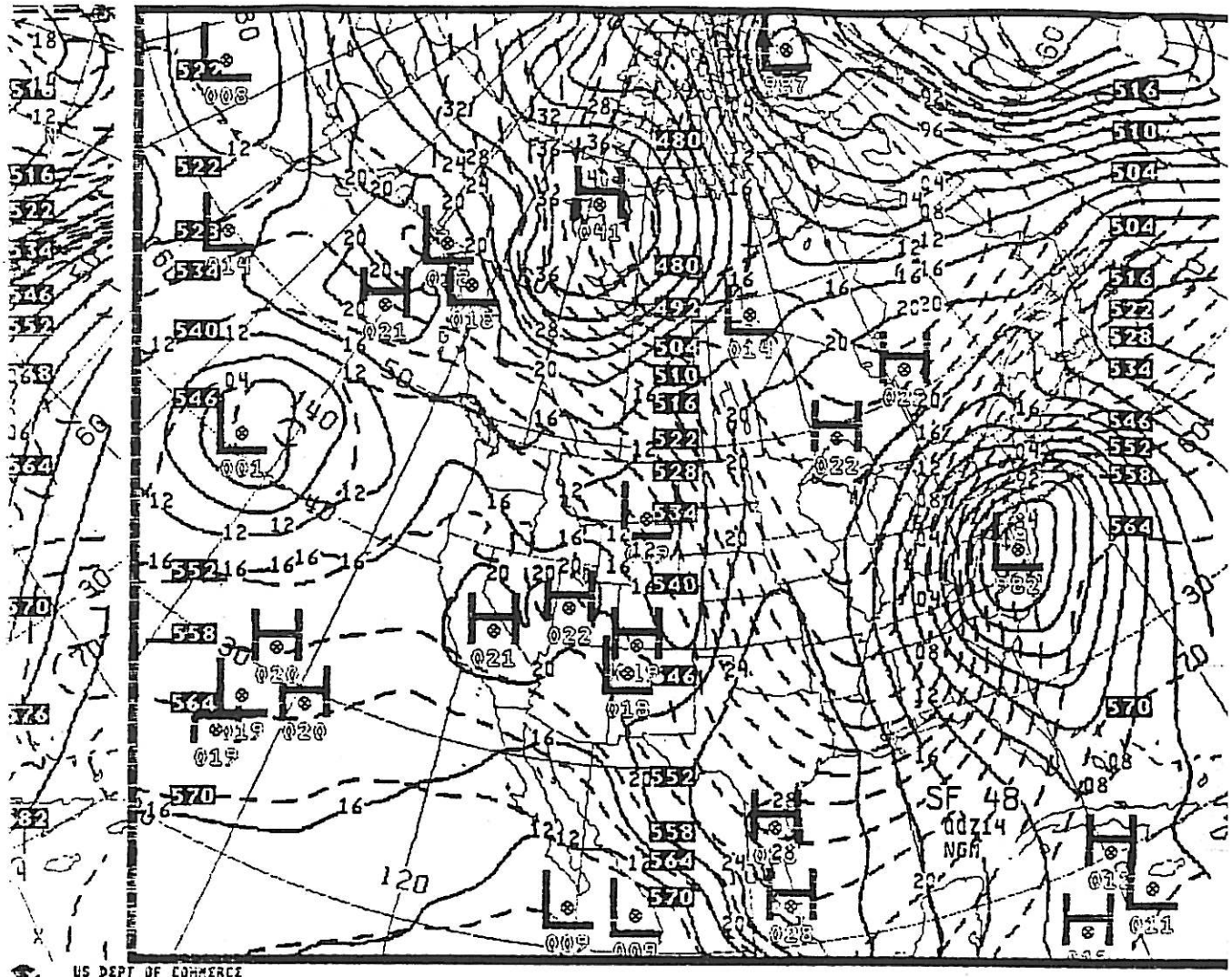

US DEPT OF COMMERCE
NOAA/NWS/NMC WASHINGTON D044 .. 48HR FCST MSL PRES/1000-500 THK VALID 00Z SUN 14 MAR 93

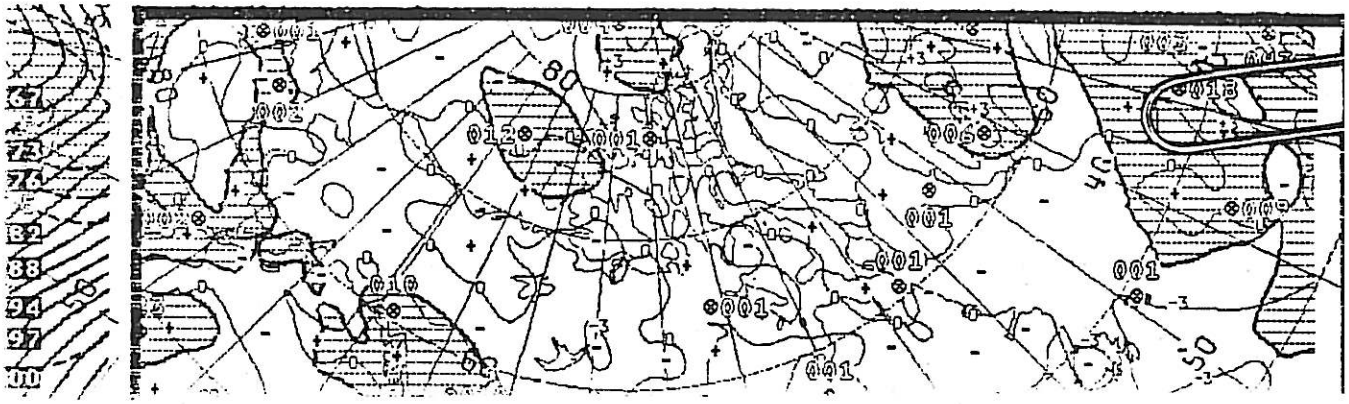

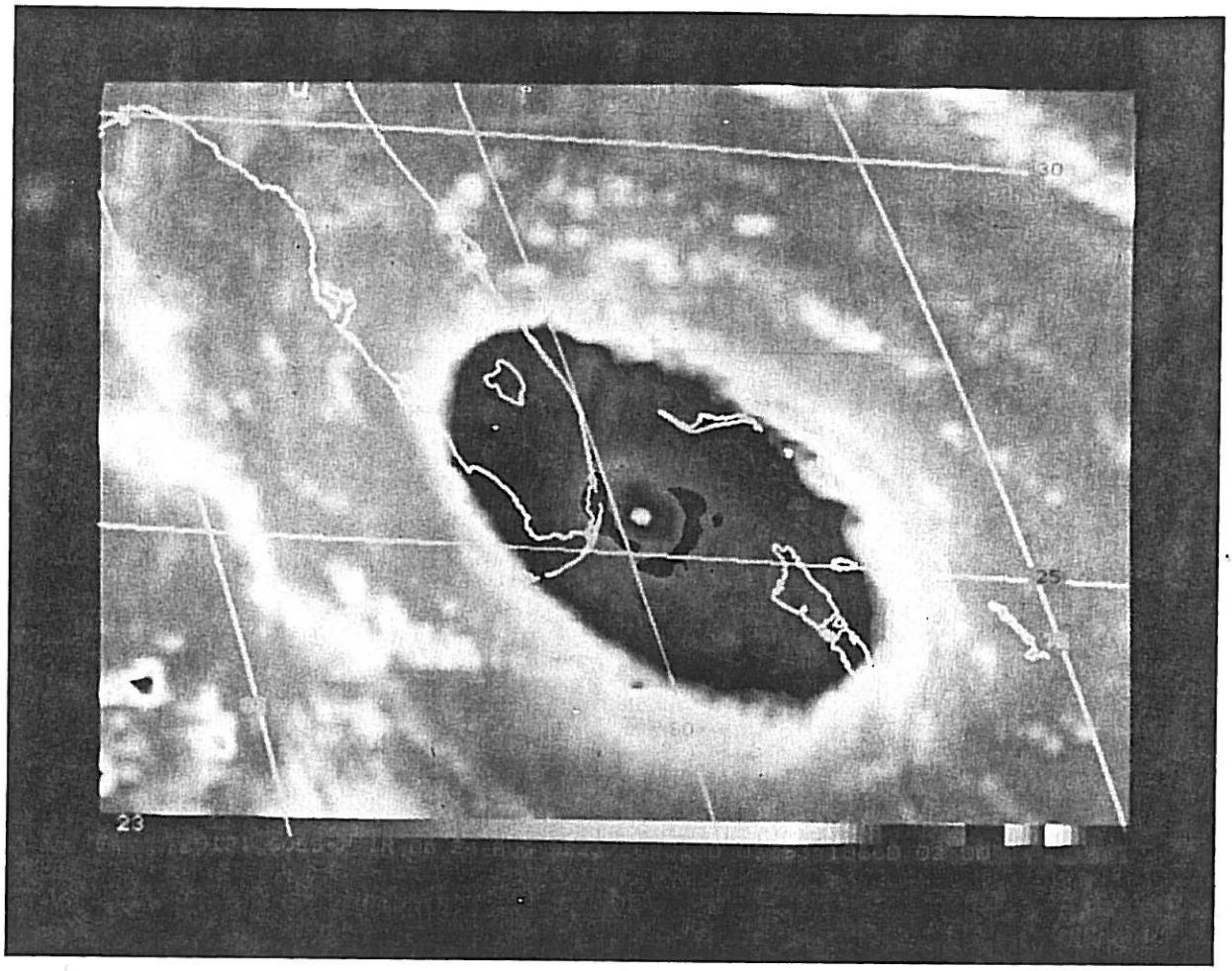

Figure 9.4: (a) satellite image of hurricane

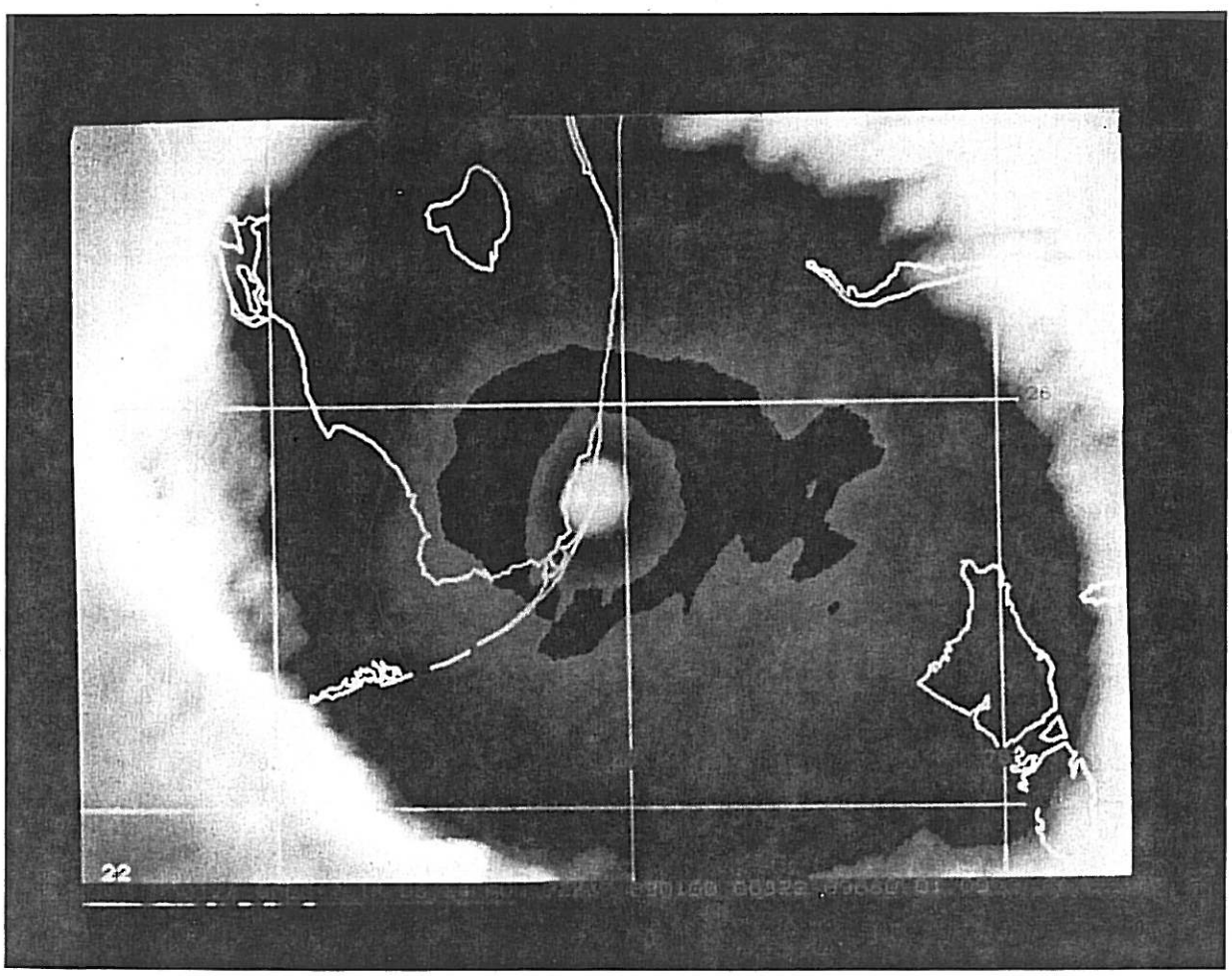

Figure 9.4: (b) satellite image of hurricane